

The Cryotron Reborn: Superconducting-Nanostrip-Based Electronics

Karl K. Berggren

Professor of Electrical Engineering
at Massachusetts Institute of Technology

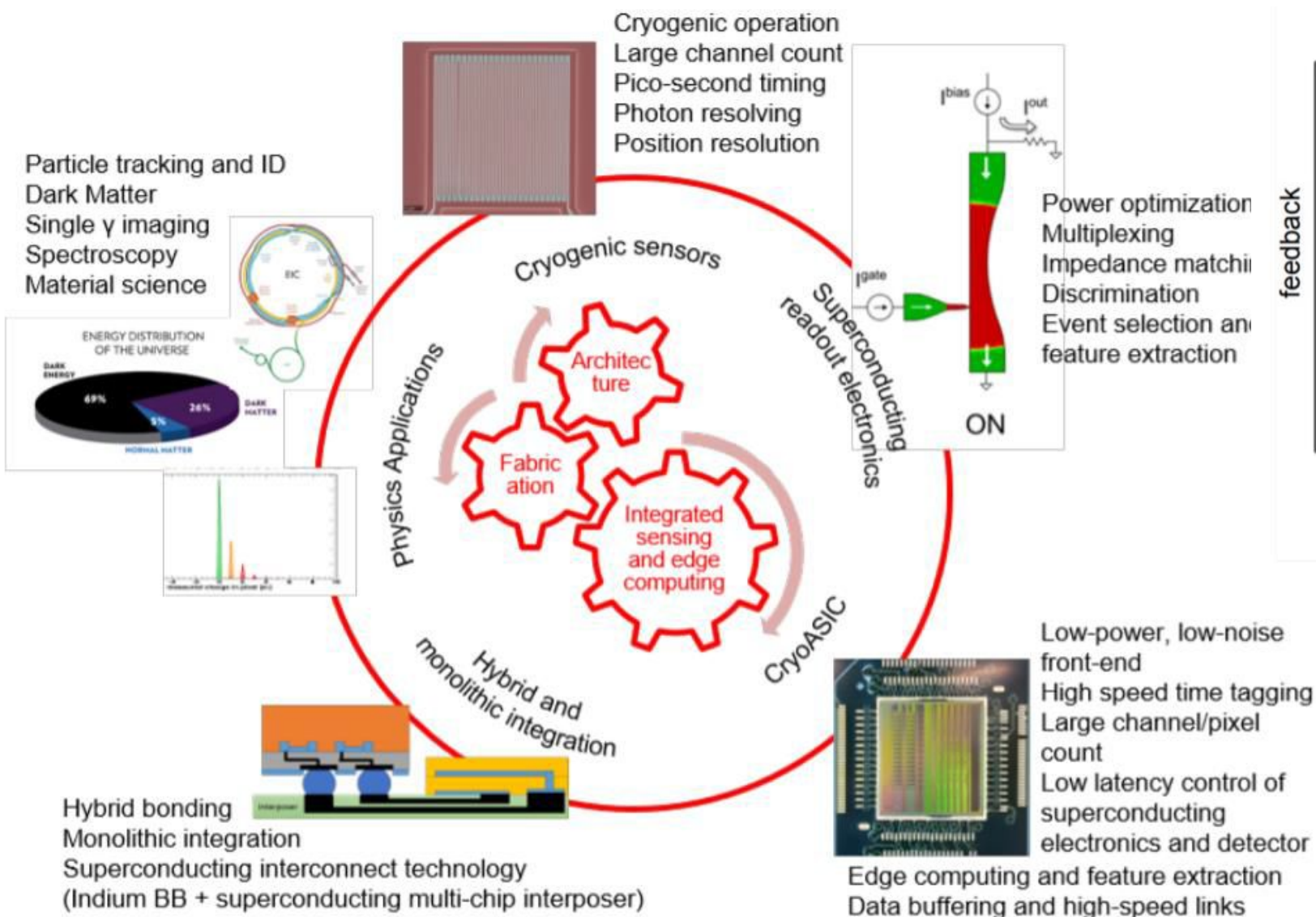
berggren@mit.edu

<https://www.rle.mit.edu/qnn/>



What do HEP Detectors Need that Superconducting Nanowires can Provide?

Hybrid superconducting detector platform

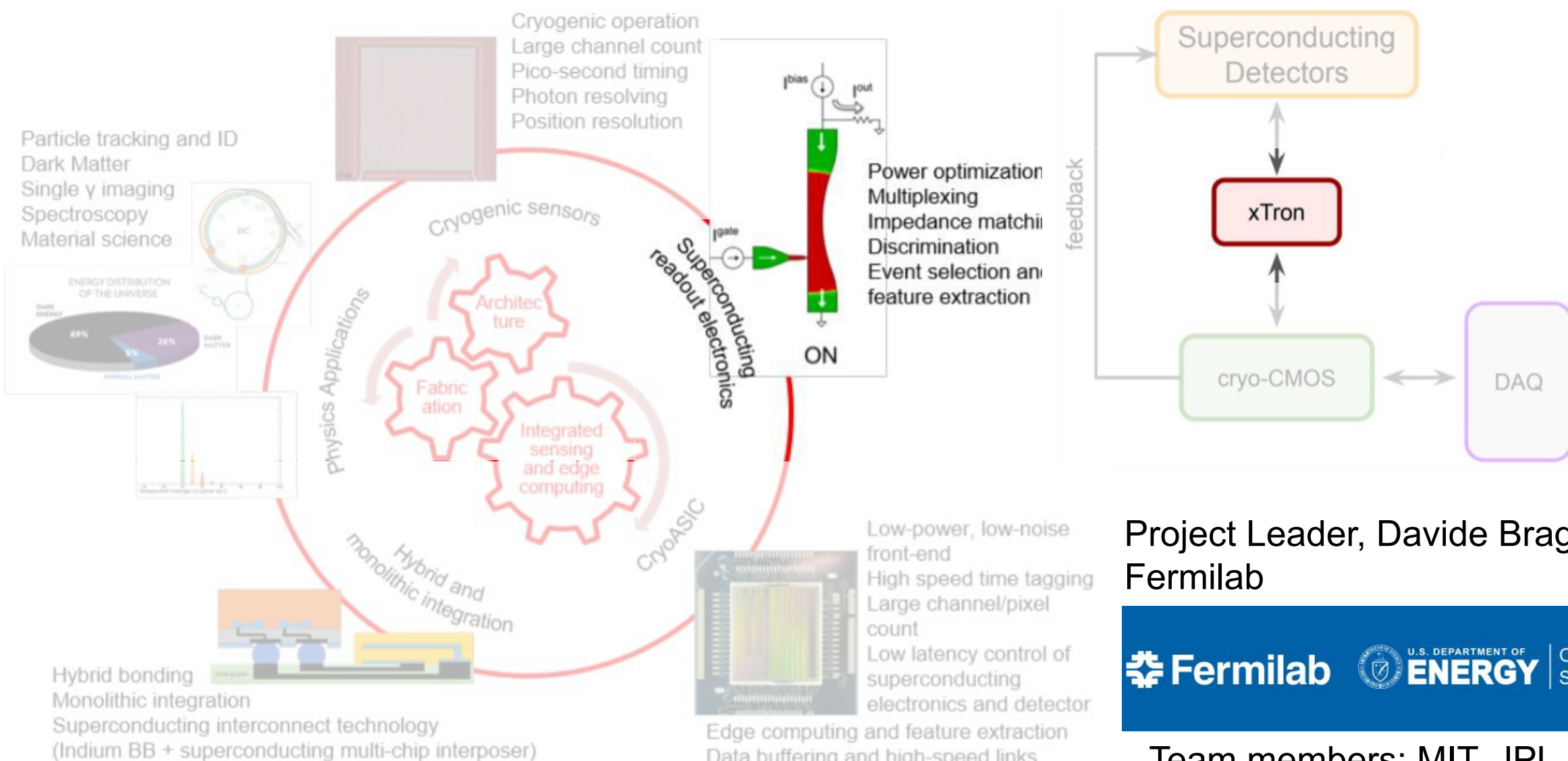


Project Leader, Davide Braga
Fermilab



Team members: MIT, JPL, NIST, Synopsys, Argonne National Lab

Hybrid superconducting detector platform



Project Leader, Davide Braga
Fermilab



Team members: MIT, JPL, NIST, Synopsys, Argonne National Lab

HEP Needs

- Operation in low-temperature environments
- Operation in high-radiation environments
- Operation in strong magnetic fields
- Basic digital functions (counting, shifting, mux/demux)
- Basic analog functions (amplification, threshold detection)
- Integration with superconducting detectors
- Integration with CMOS

What can be sacrificed?

- Ultra-high integration scale (warmer CMOS can be used, outside of the B field)
- Ultra-high speeds (need to keep up with data rate, not CMOS clock rate)

Efficient single particle detection with a superconducting nanowire

Unconventional Applications of Superconducting Nanowire Single Photon Detectors

by  Tomas Polakovic^{1,2} ,  Whitney Armstrong¹ ,  Goran Karapetrov^{2,3} ,
 Zein-Eddine Meziani¹   and  Valentine Novosad^{1,4,*} 

¹ Physics Division, Argonne National Laboratory, Argonne, IL 60439, USA

² Department of Physics, Drexel University, Philadelphia, PA 19104, USA

³ Department of Materials Science and Engineering, Drexel University, Philadelphia, PA 19104, USA

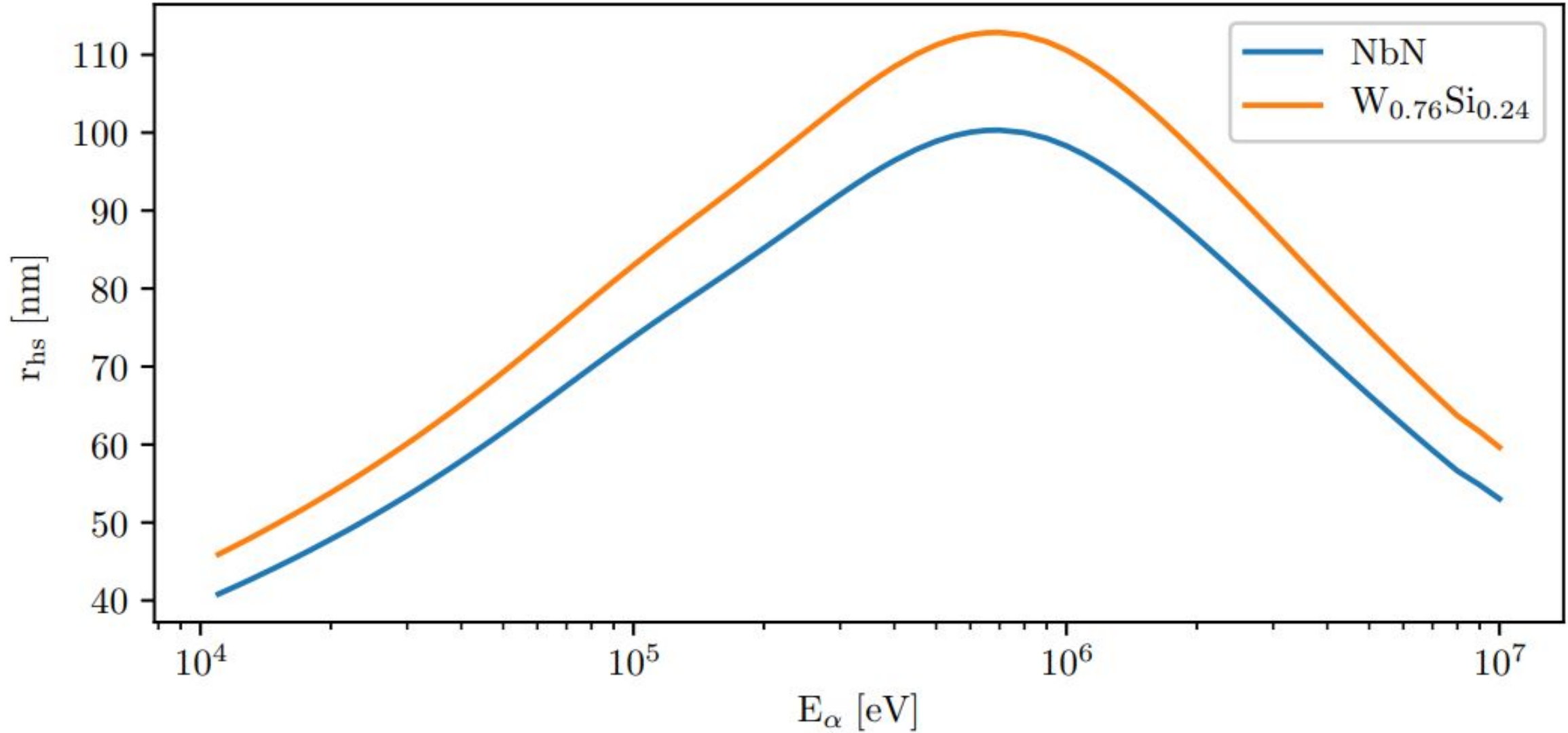
⁴ Materials Science Division, Argonne National Laboratory, Argonne, IL 60439, USA

* Author to whom correspondence should be addressed.

Nanomaterials **2020**, *10*(6), 1198; <https://doi.org/10.3390/nano10061198>

Received: 18 May 2020 / Revised: 7 June 2020 / Accepted: 8 June 2020 / Published: 19 June 2020

(This article belongs to the Special Issue Superconductivity in Nanoscaled Systems)



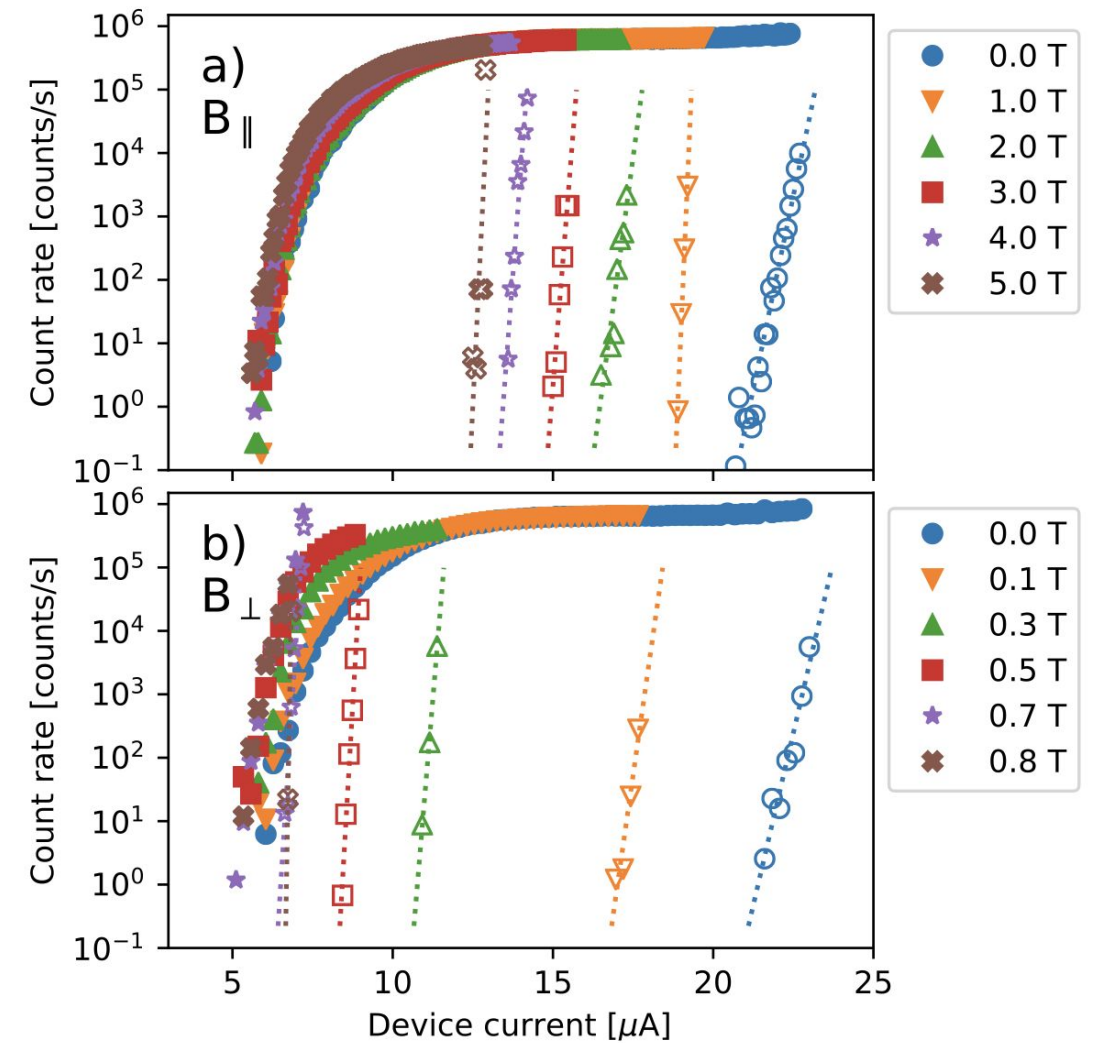
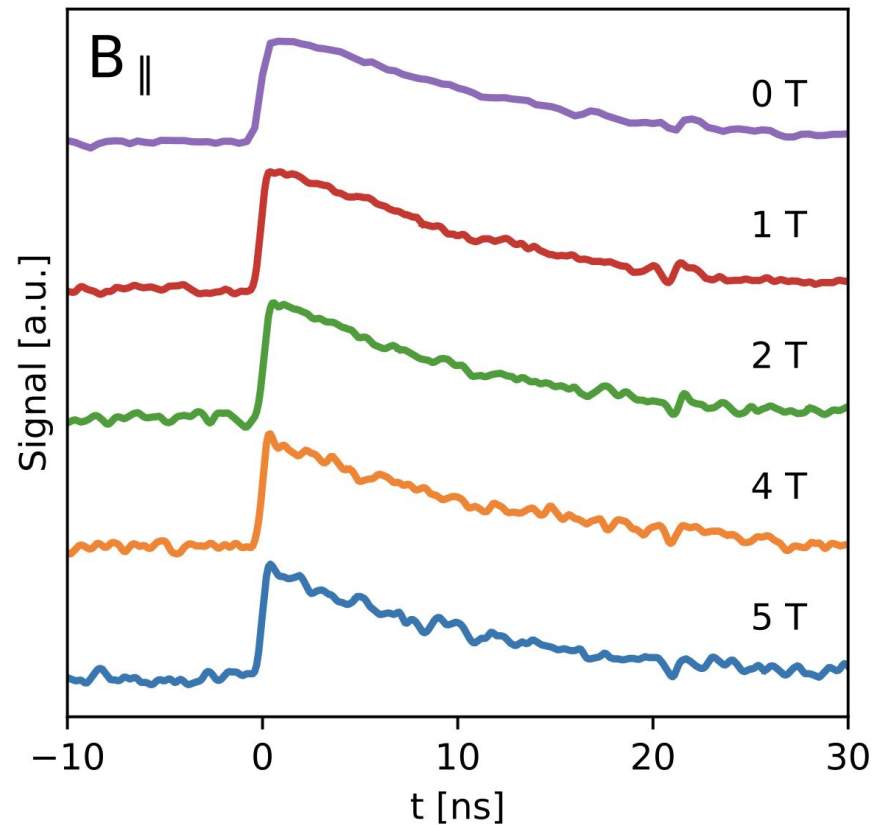
Polakovic 2020

Figure 4. Approximate thermal hotspot radius r_{hs} as a function of α -particle kinetic energy in NbN film with $T_C = 8\text{K}$ and $W_{0.76}Si_{0.24}$ film with $T_C = 3.35 \text{ K}$. Both films are assumed to be held at $T_0 = \frac{T_C}{2}$.

Operation in Strong Magnetic Field

Superconducting nanowires as high-rate photon detectors in strong magnetic fields

T. Polakovic^{a,d}, W.R. Armstrong^a, V. Yefremenko^b, J.E. Pearson^c, K. Hafidi^a, G. Karapetrov^{d,e}, Z.-E. Meziani^a, V. Novosad^{c,*}



Polakovic, Tomas et al. *Nuclear Instruments and Methods in Physics Research Section A: Accelerators, Spectrometers, Detectors and Associated Equipment* 959 (2020): 163543.

Multifunctional Superconducting Nanowire Quantum Sensors

Benjamin J. Lawrie^{1,*}, Claire E. Marvinney^{1,†}, Yun-Yi Pai¹, Matthew A. Feldman,¹ Jie Zhang,¹ Aaron J. Miller,² Chengyun Hua¹, Eugene Dumitrescu¹, and Gábor B. Halász¹

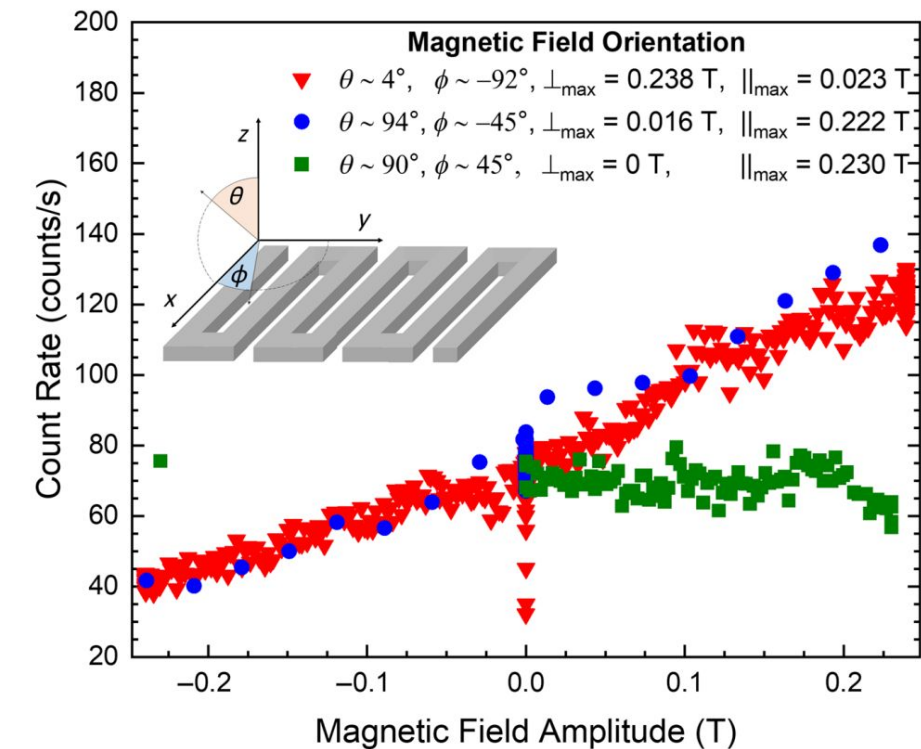
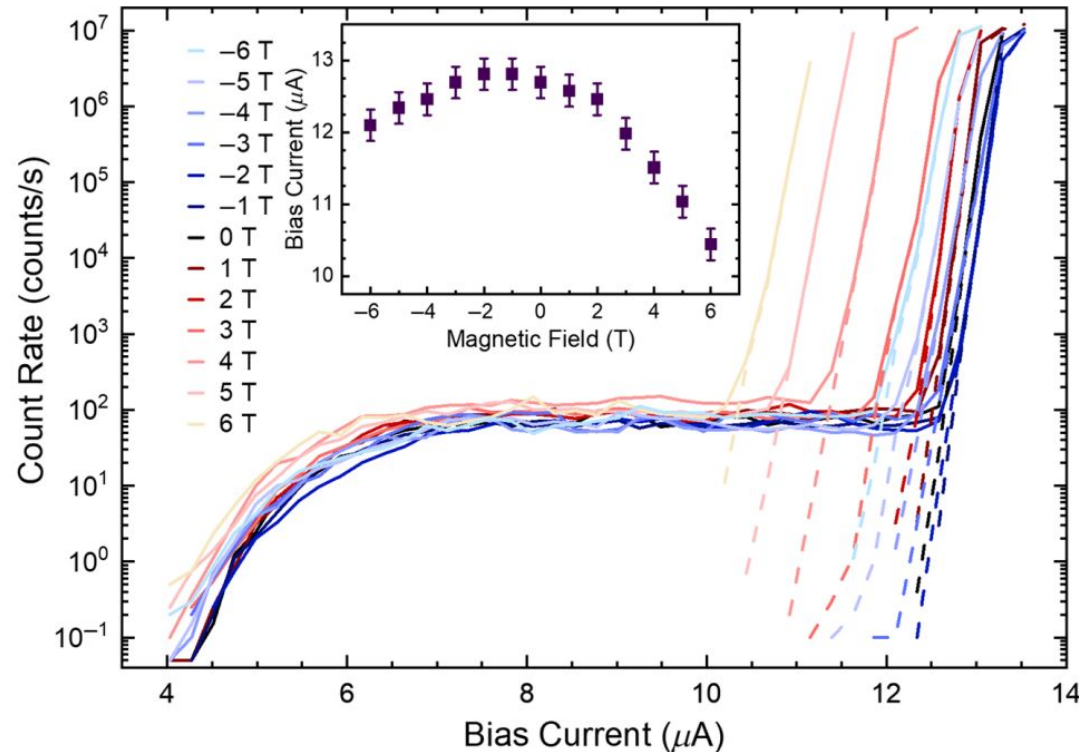
¹ Materials Science and Technology Division, Oak Ridge National Laboratory, 1 Bethel Valley Road, Oak Ridge, Tennessee 37831, USA

² Quantum Opus LLC, Novi, Michigan 48375, USA

³ Computational Science and Engineering Division, Oak Ridge National Laboratory, 1 Bethel Valley Road, Oak Ridge, Tennessee 37831, USA



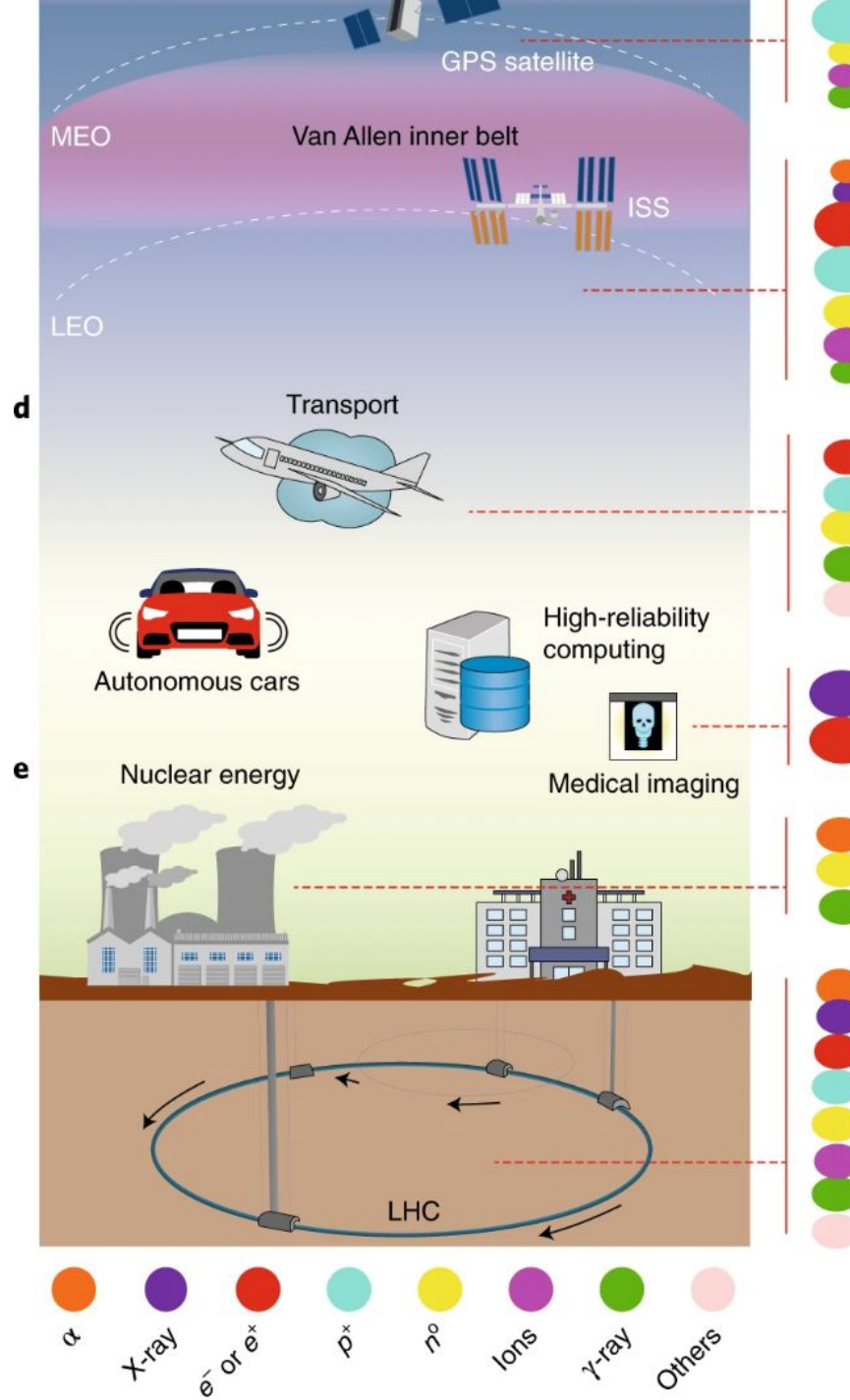
(Received 18 March 2021; revised 19 September 2021; accepted 9 November 2021; published 23 December 2021)



A colorful, abstract painting of a landscape. The scene features rolling hills and mountains in shades of yellow, green, blue, and red. A winding path or riverbed cuts through the center of the composition, leading the eye towards the horizon. The brushwork is visible and expressive throughout the piece.

Radiation Hard

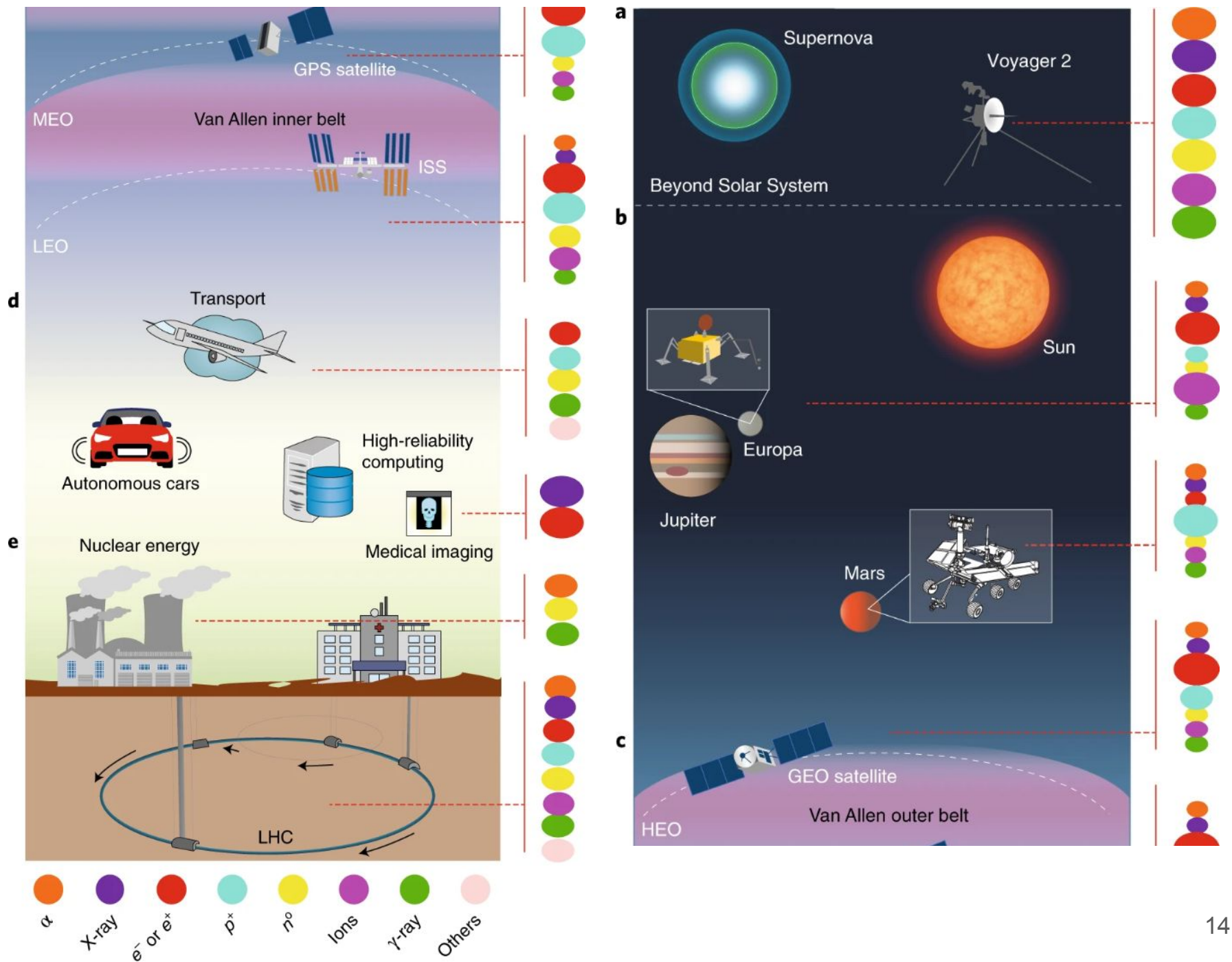
Radiation Environment



Prinzie, J., Simanjuntak, F.M., Leroux, P. et al.
Low-power electronic technologies for harsh
radiation environments. *Nat Electron* 4,
243–253 (2021).
<https://doi-org.libproxy.mit.edu/10.1038/s41928-021-00562-4>

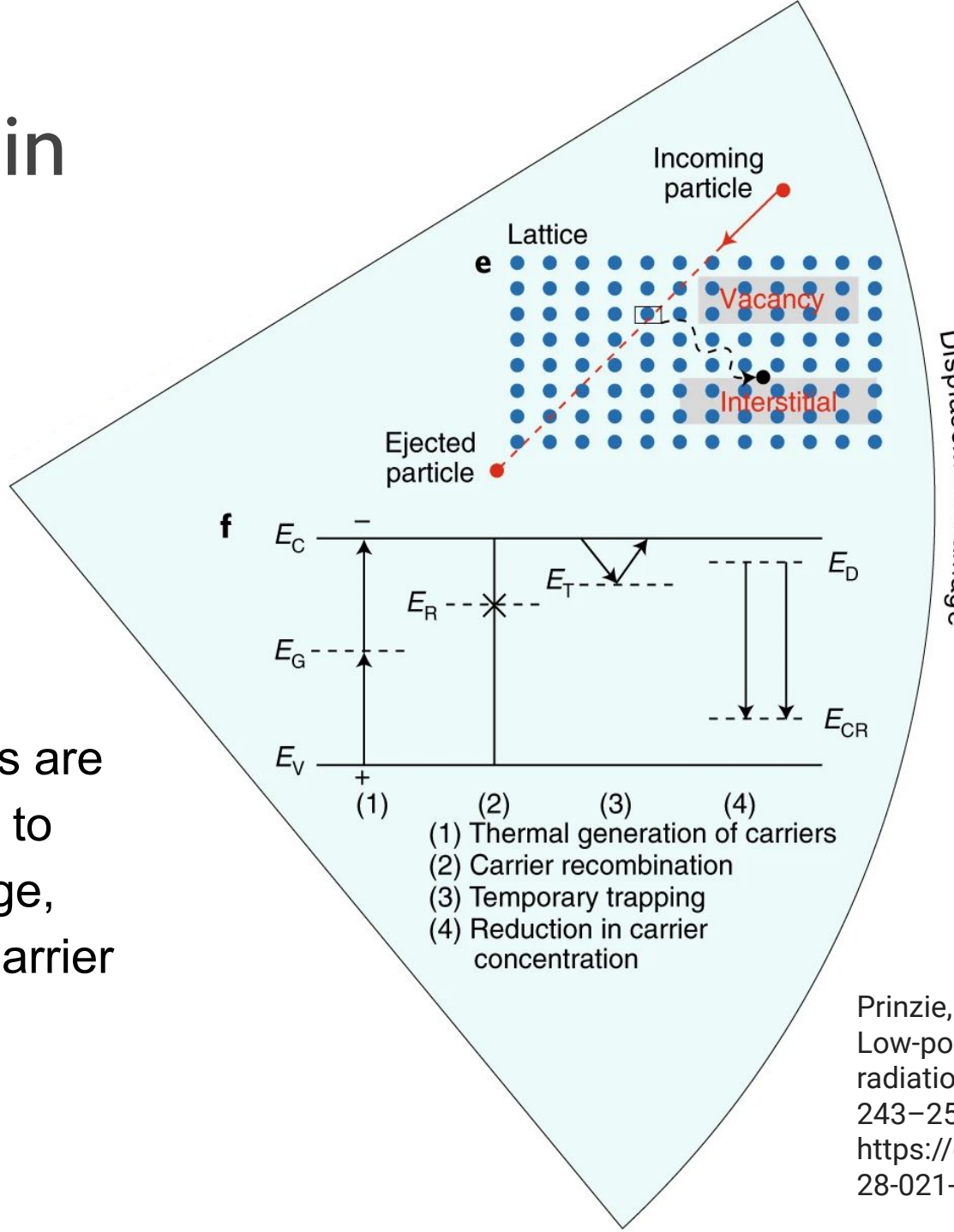
Radiation Environment

Prinzie, J., Simanjuntak, F.M., Leroux, P. et al.
Low-power electronic technologies for harsh
radiation environments. *Nat Electron* 4,
243–253 (2021).
<https://doi-org.libproxy.mit.edu/10.1038/s41928-021-00562-4>



Lattice Damage in CMOS and JJs

- Josephson Junctions are likely to be sensitive to displacement damage, which will alter the barrier shape and height



Prinzie, J., Simanjuntak, F.M., Leroux, P. et al.
Low-power electronic technologies for harsh
radiation environments. *Nat Electron* 4,
243–253 (2021).
<https://doi-org.libproxy.mit.edu/10.1038/s41928-021-00562-4>

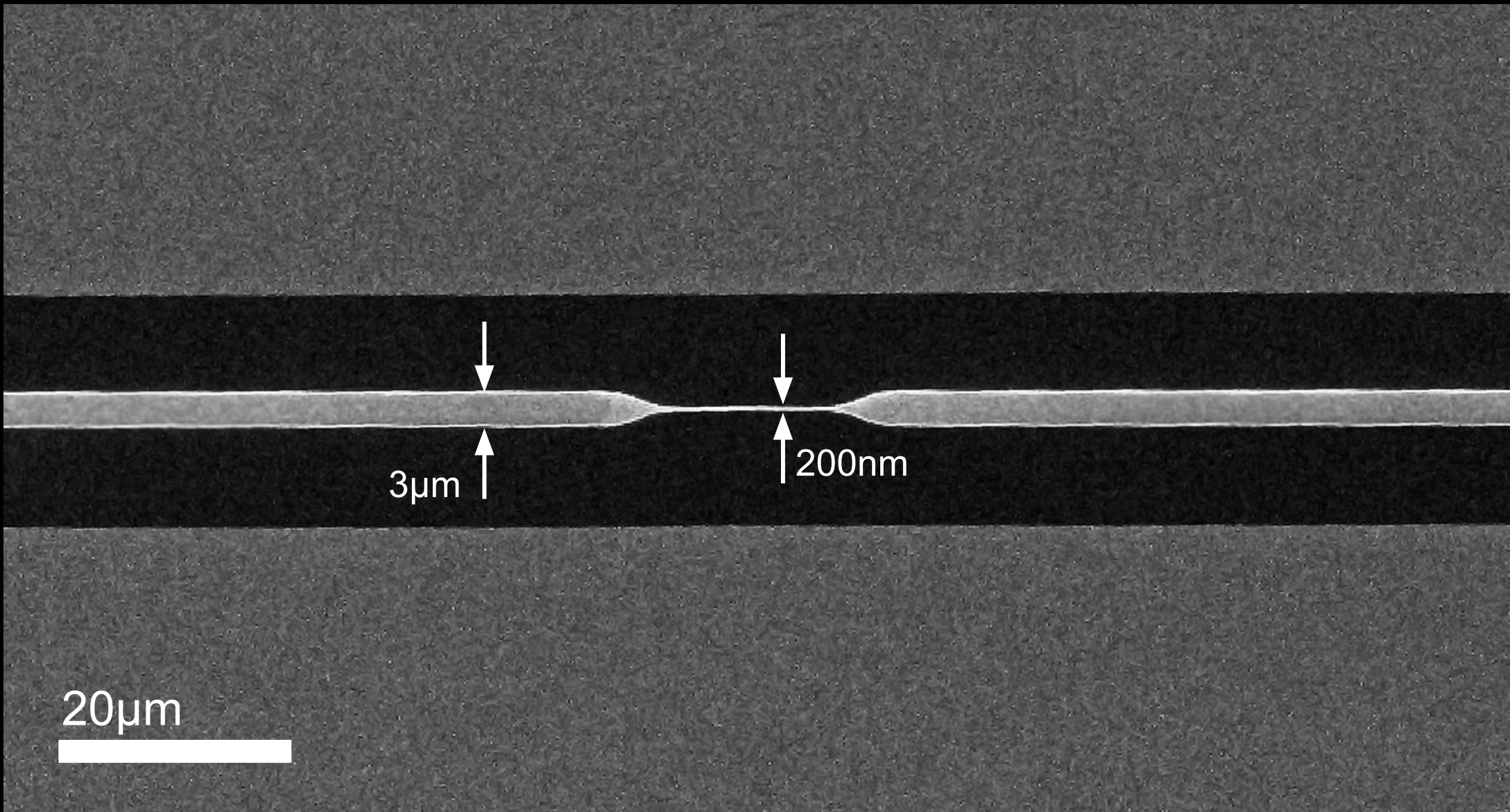
Radiation Tolerance of Niobium Nitride

- Previous NbN radiation study¹ with fast neutron fluence of 10^{23} m^{-2}
 - In low orbit (297 km altitude²), fast neutron flux of $3.4 \times 10^8 \text{ m}^{-2}\text{day}^{-1}$
 - T_c decreased by 5.7%
 - ρ increased by 6.3%
 - J_c did not change

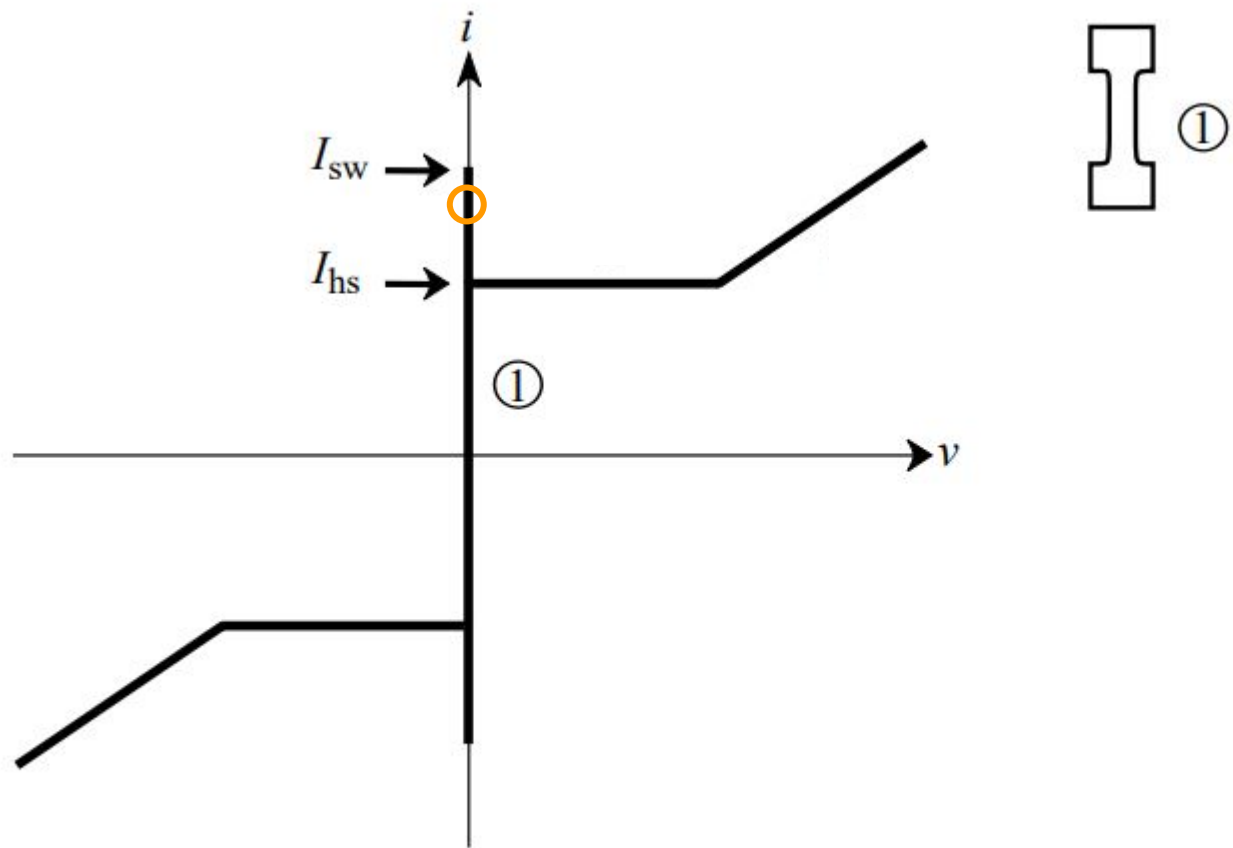
¹*Journal of Applied Physics* **64**, 1301 (1988); <https://doi.org/10.1063/1.341850>

²*Nucl. Tracks Radiat. Meas.* **17**, 87-91 (1990)

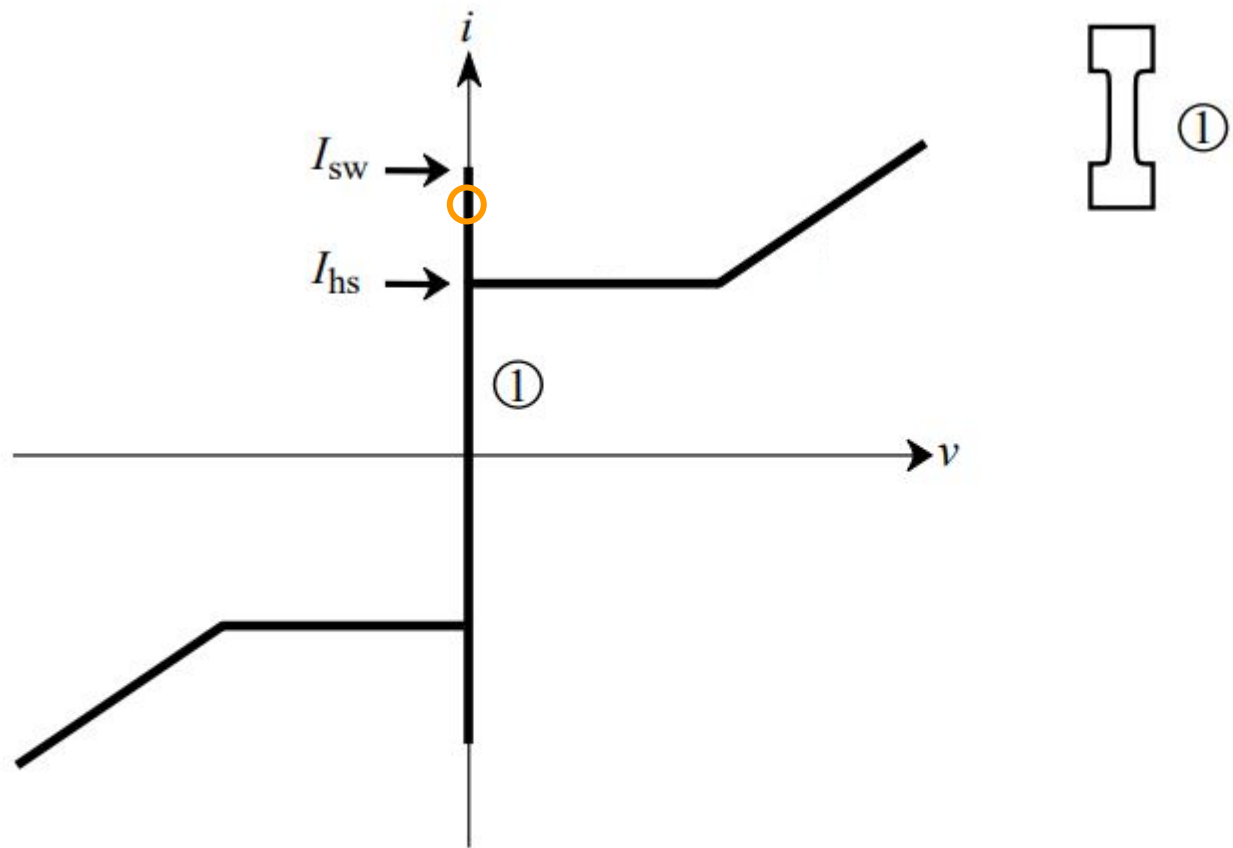
Superconducting Nanowire Device



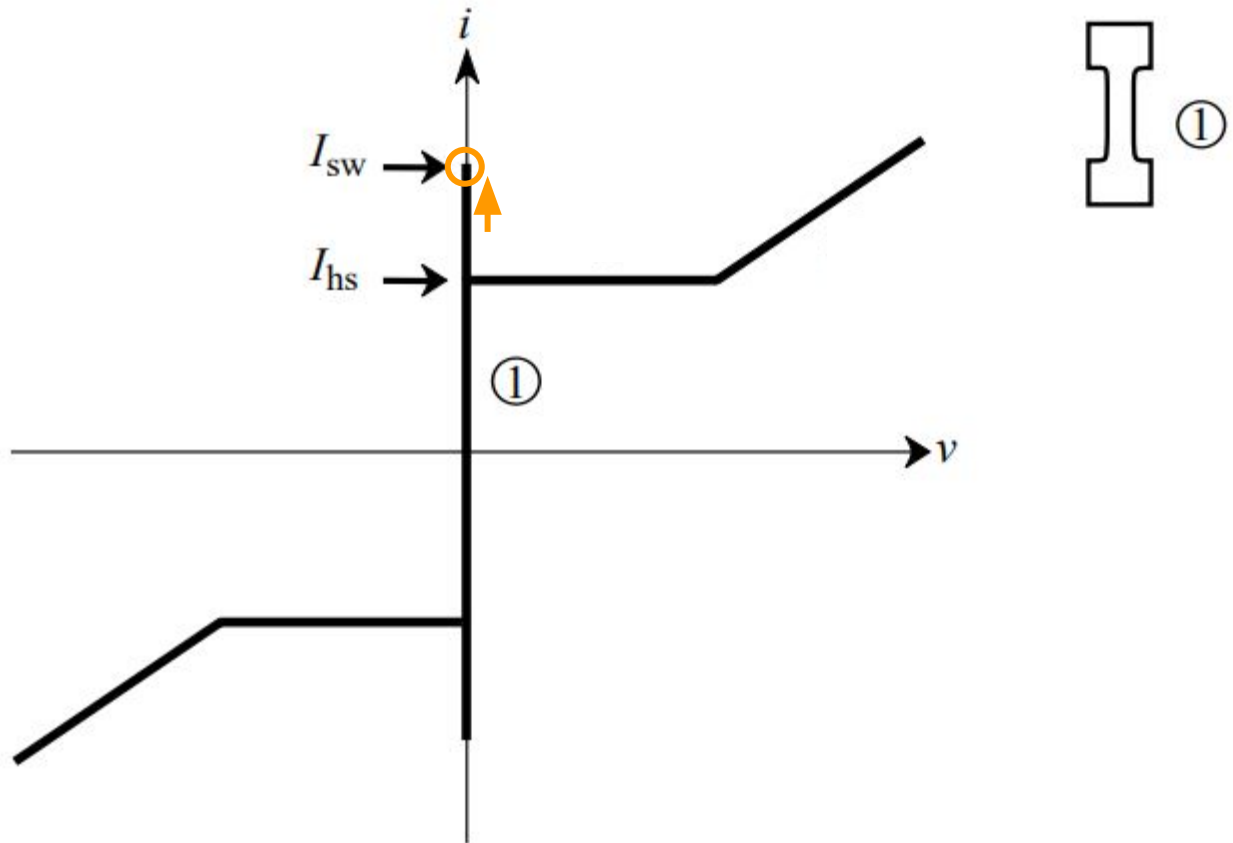
Initial Bias Condition



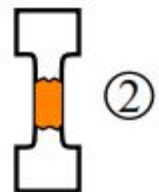
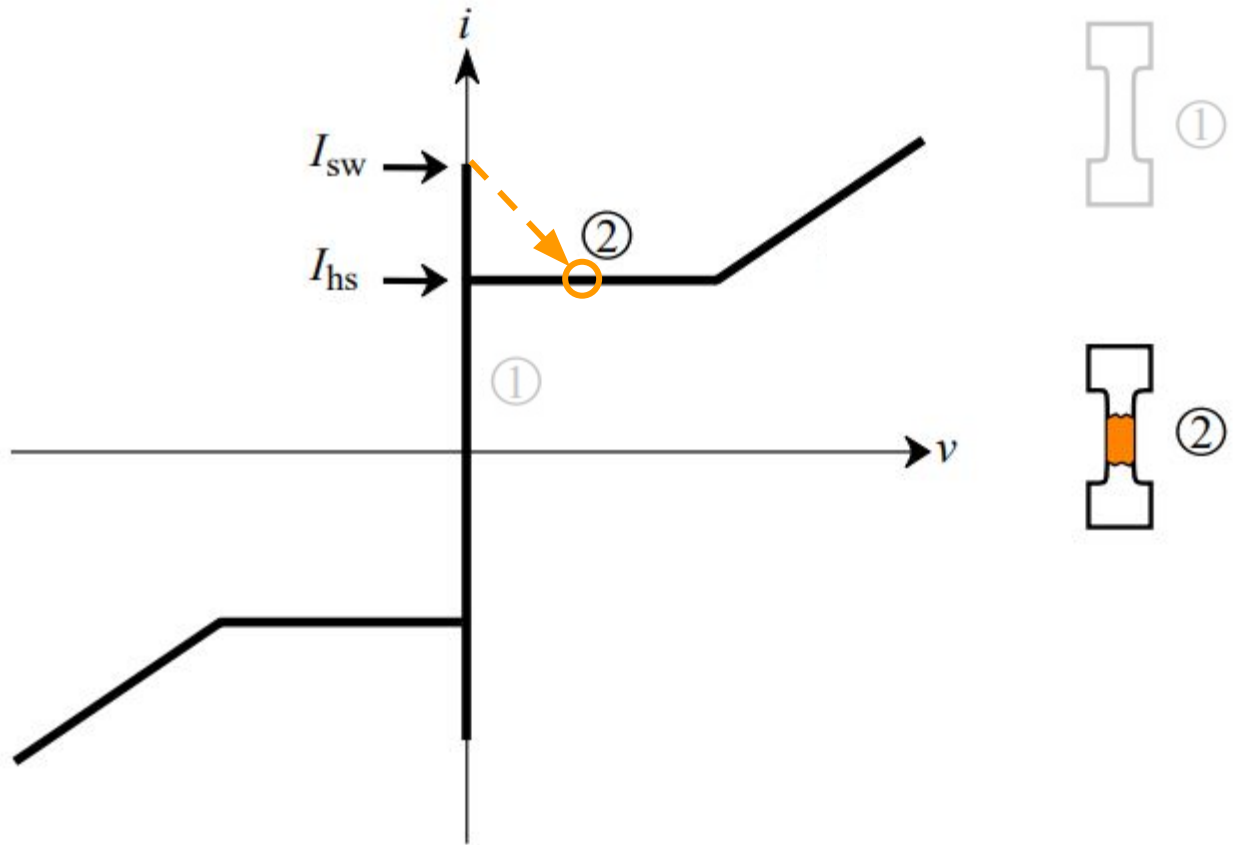
Initial Bias Condition



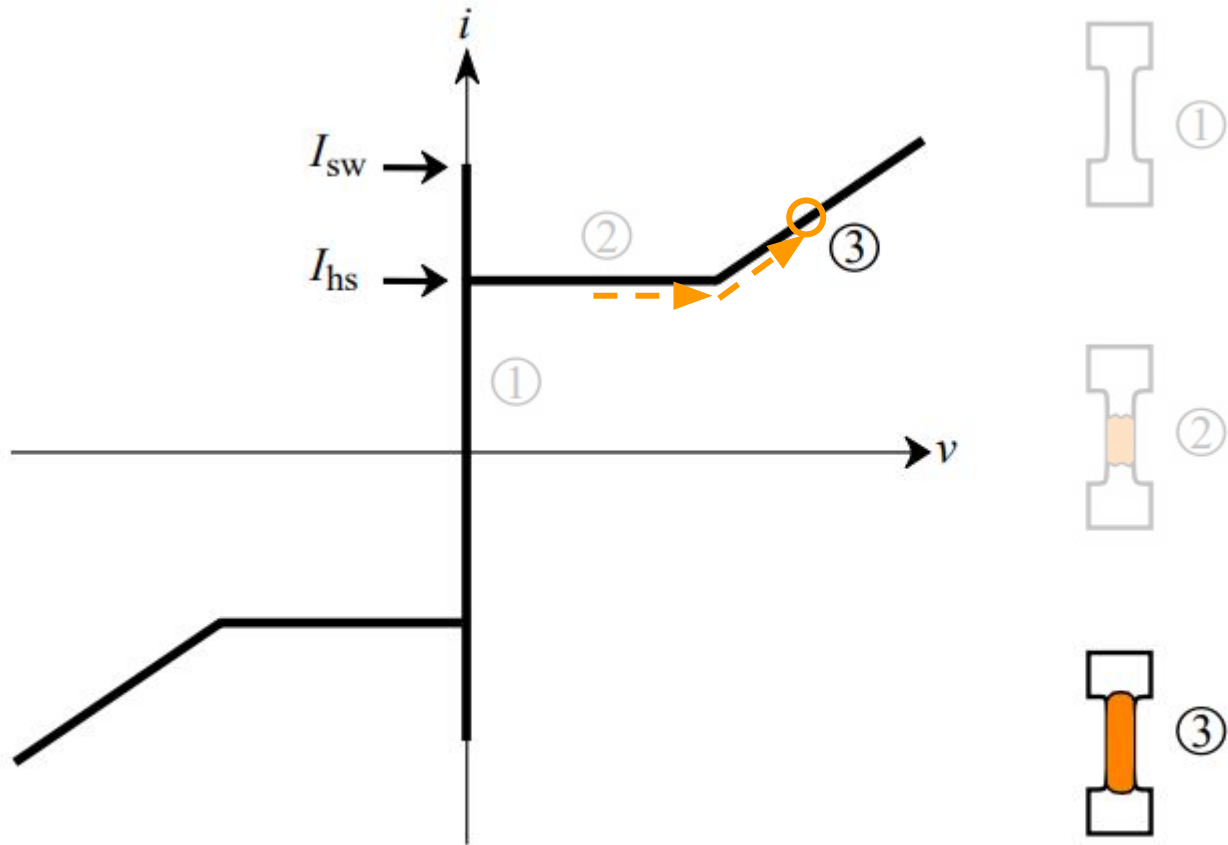
Trigger Event



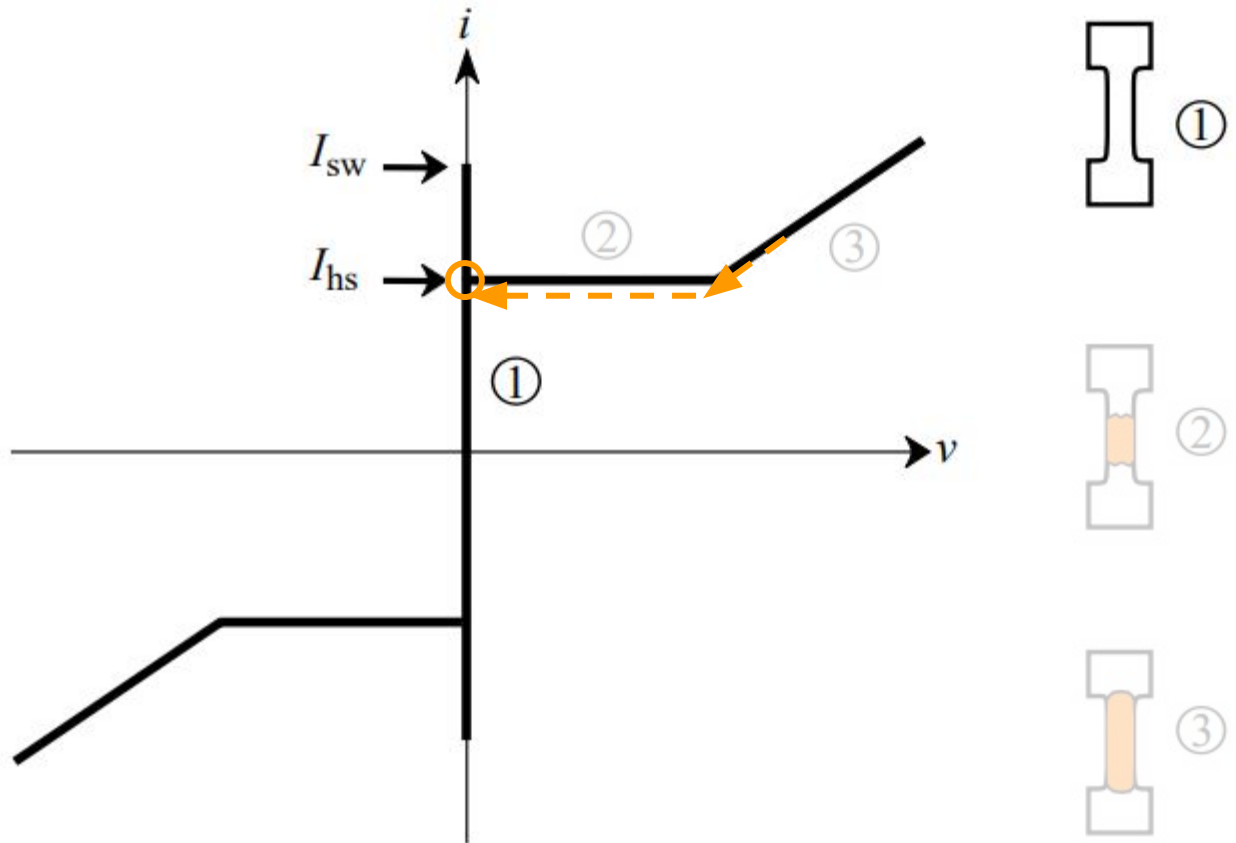
Hot Spot Creation and Growth



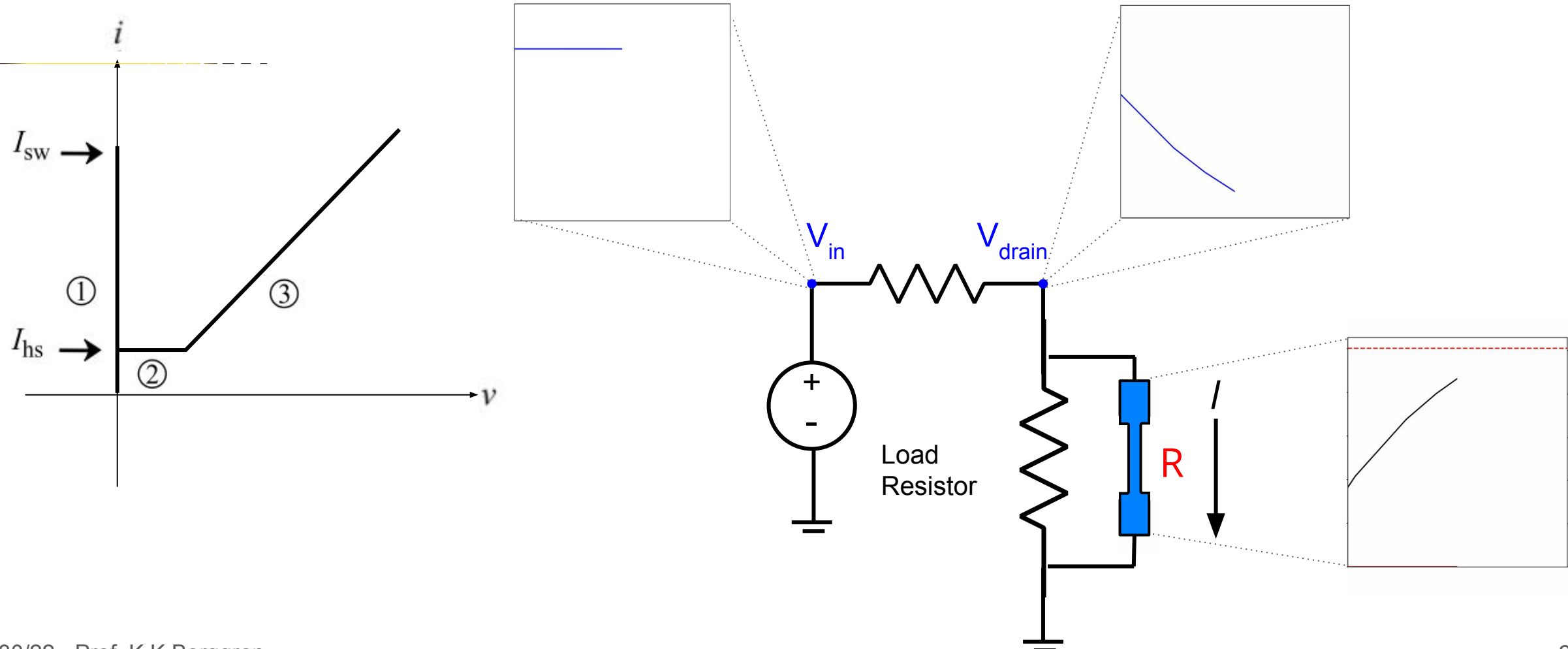
Hot Spot Saturation



Collapse and Reset



Superconducting Nanowire in a Circuit



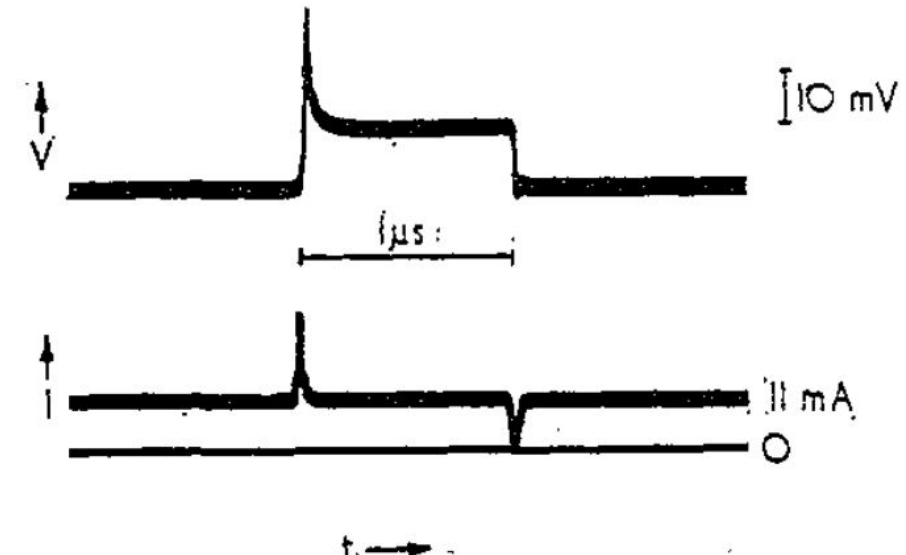
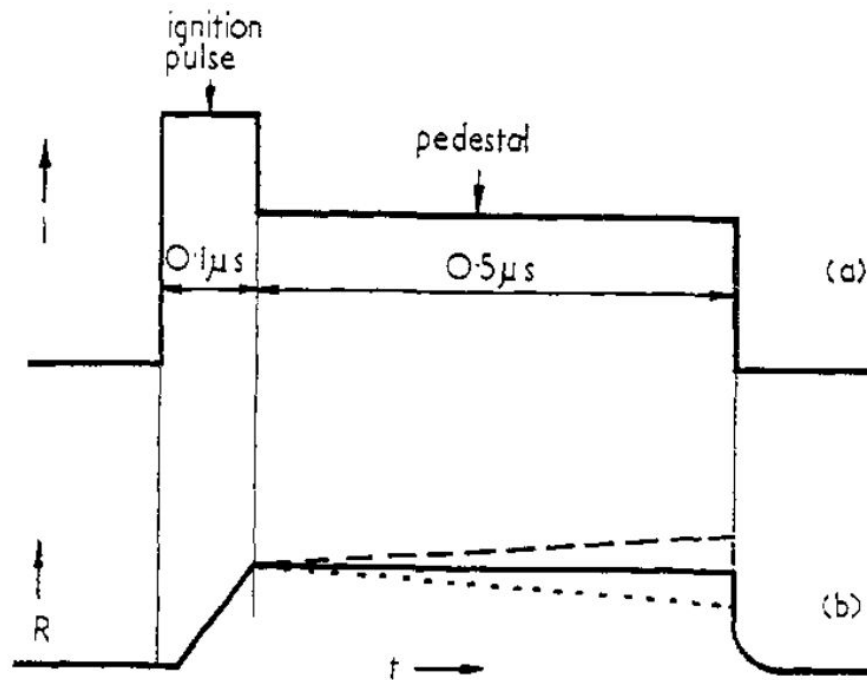
Calotron: Broom and Rhoderick 1960 Br.J.Appl.Phys II 292

Thermal propagation of a normal region in a thin superconducting film and its application to a new type of bistable element

- Dual device to a DIAC

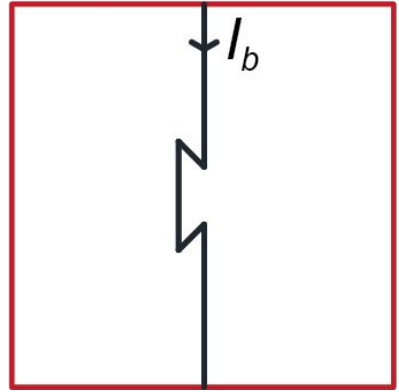
by R. F. BROOM, B.Sc., and E. H. RHODERICK, M.A., Ph.D., Services Electronics Research Laboratory, Baldock, Hertfordshire

[Paper first received 12 January, and in final form 13 February, 1960]



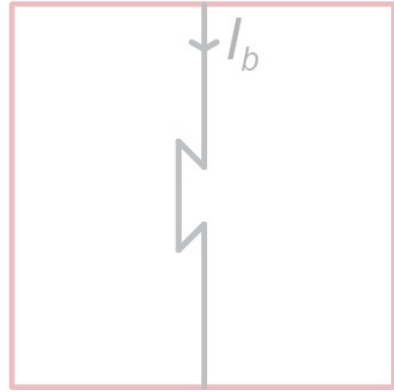
Bestiary of Nanowire Devices

constriction

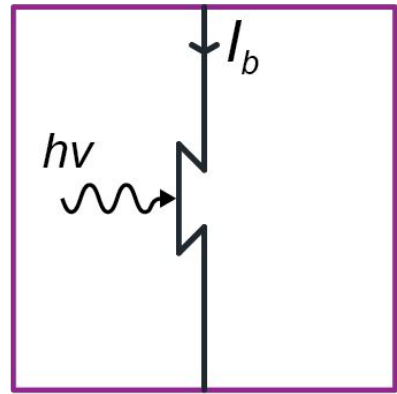


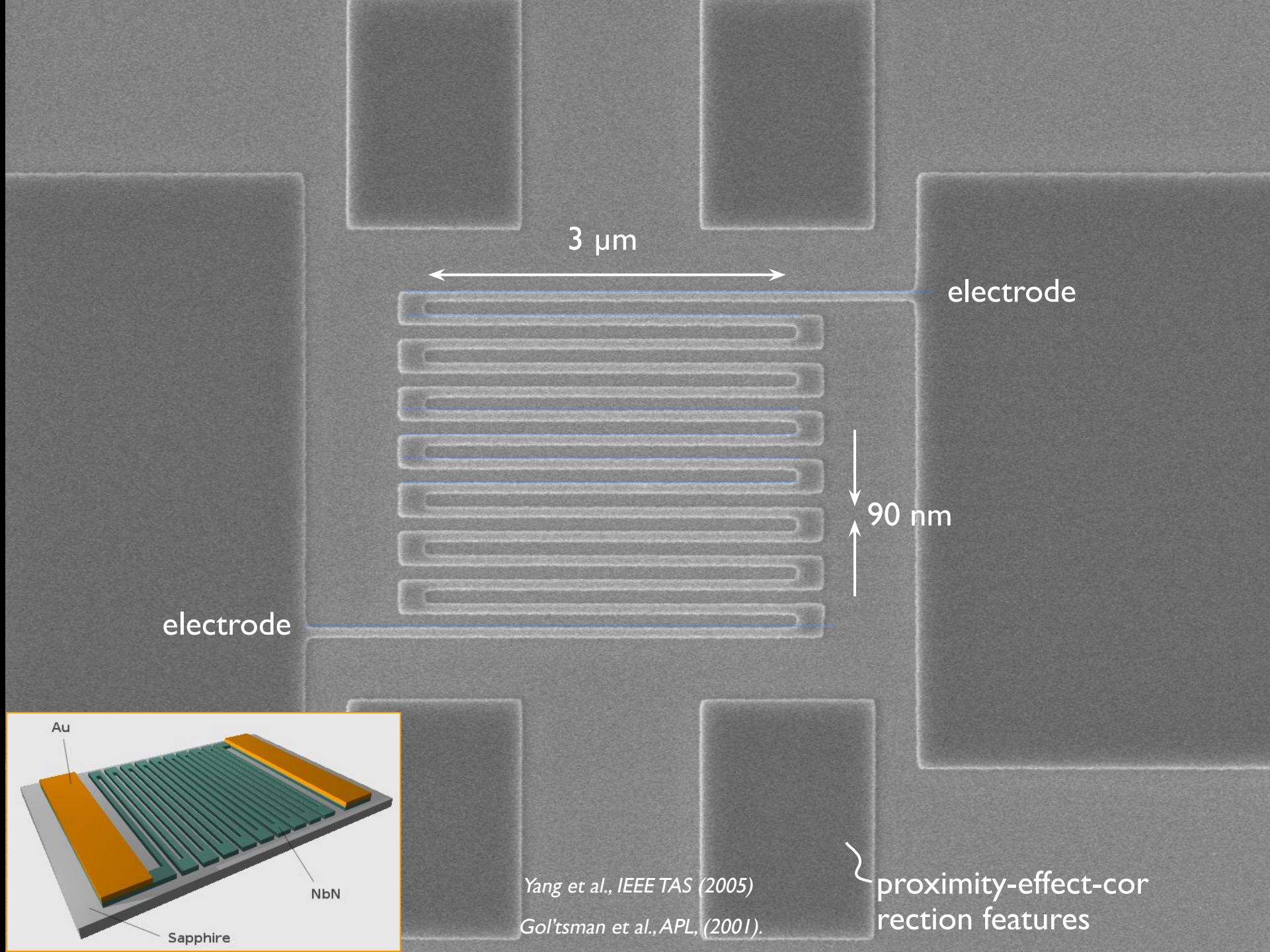
Bestiary of Nanowire Devices

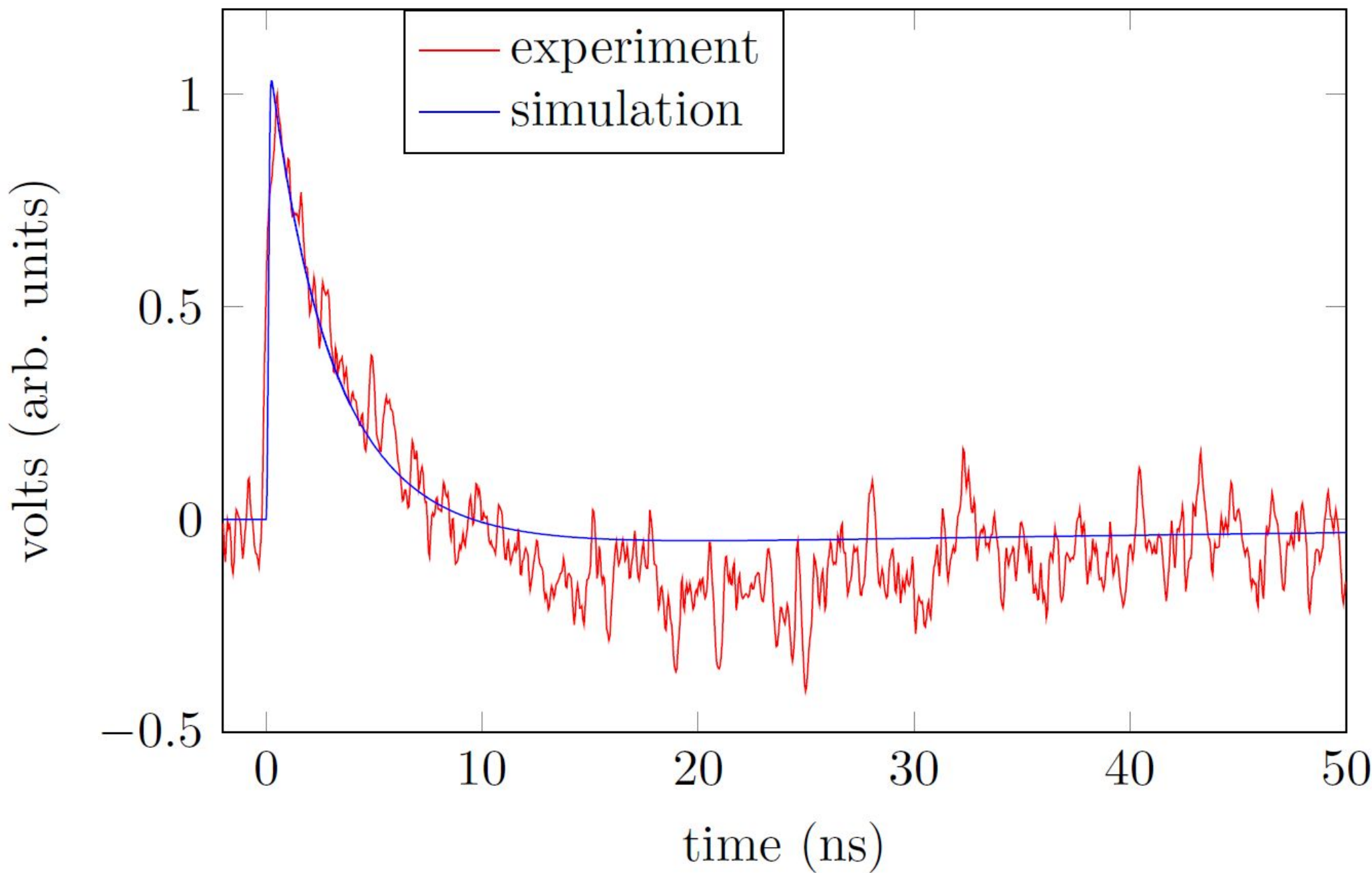
constriction



SNSPD





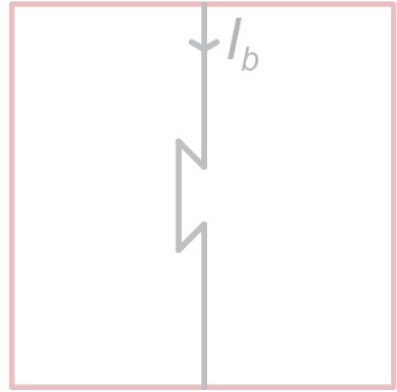


What SNSPDs tell us about Nanowire Logic

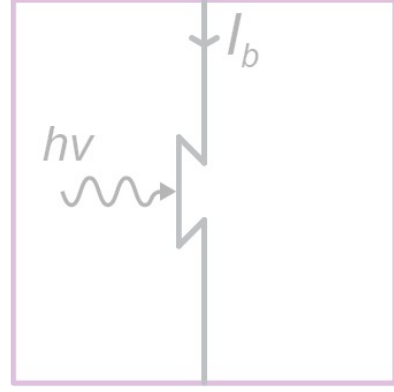
- Infrared efficiency for single photons up to 10 μm : single photon sensitivity \Rightarrow Narrow grey zone [Verma et al., APL Photonics, 2021]
- Jitter $\approx 3 \text{ ps}$ [Korzh et. al. 2020]
- Reset time runs into thermal limits at $\approx 1.5 \text{ ns}$
 - Suggestions in MgB₂ it can be as low as 150 ps [Cherednichenko et al. SUST 2021]
- Dark-count rate (~ 1 per day) : consistent with cosmic rays [Chiles and Charaev, unpublished result]
- Convenient fabrication, shielding, amplification, temperature

Bestiary of Nanowire Devices

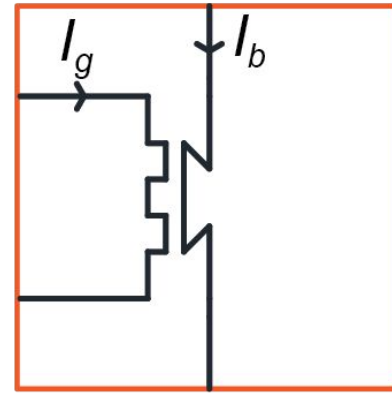
constriction



SNSPD

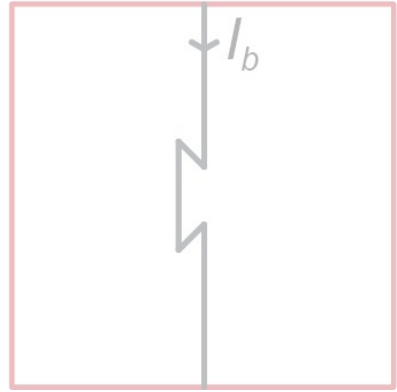


hTron

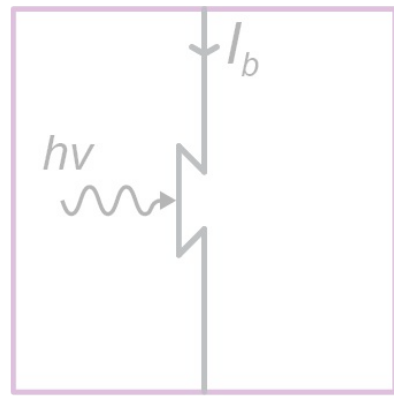


Bestiary of Nanowire Devices

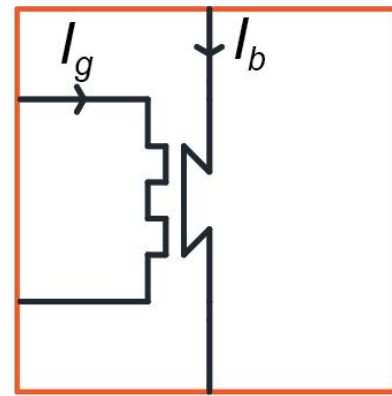
constriction



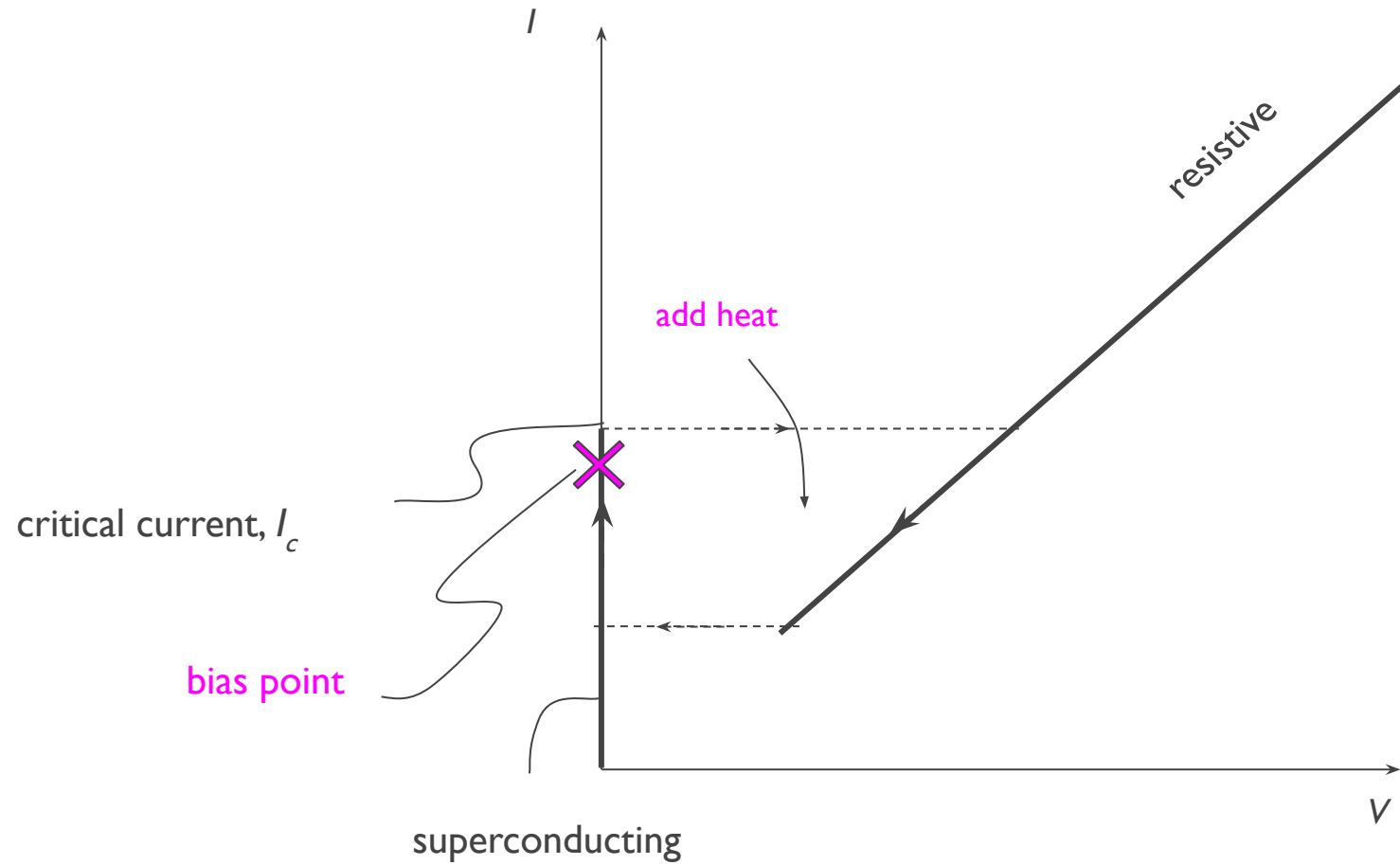
SNSPD



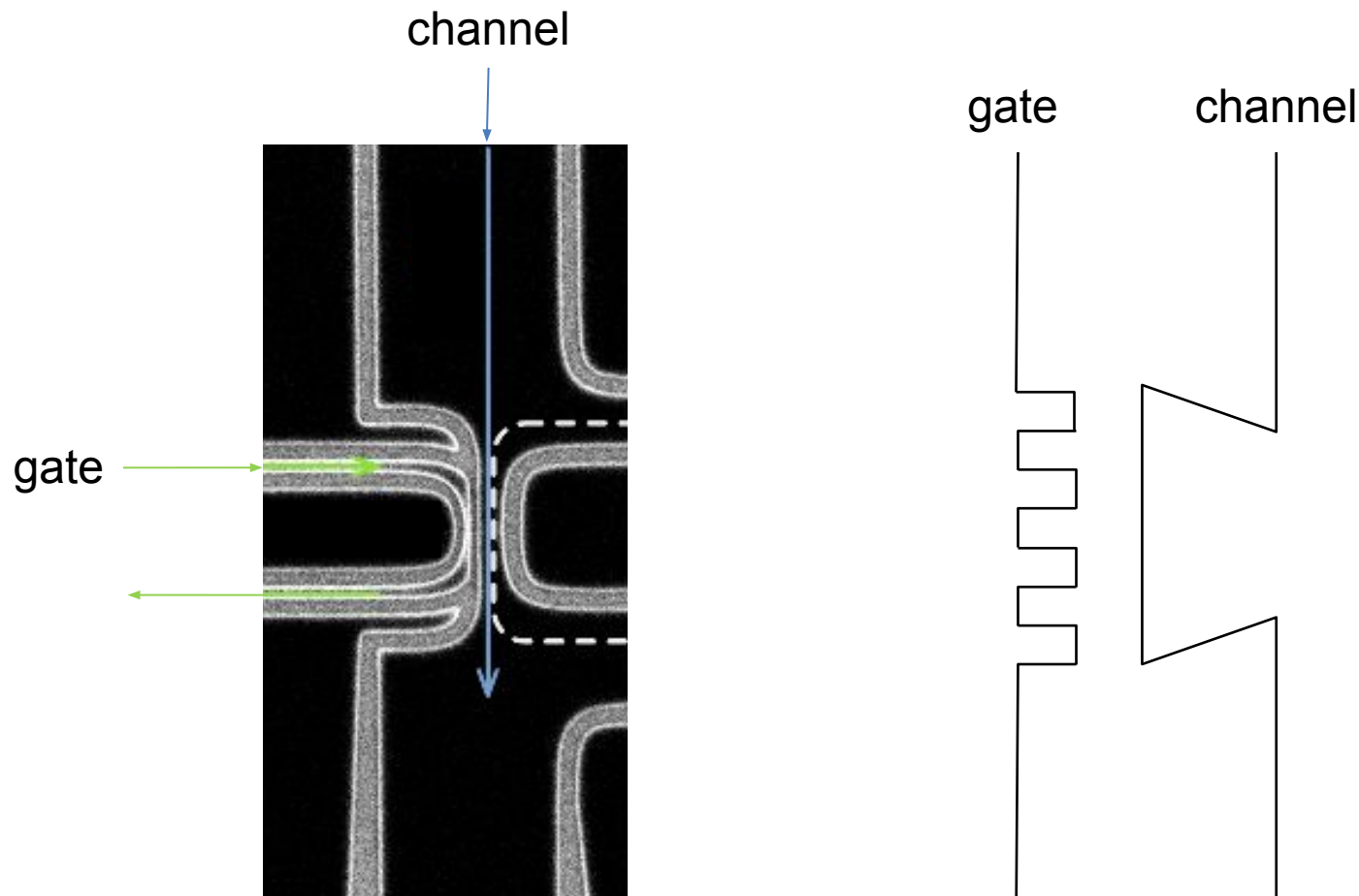
hTron



Thermo-Electric Switch

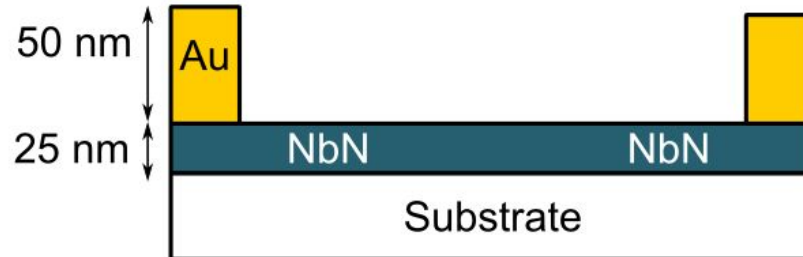


Thermal Cryotron: heater (h)Tron

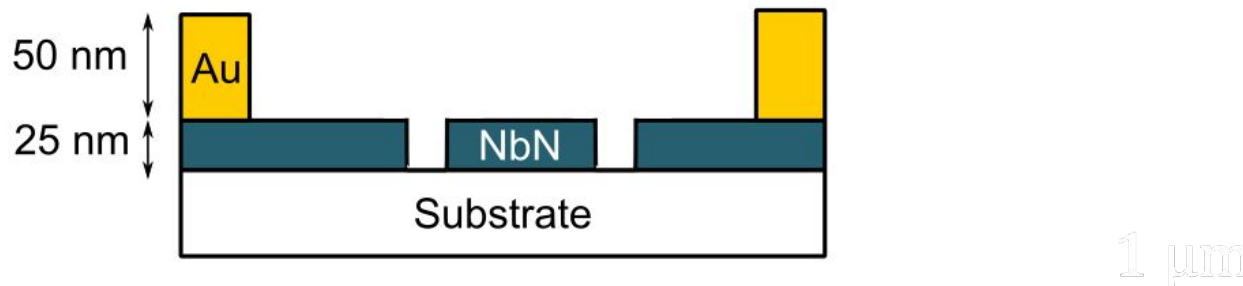


Fabrication process for making multilayer hTron devices

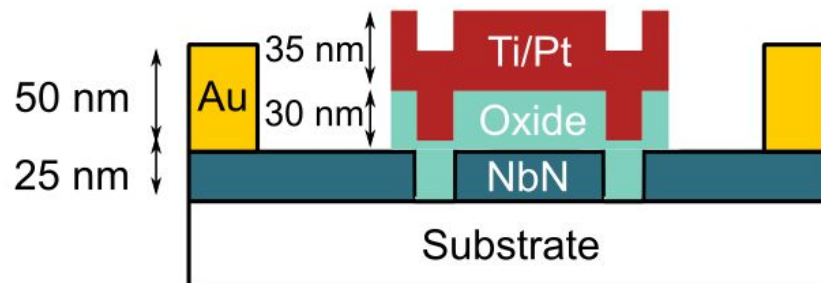
- 1 Define Au marks (lift-off).



- 2 Define the nanowire on NbN film (RIE).



- 3 Define the heater on top of the nanowire (lift-off).

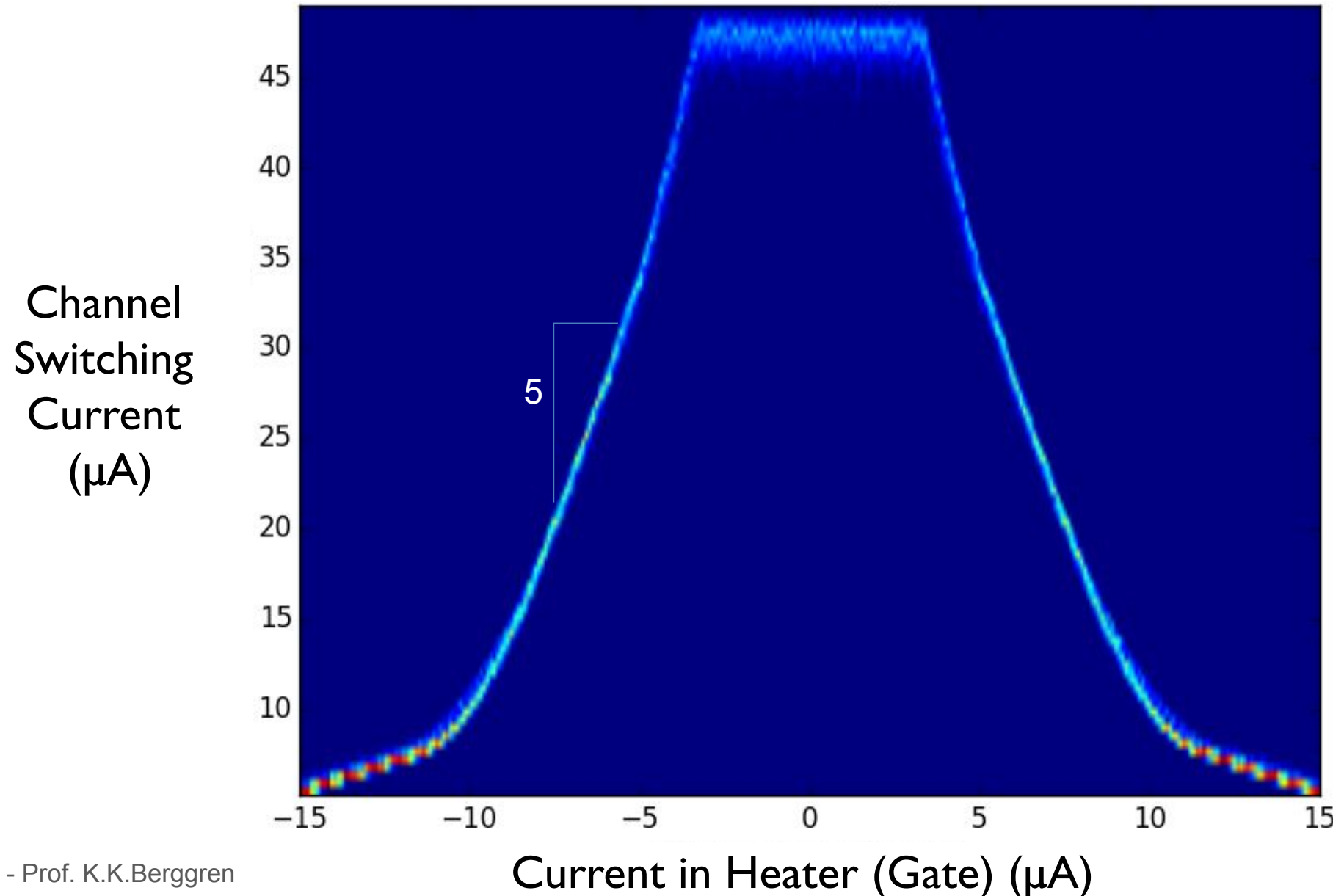


"Multilayered Heater Nanocryotron: A Superconducting-Nanowire-Based Thermal Switch" Phys. Rev. Applied 14, 054011 – Published 6 November 2020

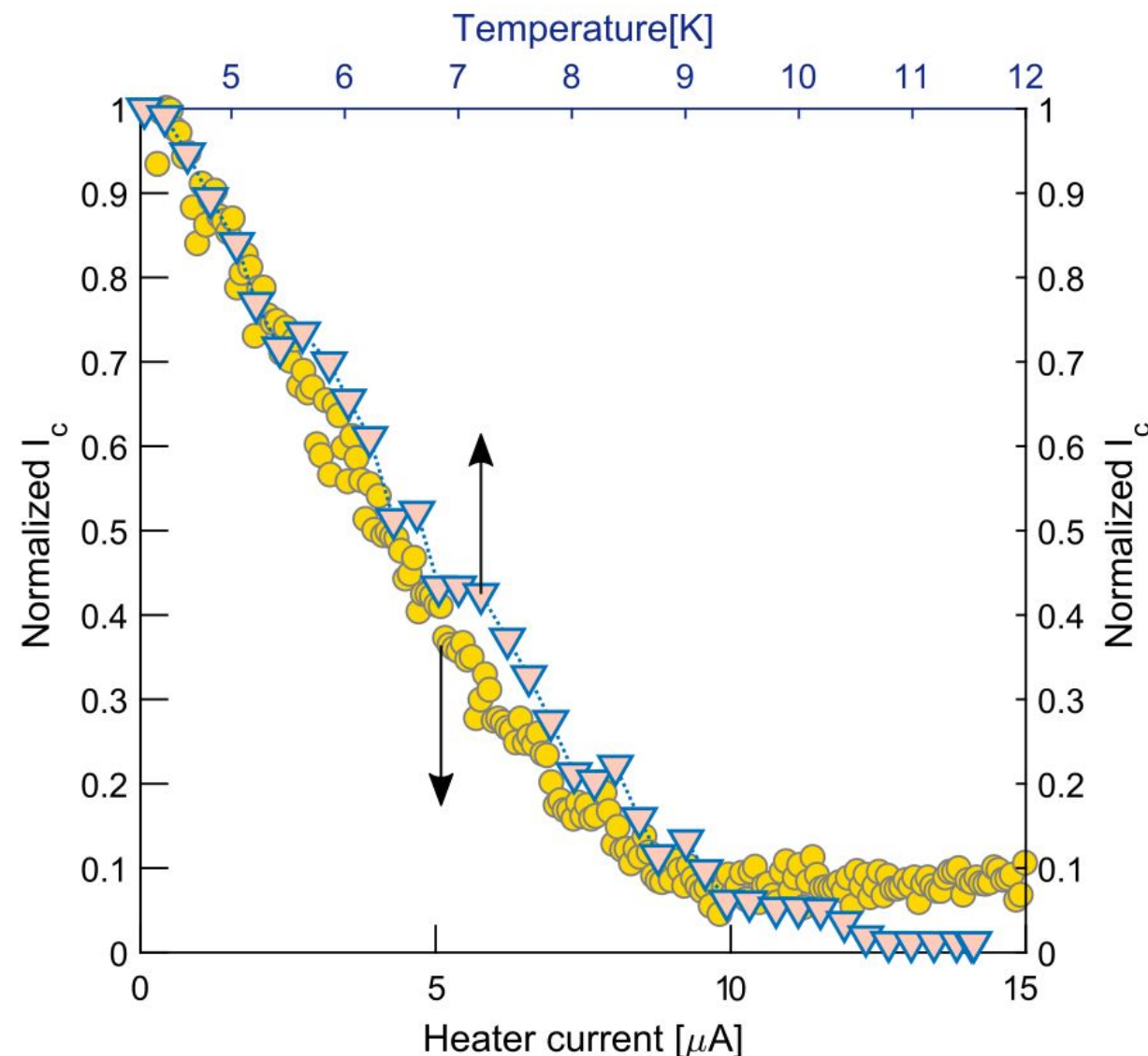


Reza Baghdadi

hTron Switching Characteristics

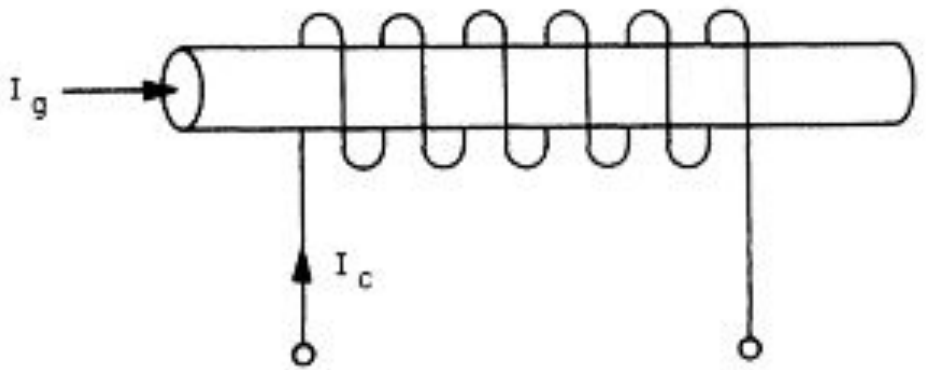


Operation of an hTron: Translate Joule heating to temperature



The cryotron: magnetic suppression

- 1956, Dudley Buck at MIT
- Gate induces magnetic field
 - Suppresses channel I_c



Buck, D. (1956). The Cryotron - A Superconductive Computer Component. *Proceedings of the IRE*, 44(4), 482–493. doi:10.1109/JRPROC.1956.274



“A cryotron multi-level logic and memory circuit”

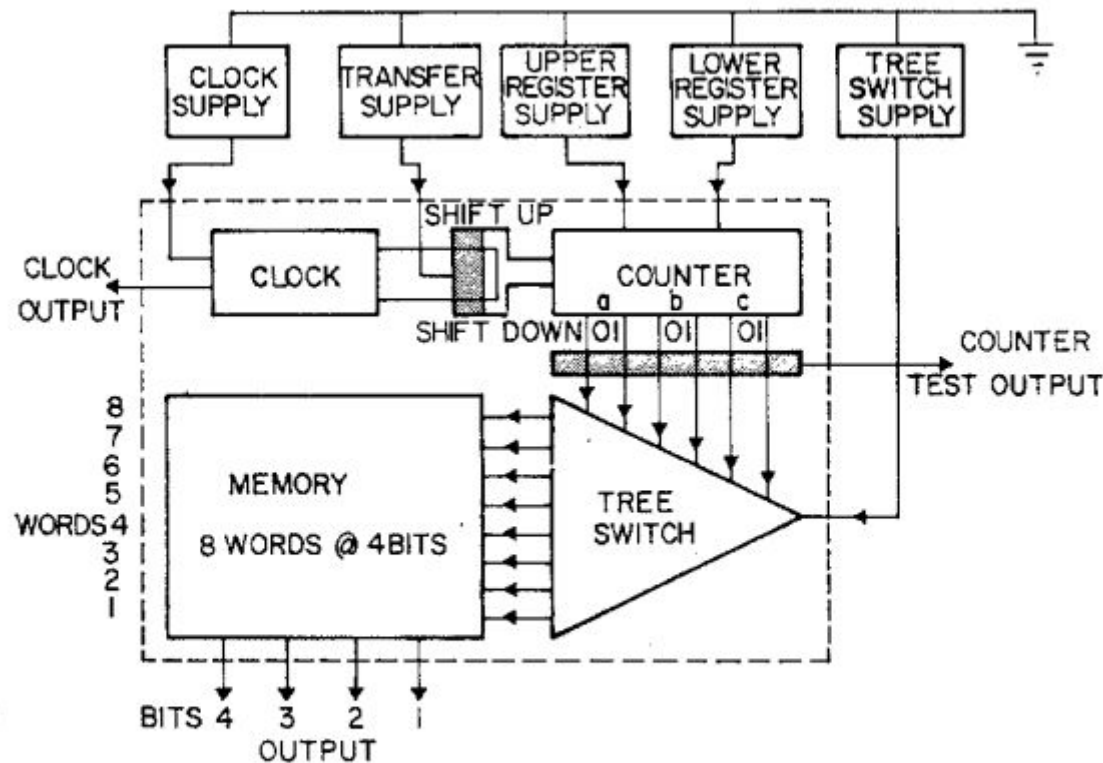


FIGURE 1—Block diagram of cryotron logic and memory circuit.

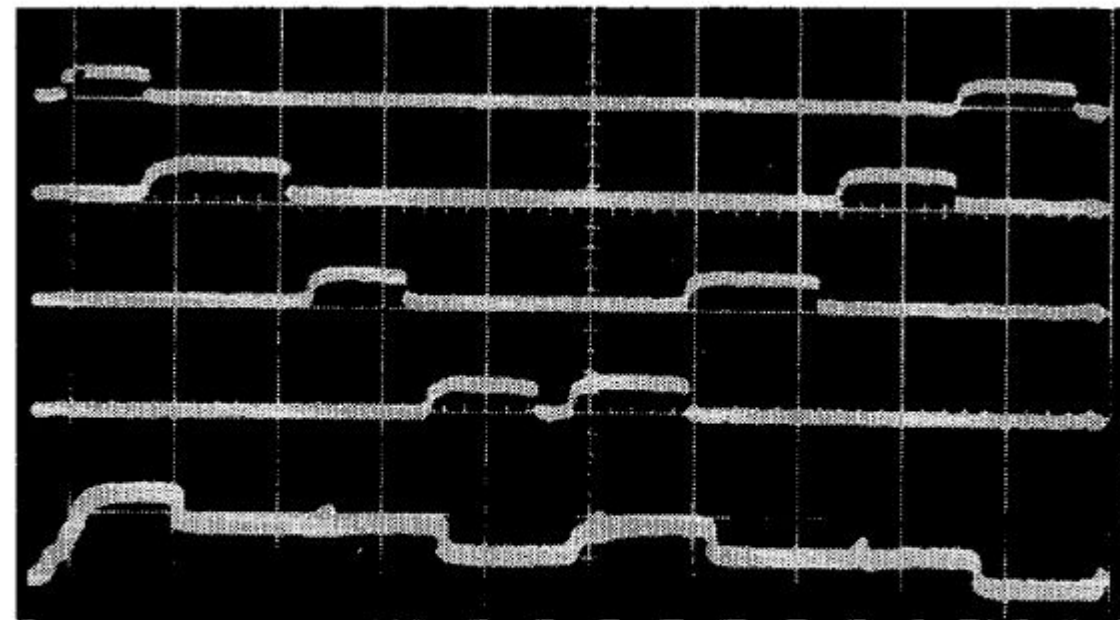
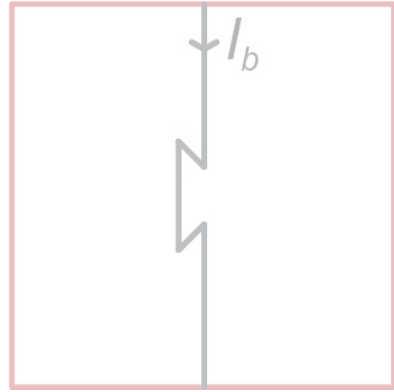


FIGURE 3—Output waveforms at 200 kc; 5 μ sec word time. Top to bottom: bit 1, bit 2, bit 3, bit 4, and counter test output. Vertical scale: 0.5 mv/em.

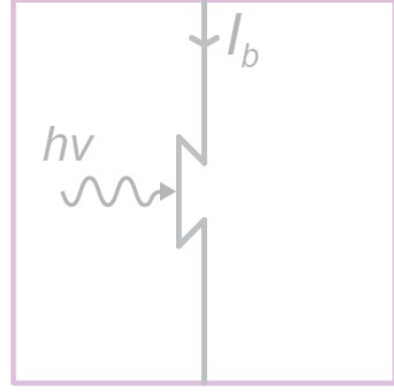
M. Cohen, A. Slade and R. Varteresian, "A cryotron multi-level logic and memory circuit," 1964 IEEE International Solid-State Circuits Conference. Digest of Technical Papers, Philadelphia, PA, USA, 1964, pp. 102-103, doi: 10.1109/ISSCC.1964.1157547.

Bestiary of Nanowire Devices

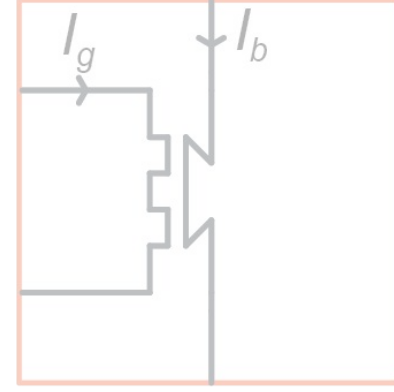
constriction



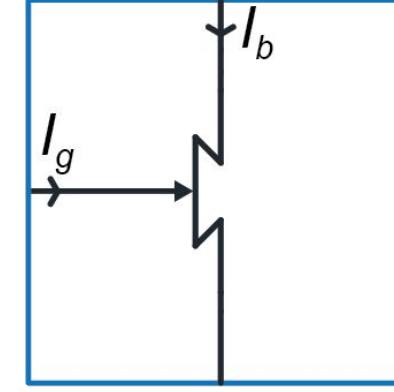
SNSPD

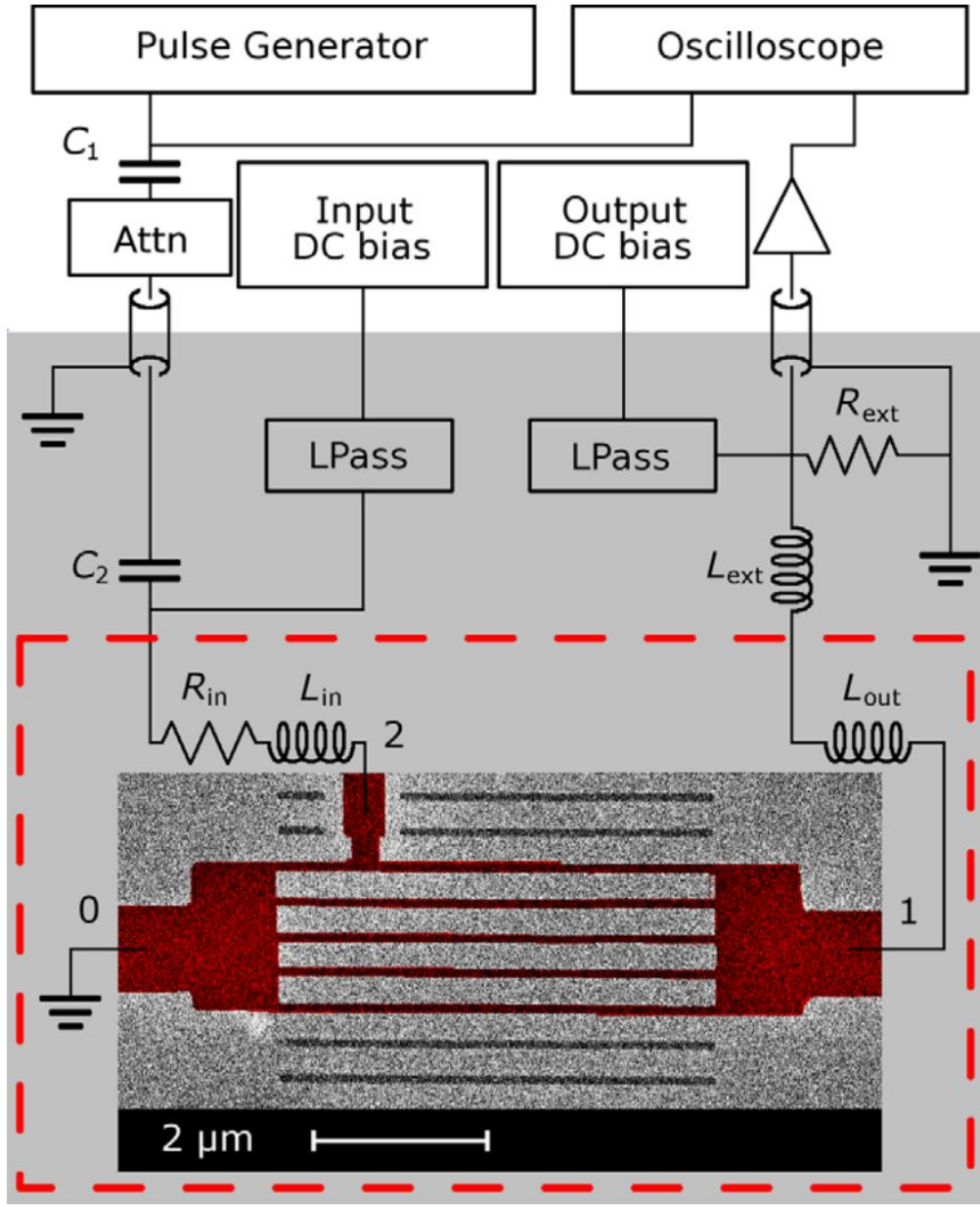


hTron



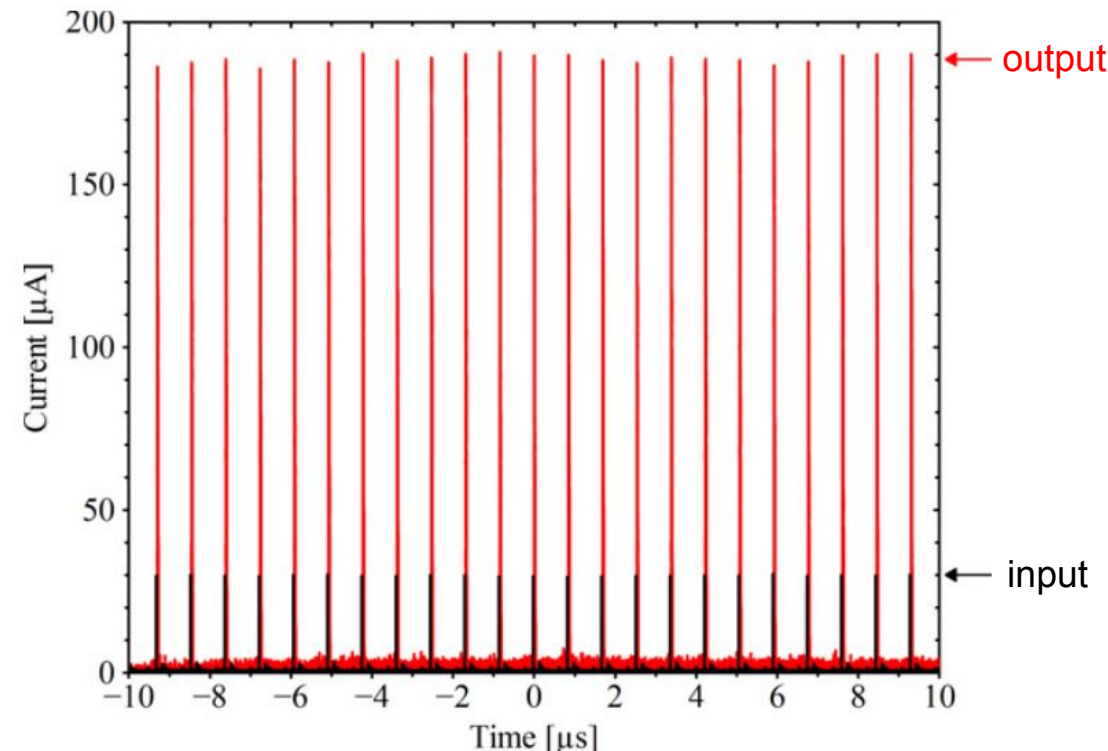
nTron





Pulse Discriminator for SNSPD Readout

M Ejrnaes et al 2011 *Supercond. Sci. Technol.* 24 035018

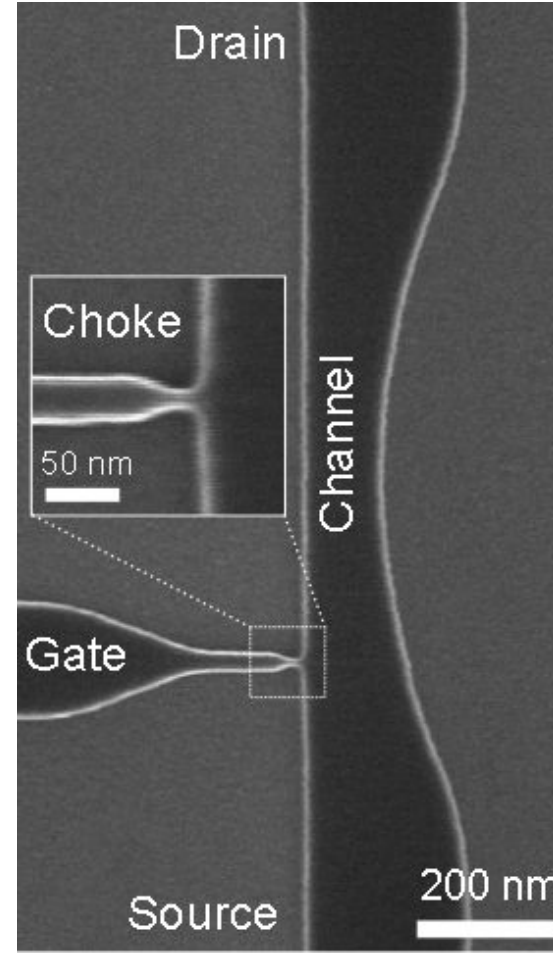
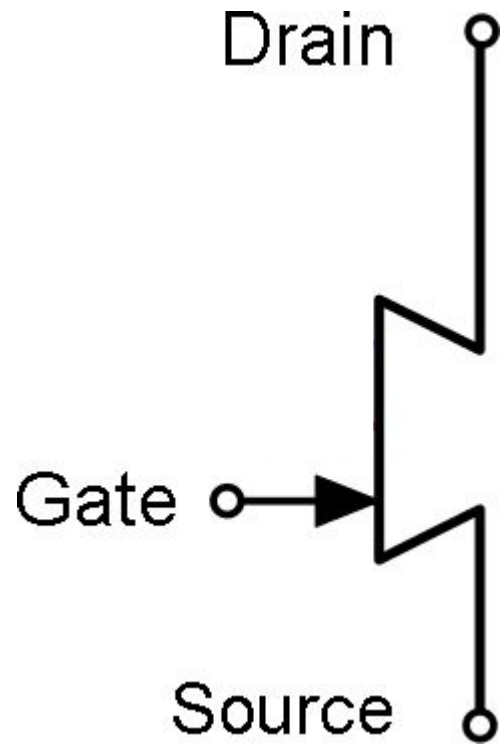


O. Qaranta



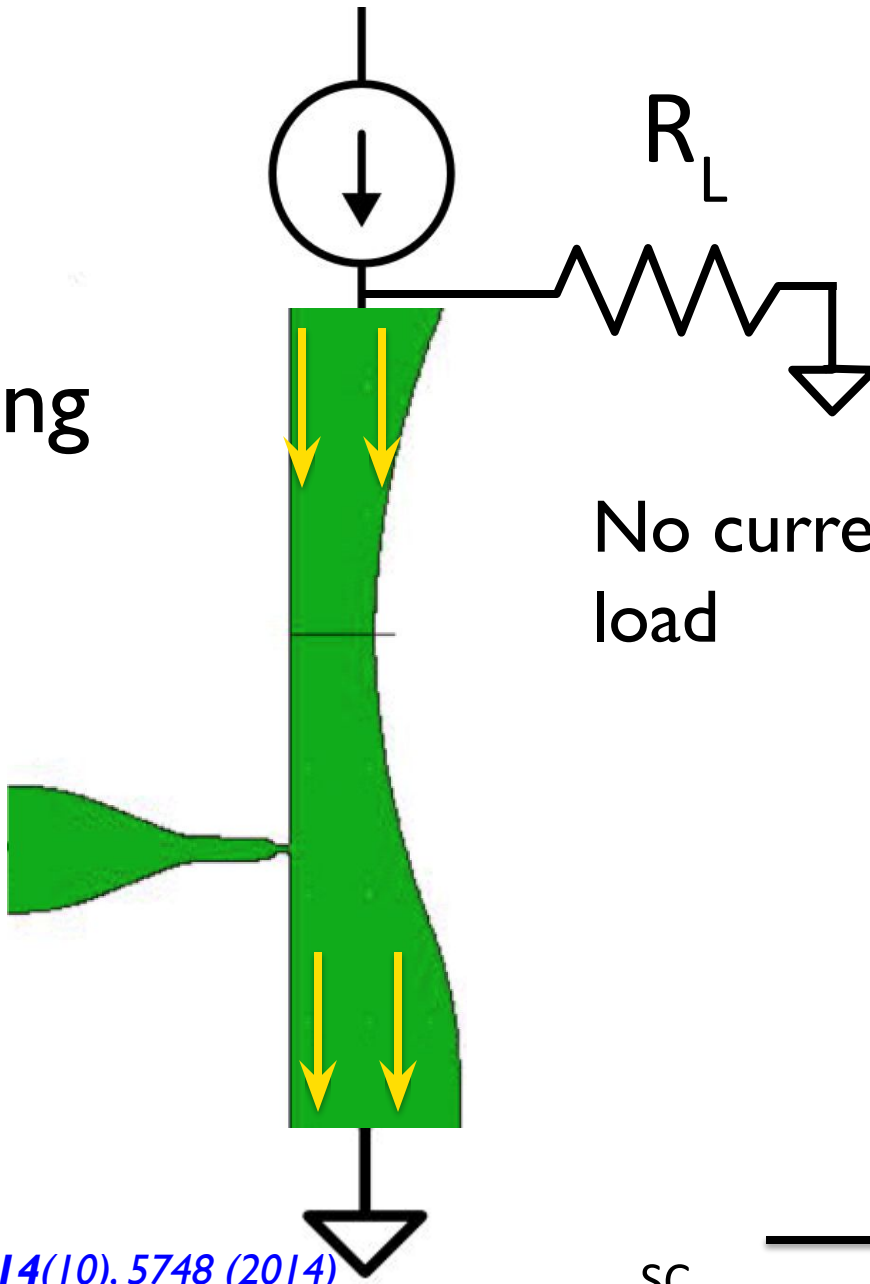
M. Ejrnaes

nTron geometry

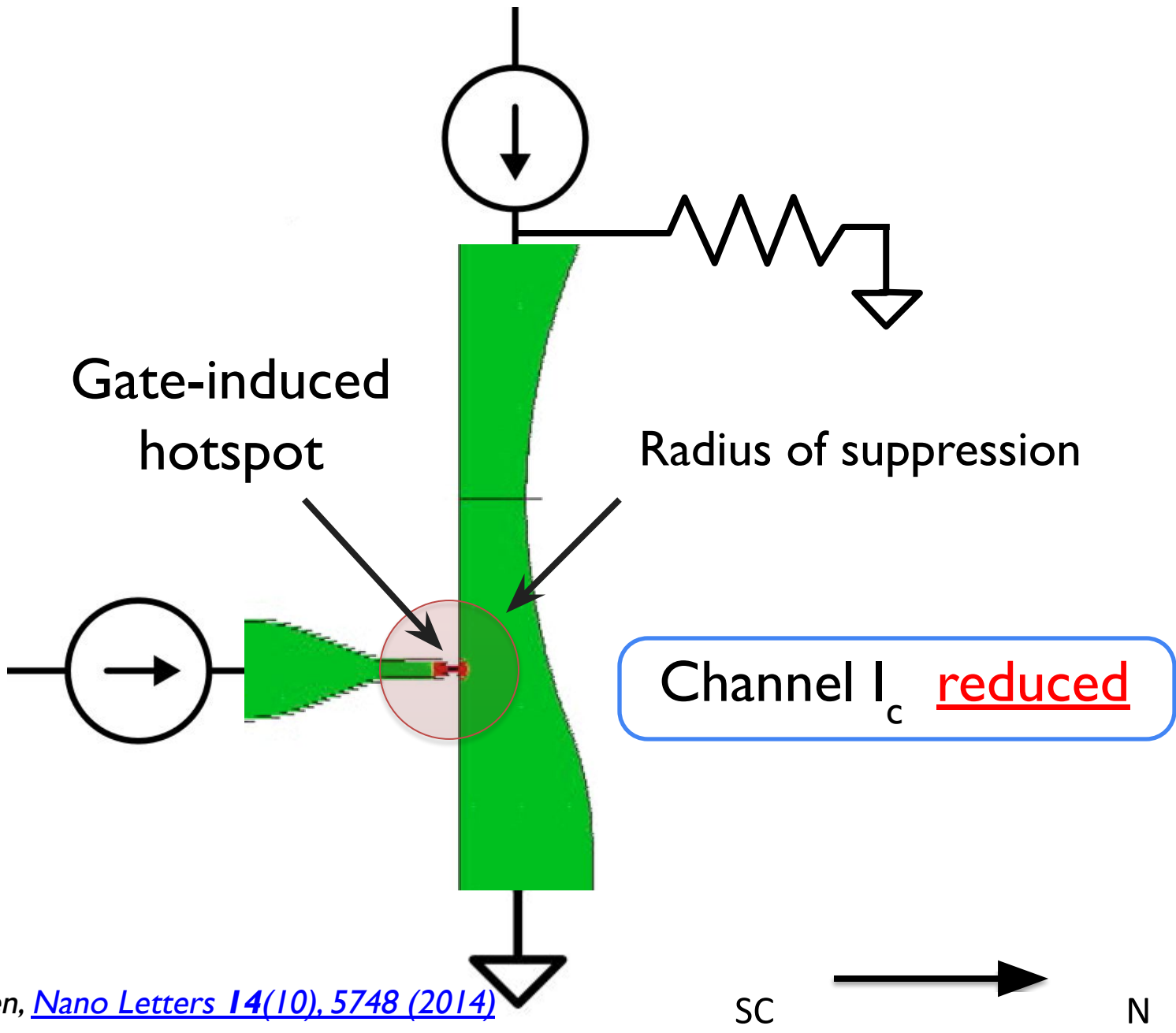


A. N. McCaughan and K. K. Berggren, [Nano Letters 14\(10\), 5748 \(2014\)](#)

Device fully
superconducting

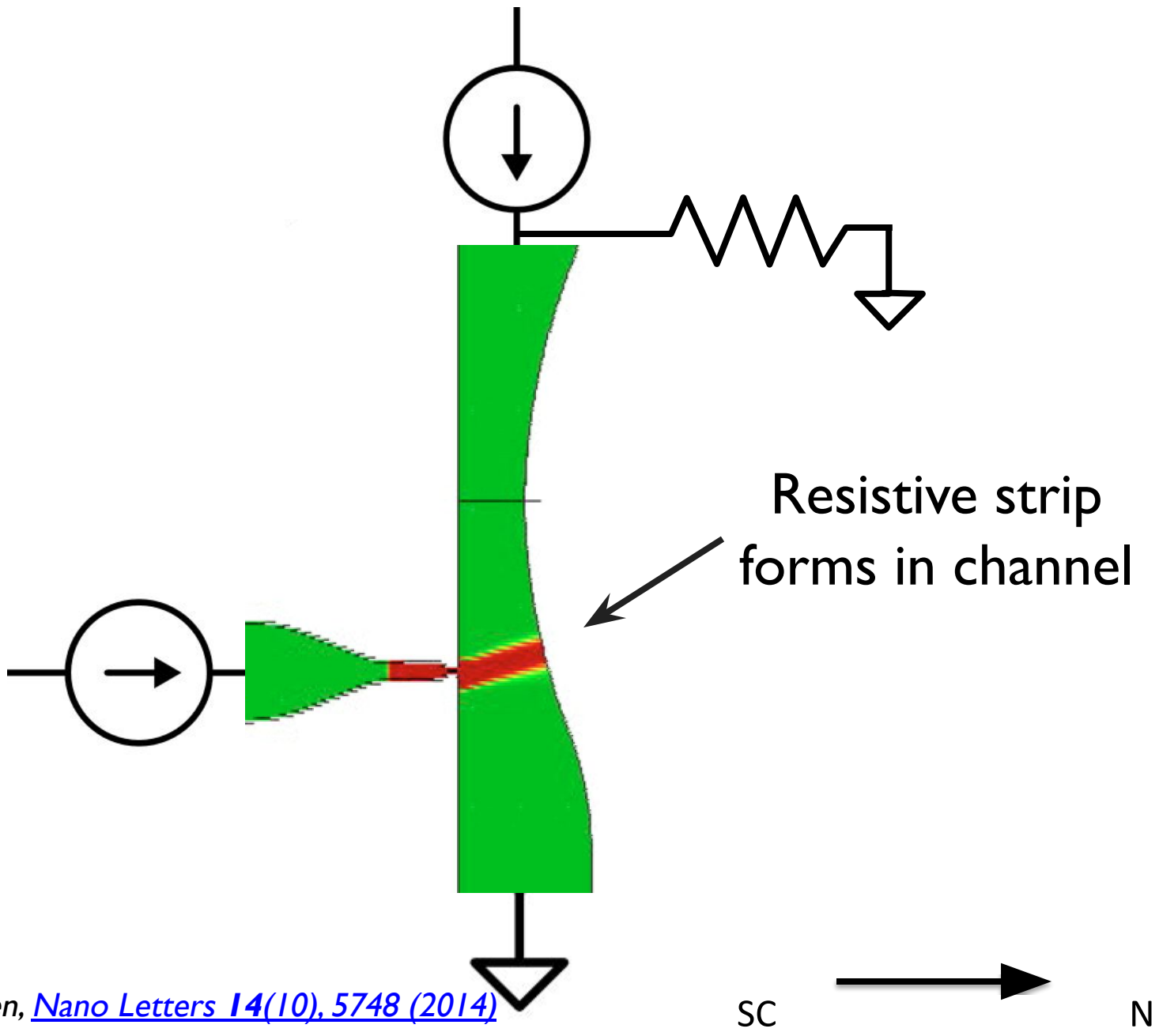


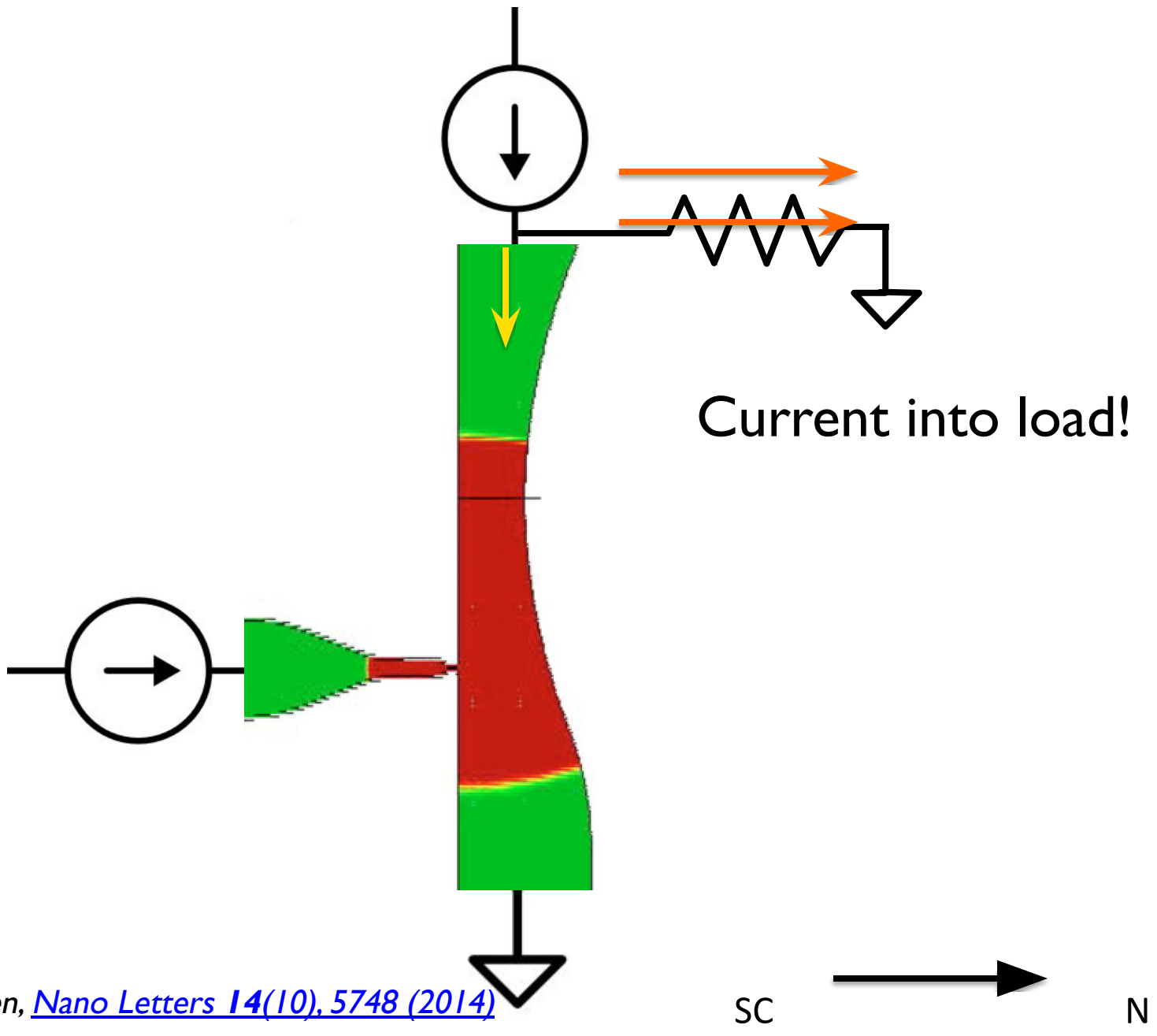
No current to
load



A. N. McCaughan and K. K. Berggren, [Nano Letters 14\(10\), 5748 \(2014\)](#)

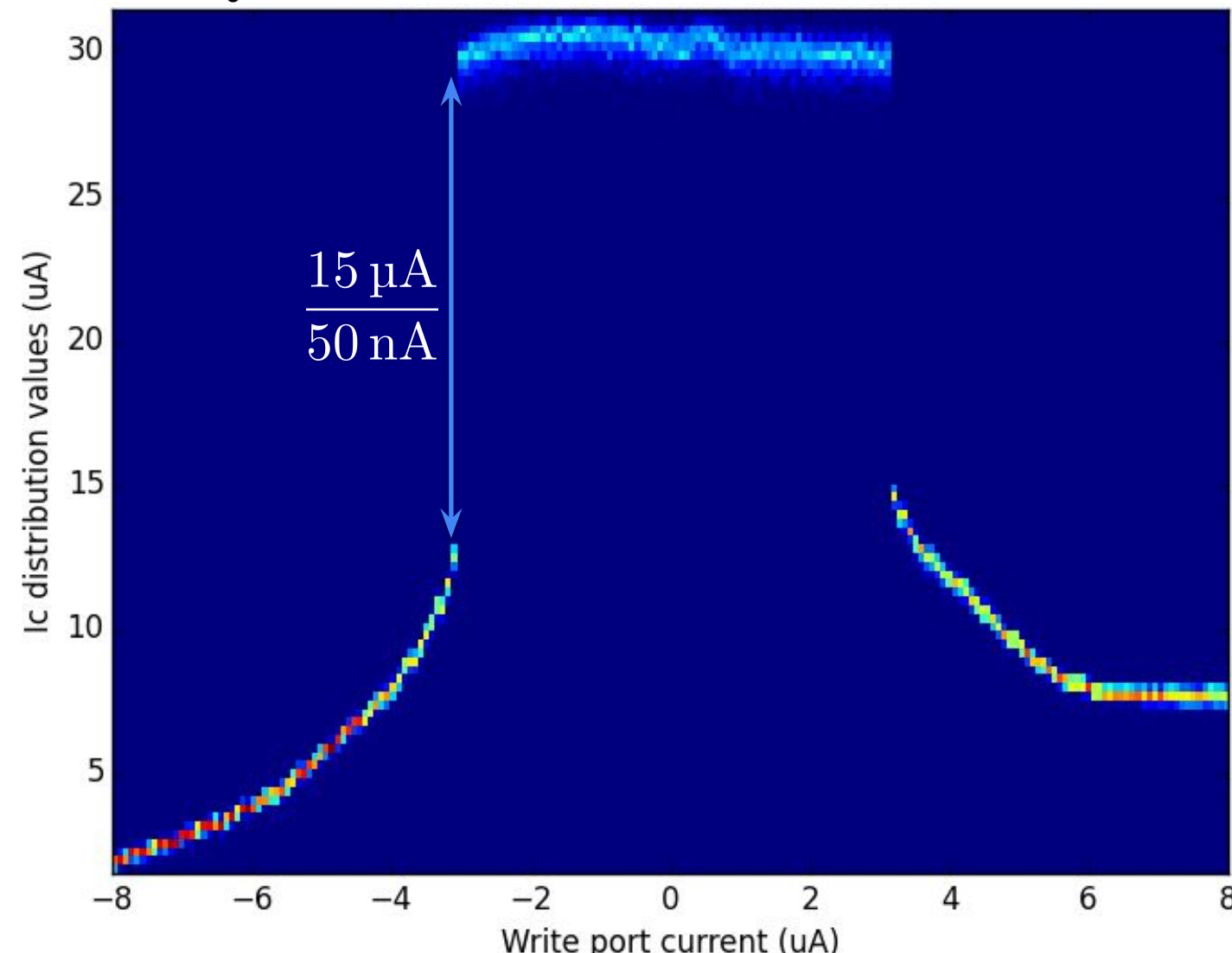
11/30/22 - Prof. K.K.Berggren



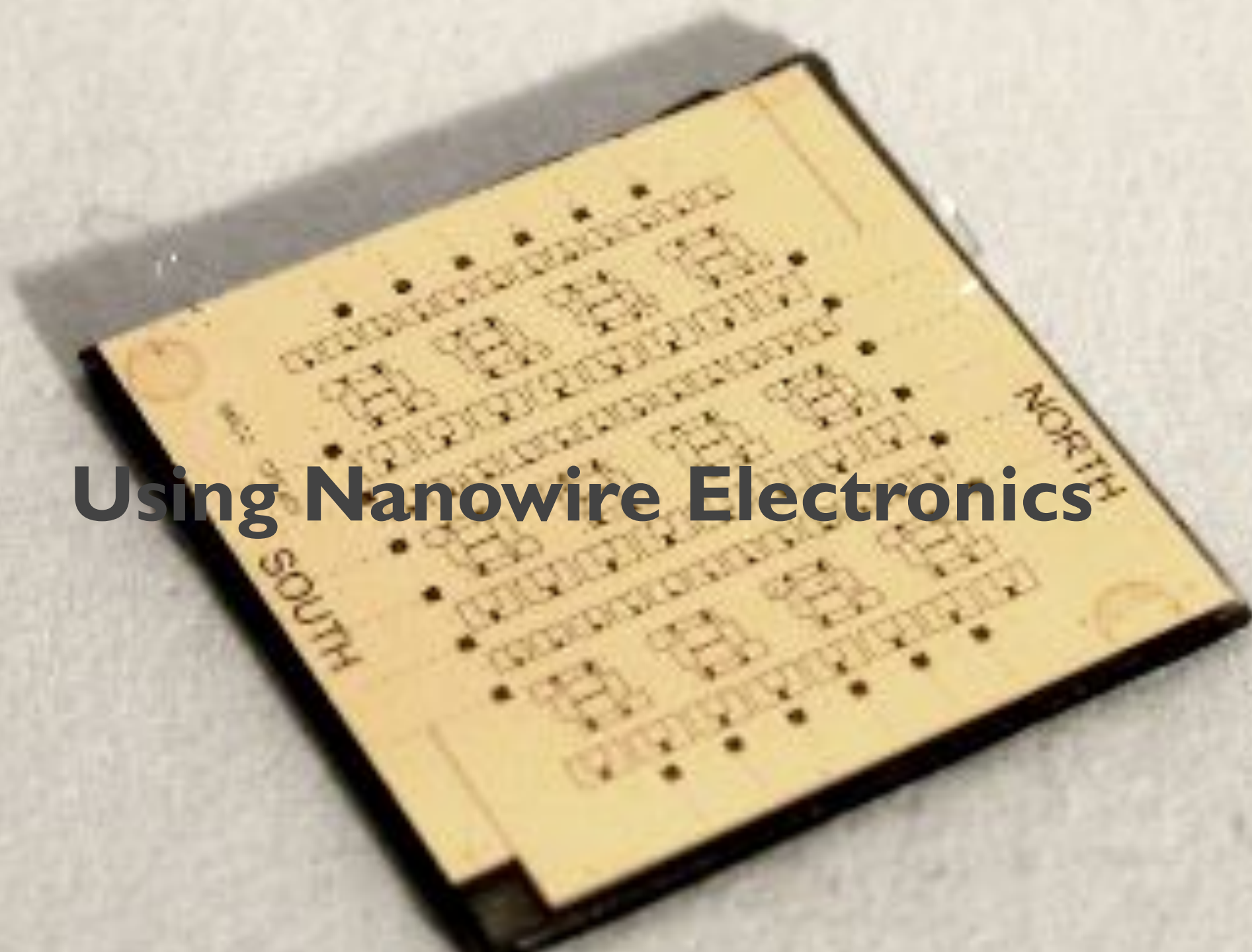


nanowire Cryotron Characteristics

Channel switching current I_c vs gate input current (write port current) for nTron reference device



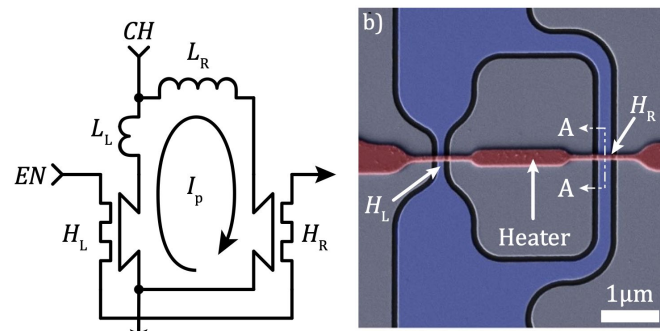
Using Nanowire Electronics



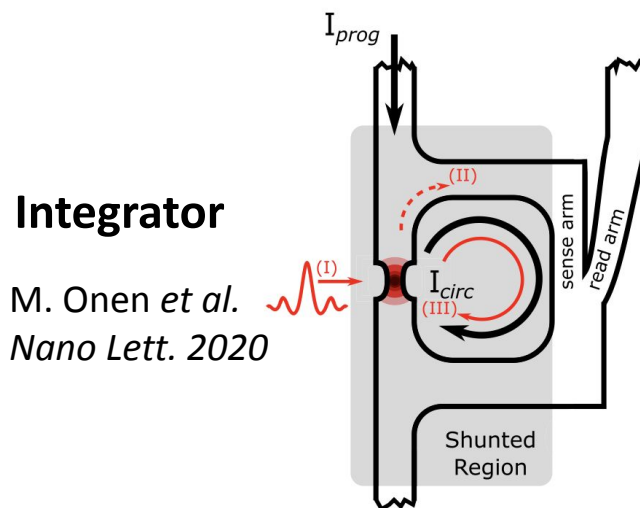
Logic Circuits

Superconducting nanowire electronics

Non-volatile memory

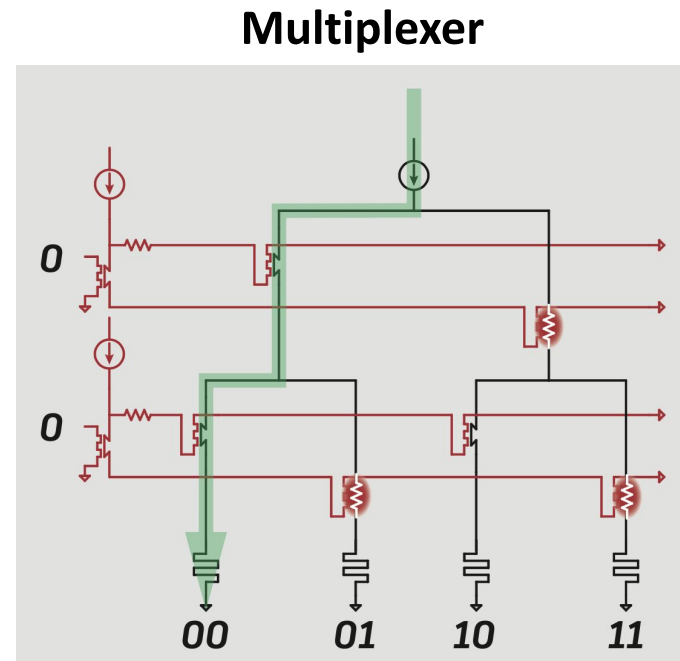


B. A. Butters *et al.* SUST 34 2021



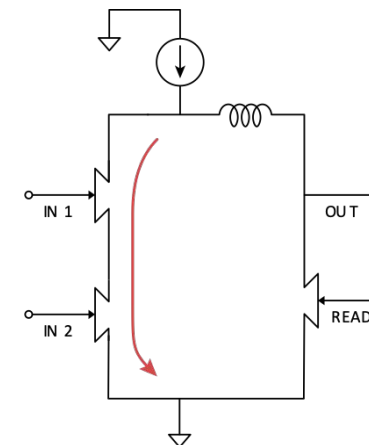
Integrator

M. Onen *et al.*
Nano Lett. 2020

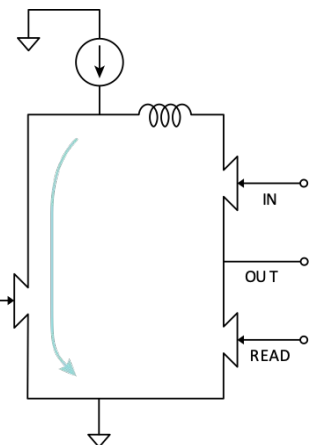


O. Medeiros *et al.* ASC 22
SNSPD: Physics, Measurement, Readout,
Applications

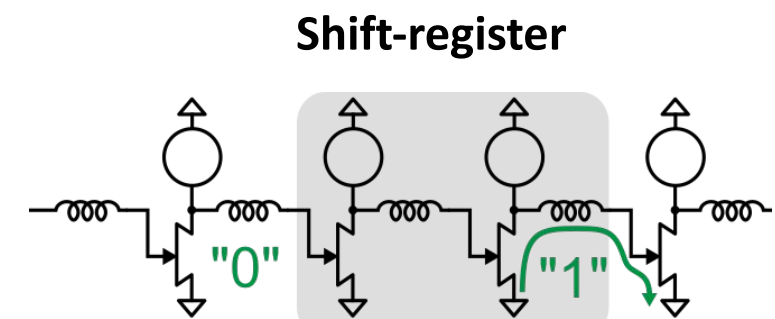
OR gate



NOT gate



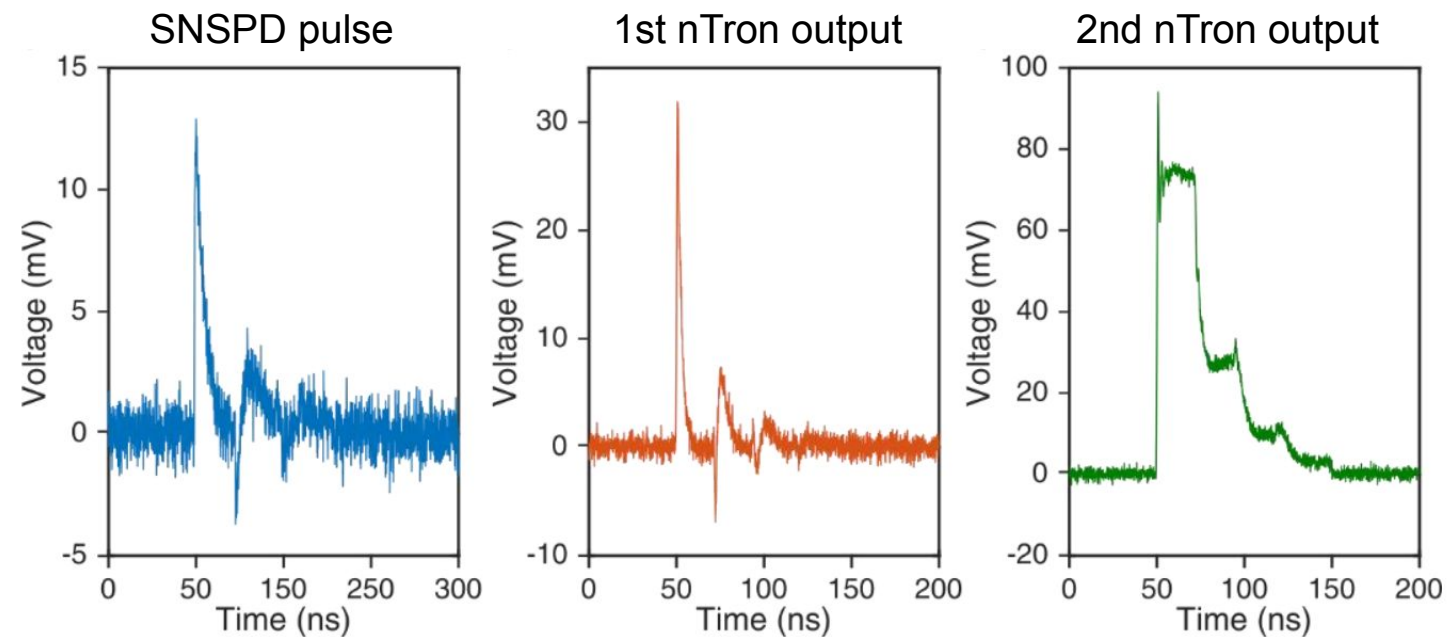
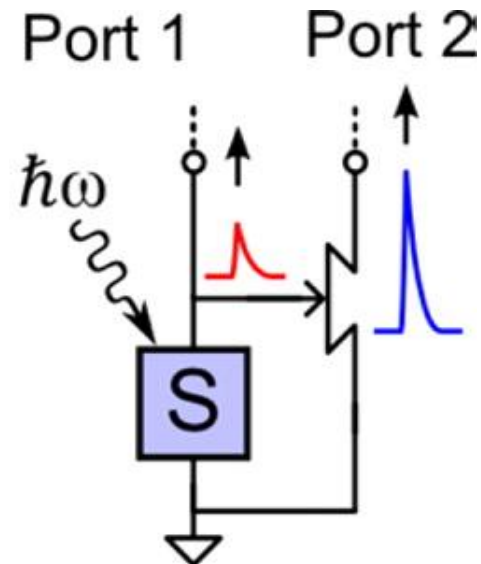
A. Buzzi *et al.* WOLTE 22



Shift-register

R. A. Foster *et al.* WOLTE 22

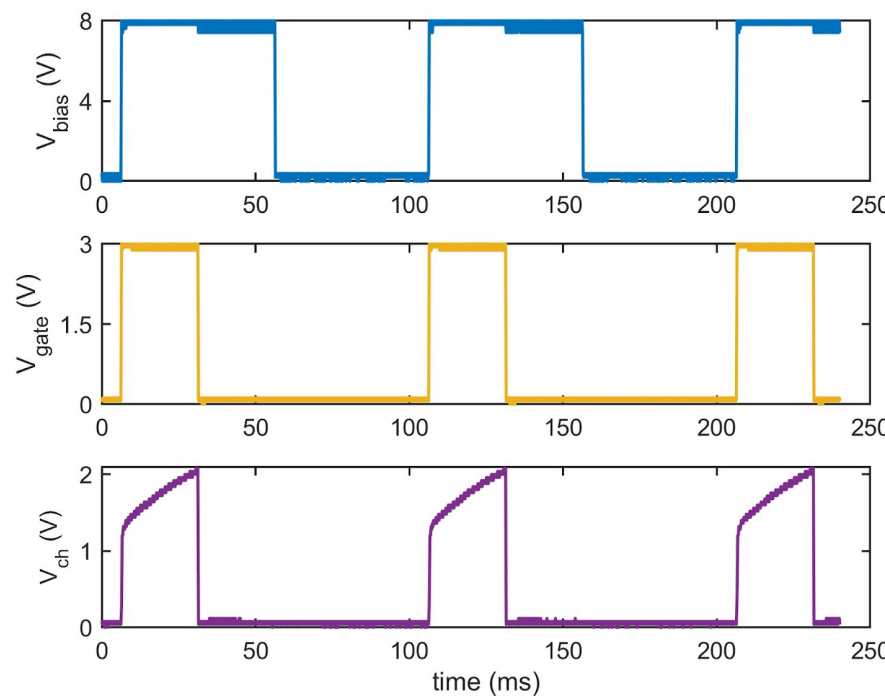
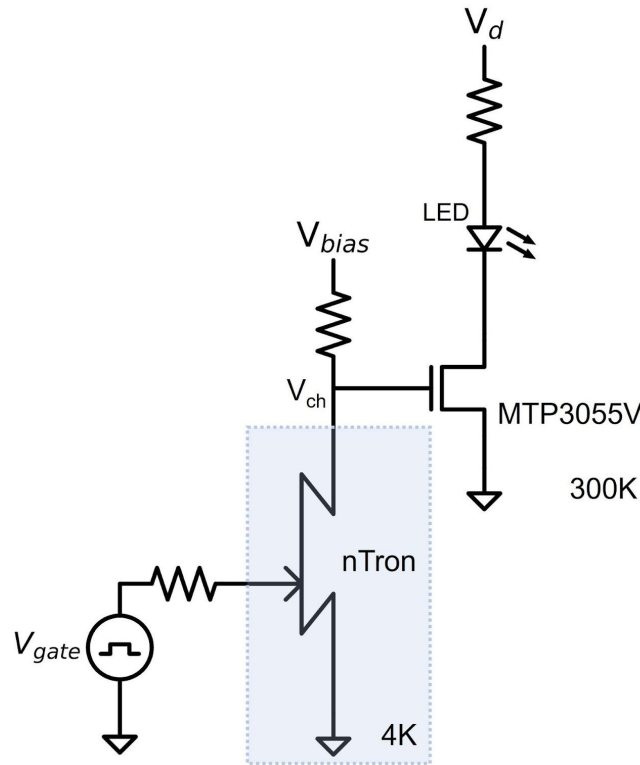
nTron Amplifier Example for SNSPDs



Zheng, K., Zhao, Q. Y., et al. "A Superconducting Binary Encoder with Multigate Nanowire Cryotrons." *Nano letters*, 20(5), (2020) 3553-3559. (Supporting Information)

Tron-CMOS interfacing demo

Driving room-temp MOSFET and LED with nTron

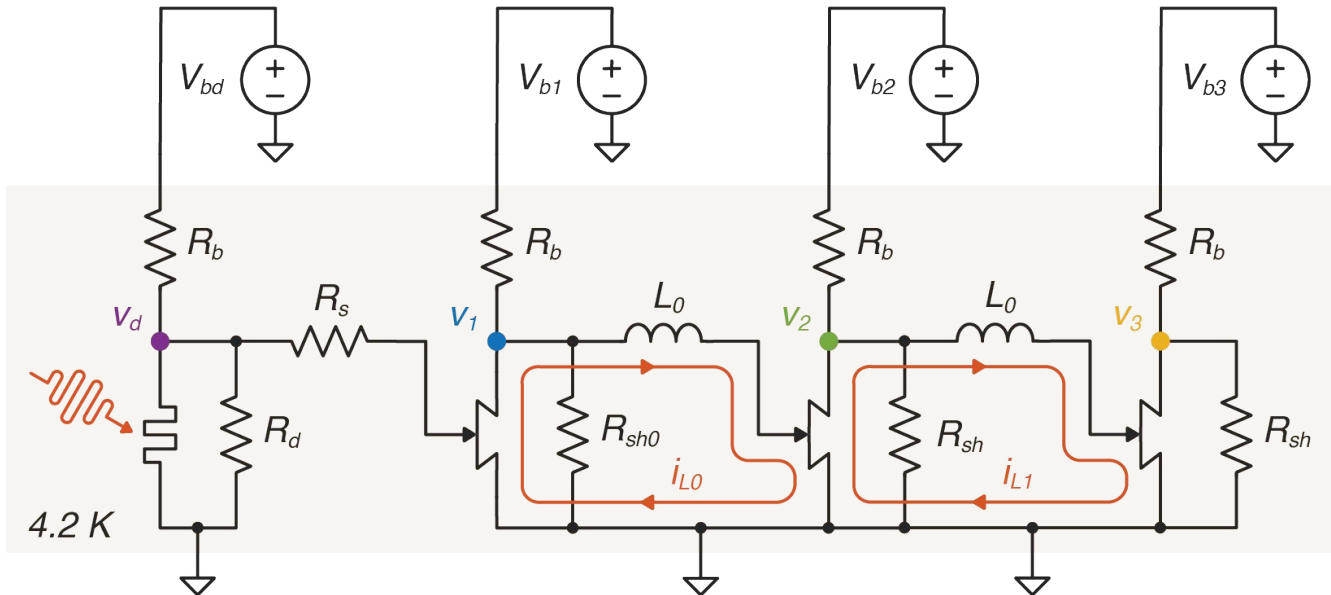


<https://www.youtube.com/shorts/fJycxwcOsO0>

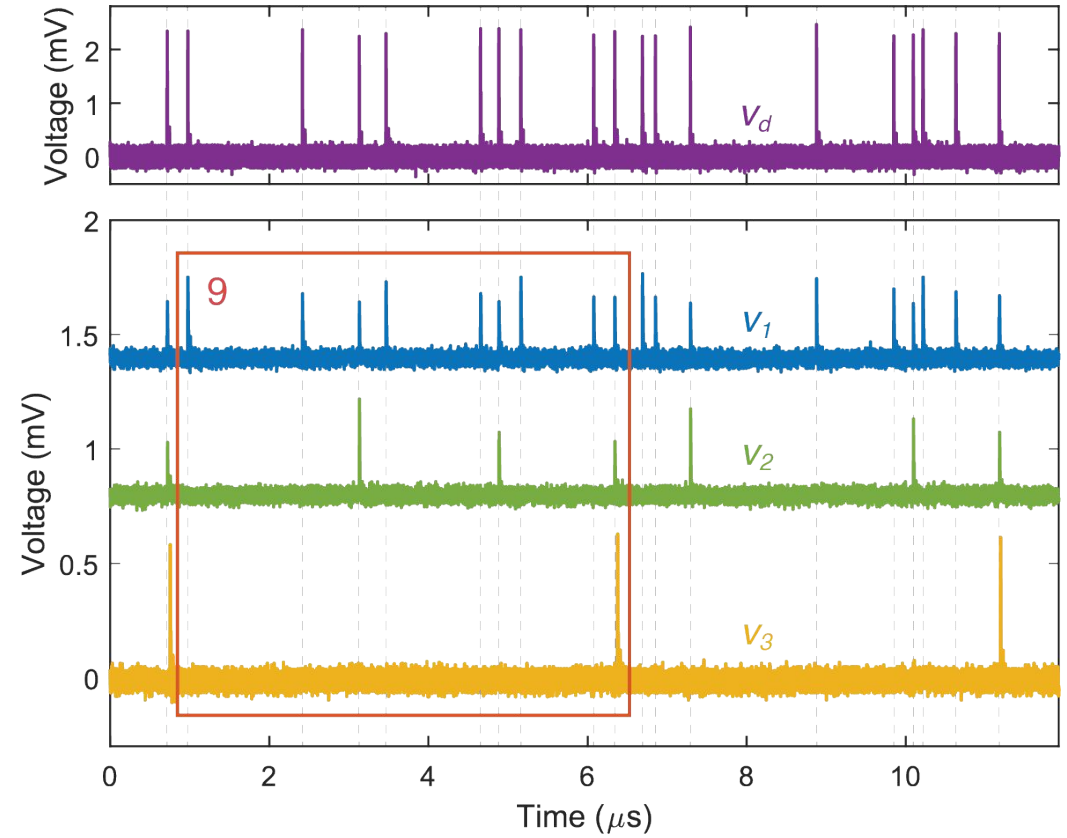
MOSFET is driven by the nTron gate pulse
FET $V_{th} = 2$ V. LED turns on, when $V_{ch} > V_{th}$

SNSPD + 2-digit counter

Tested at 1550 nm and 405 nm



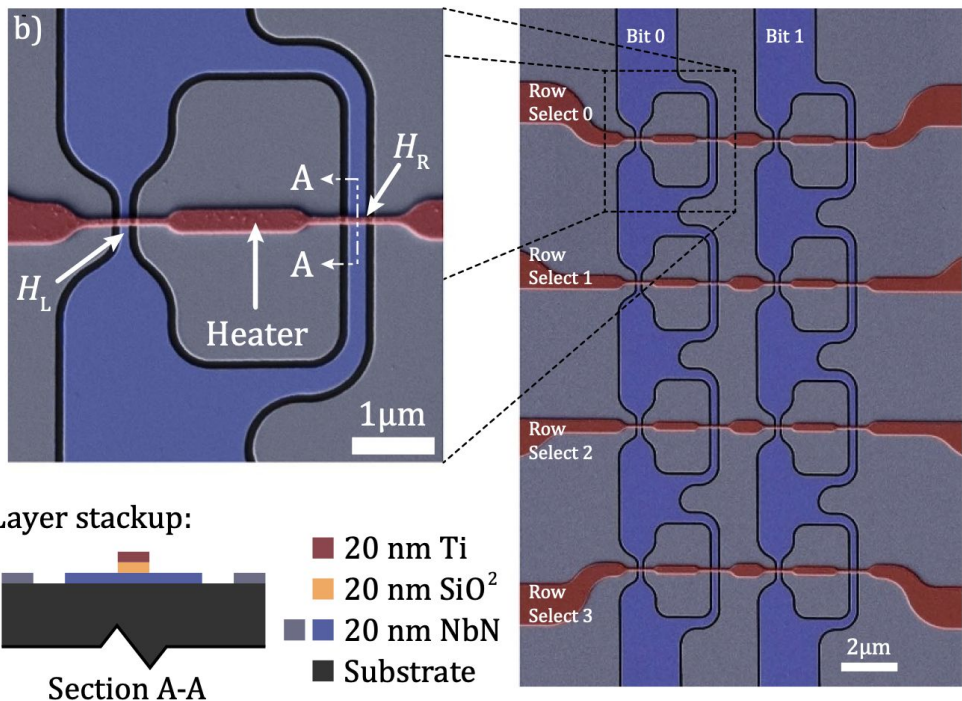
Base 3 at 405 nm



Nanowire Memory Element (nMem)

Superconducting Memories

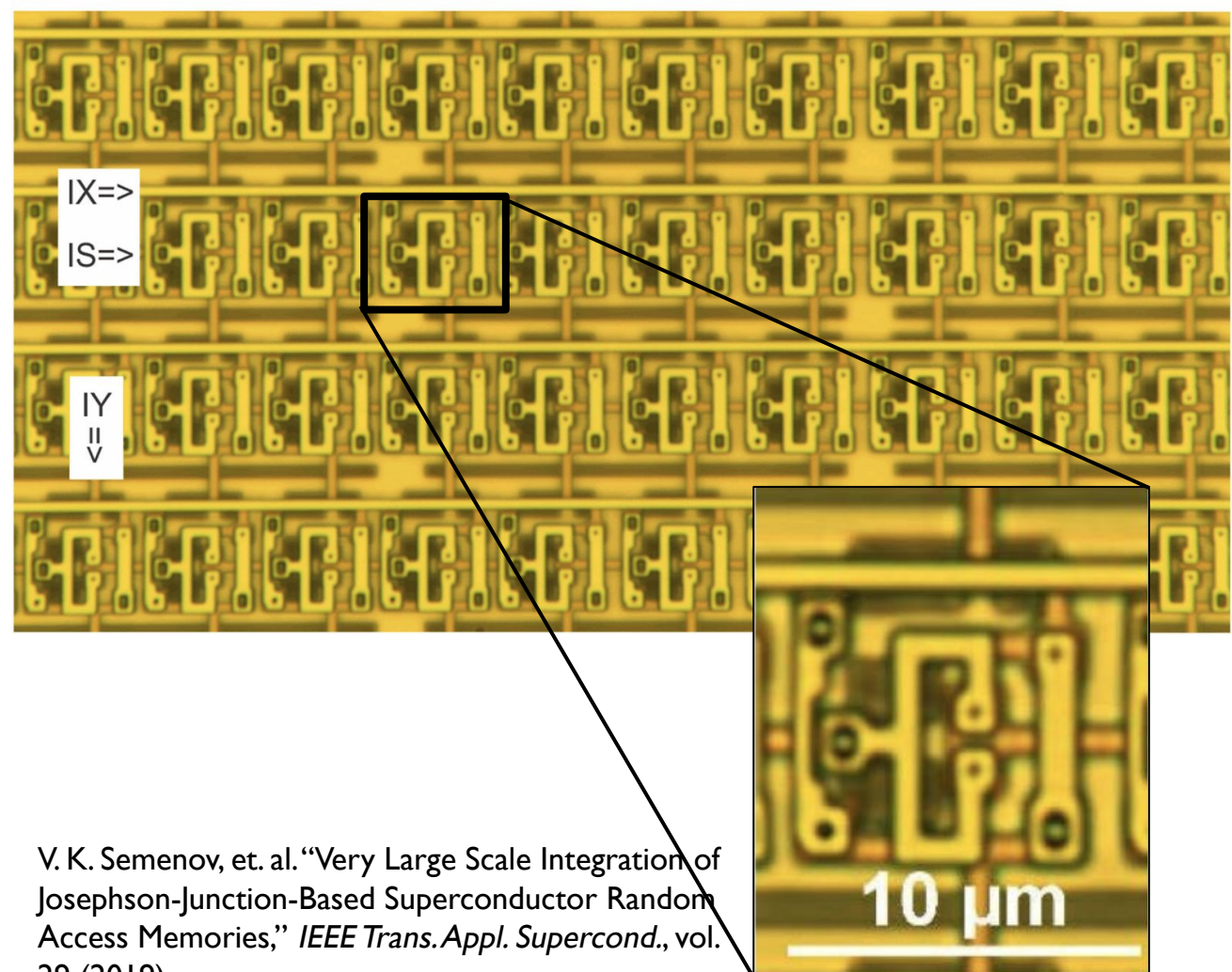
Superconducting nanowire memory



Work initiated
under IARPA C3
Program

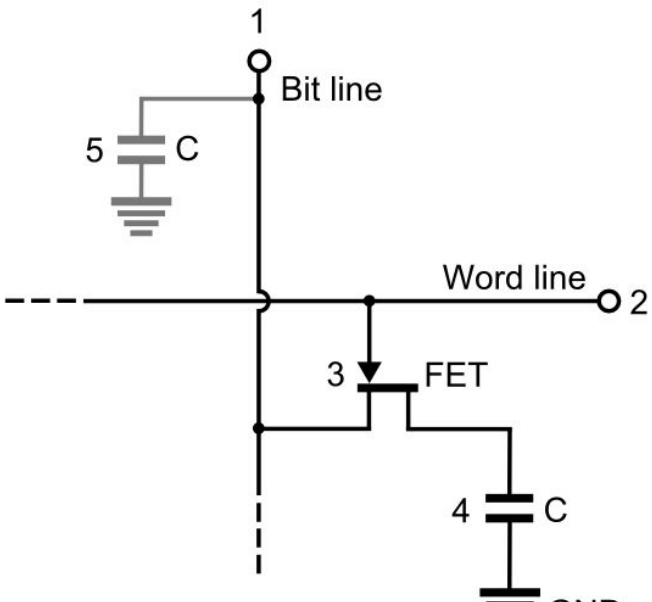
Butters, Brenden A., et al. "A scalable superconducting nanowire memory cell and preliminary array test." *Superconductor Science and Technology* 34.3 (2021)

Vortex-Transitional (VT) memory cells

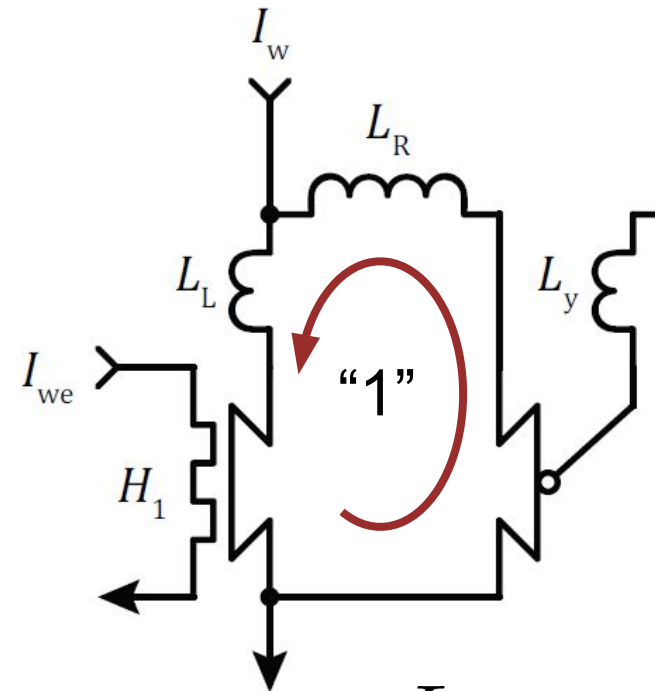


V. K. Semenov, et. al. "Very Large Scale Integration of Josephson-Junction-Based Superconductor Random Access Memories," *IEEE Trans. Appl. Supercond.*, vol. 29 (2019)

Persistent Current

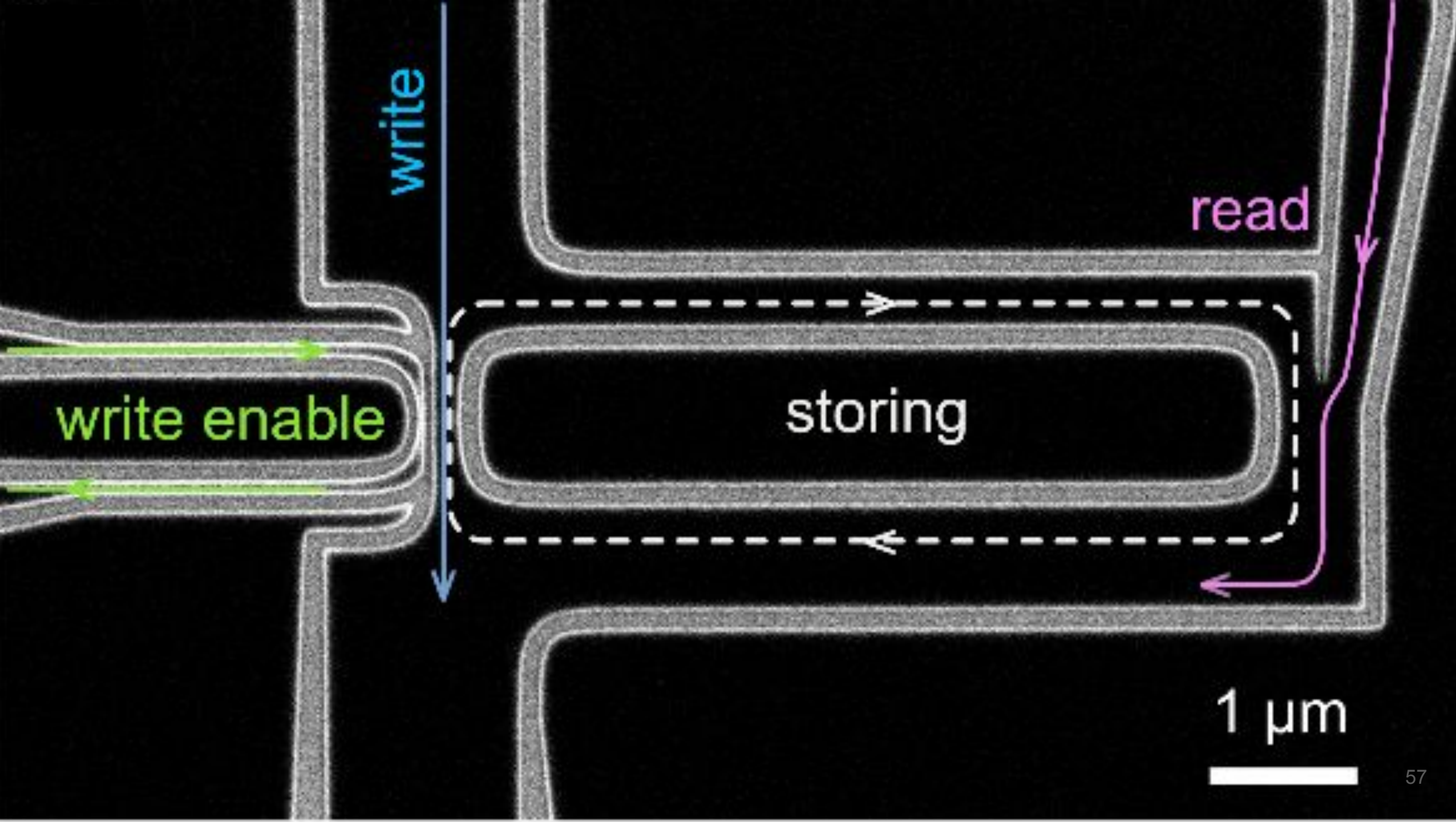


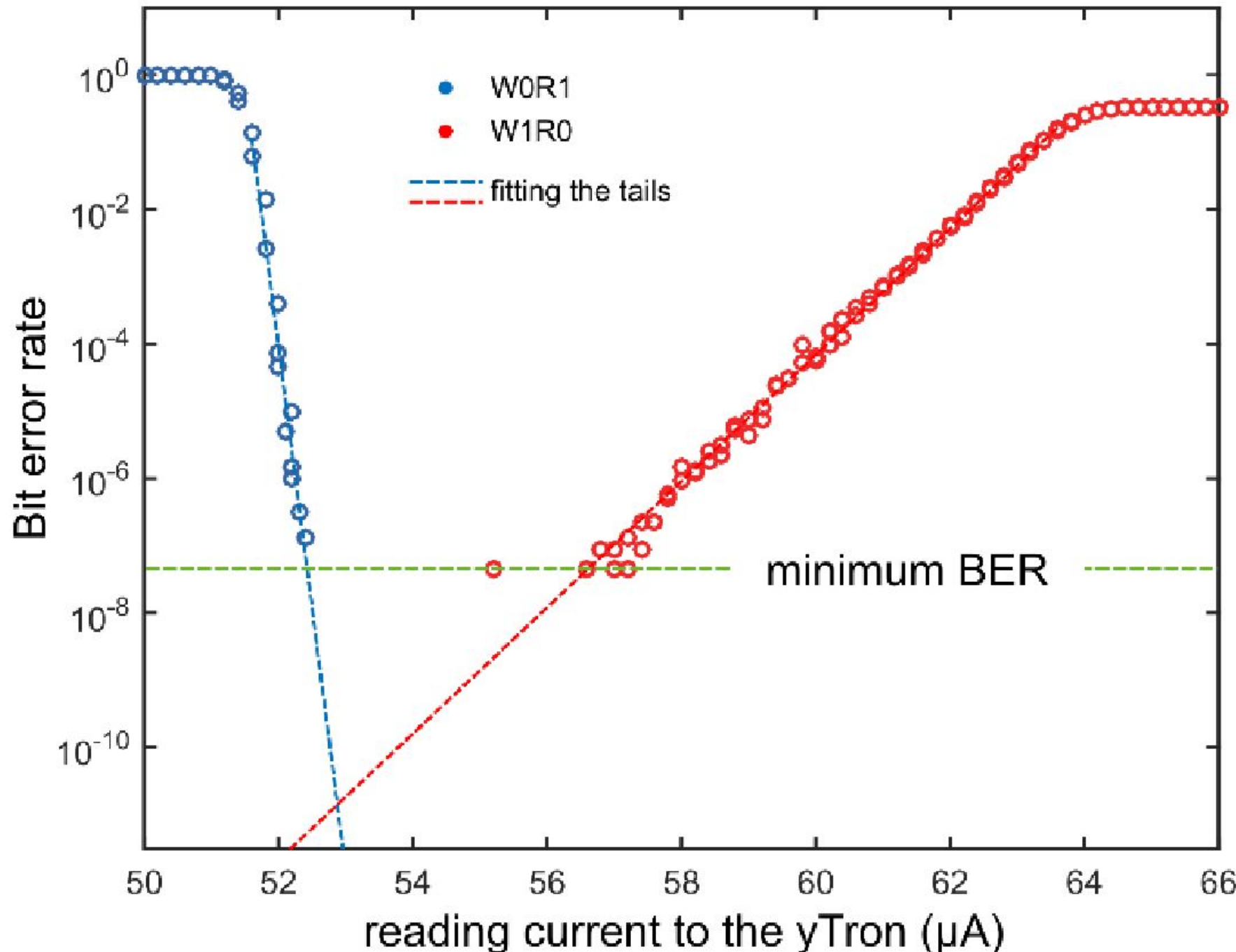
$$\tau = RC$$



$$\tau = \frac{L}{R}$$

Wikimedia Commons, DRAM Cell Structure (Model of Single Circuit Cell), Tosaka (2008)

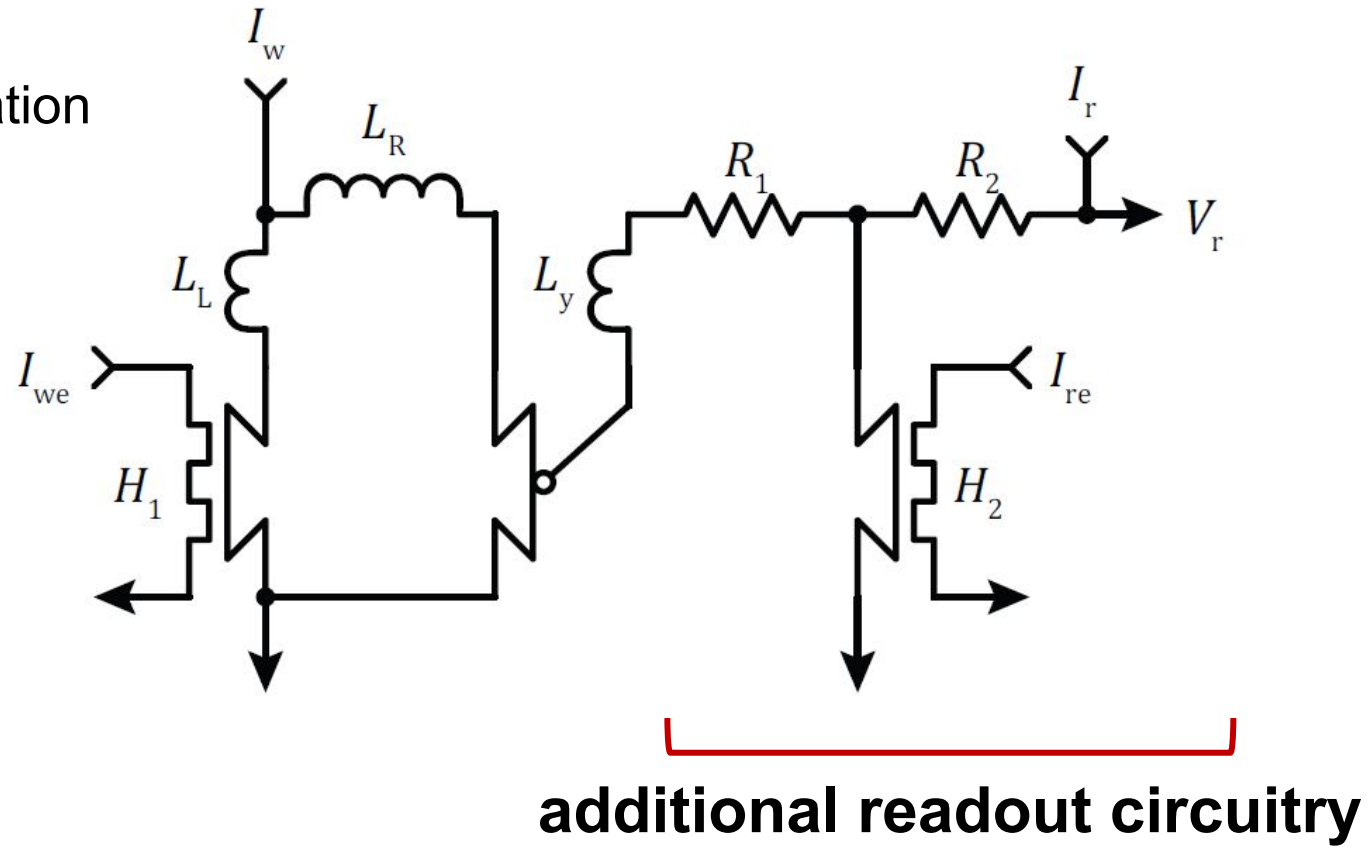




Problems with non-destructive read

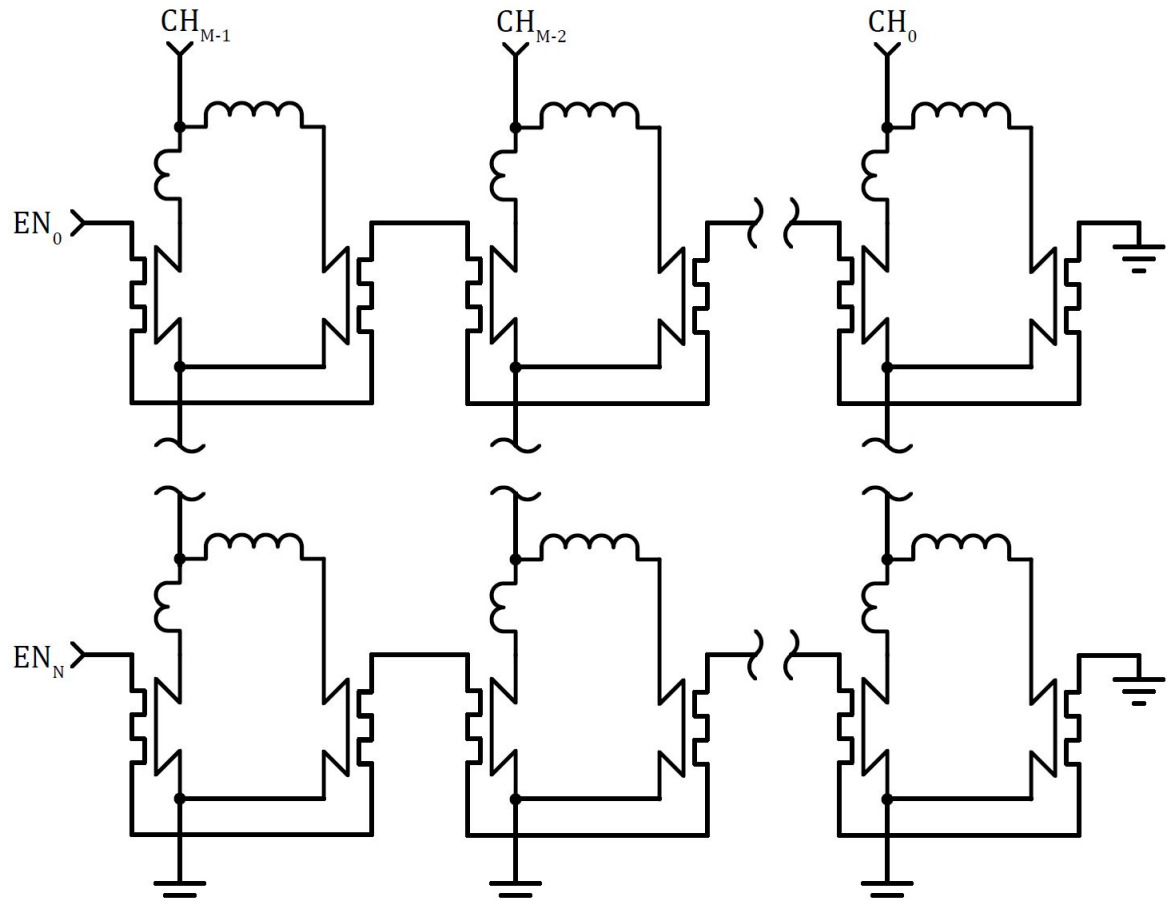
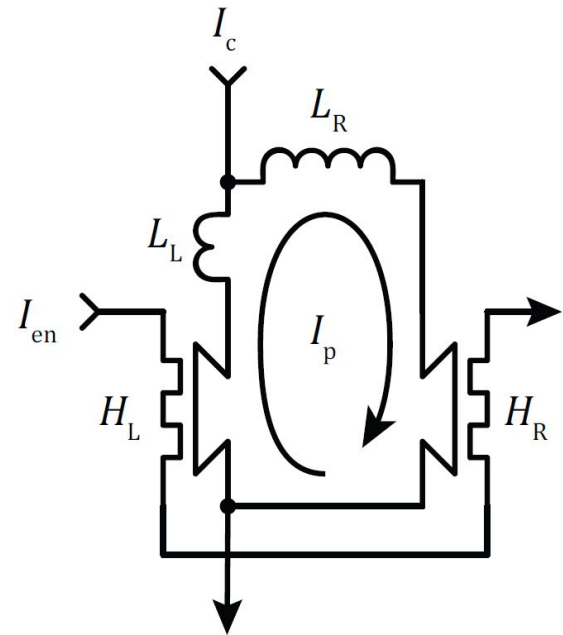
- yTron makes sneak currents hard to avoid
- Forming an array requires addressing circuitry

- Increases cell size
- Increases power dissipation
- Reduces speed

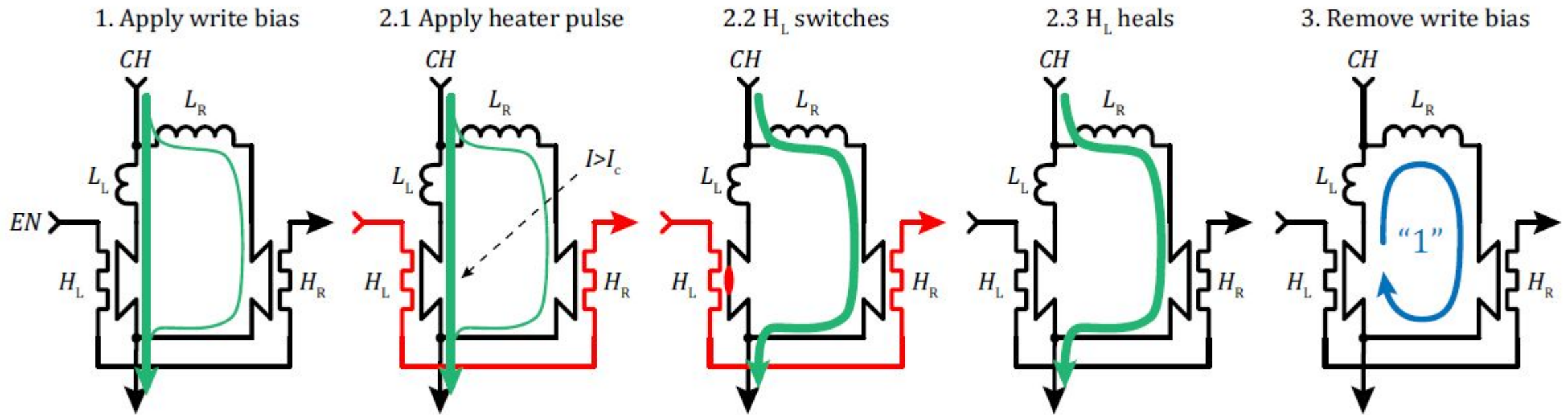


Destructive nanowire memory

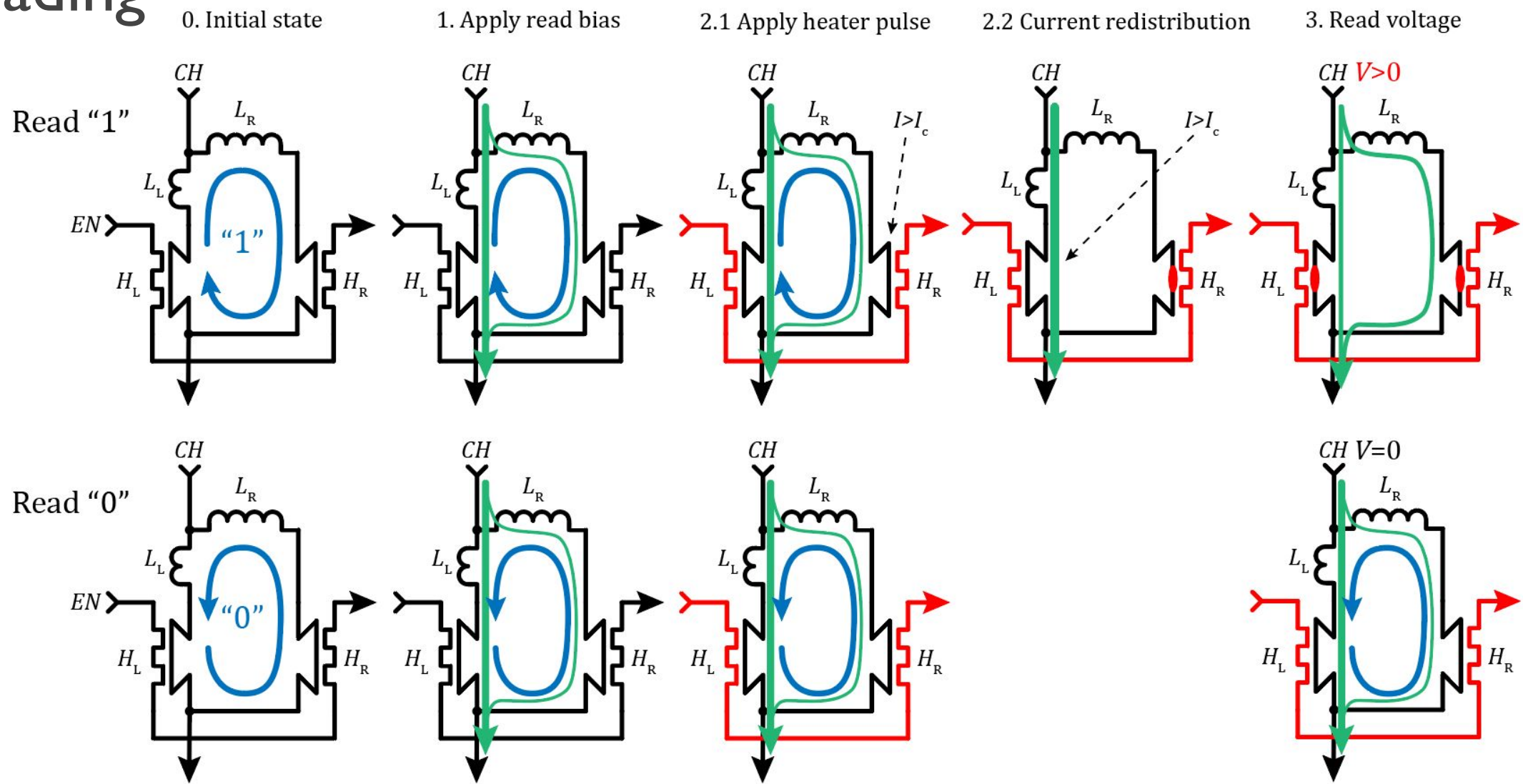
Destructive-read memory allows for simplified array geometry.



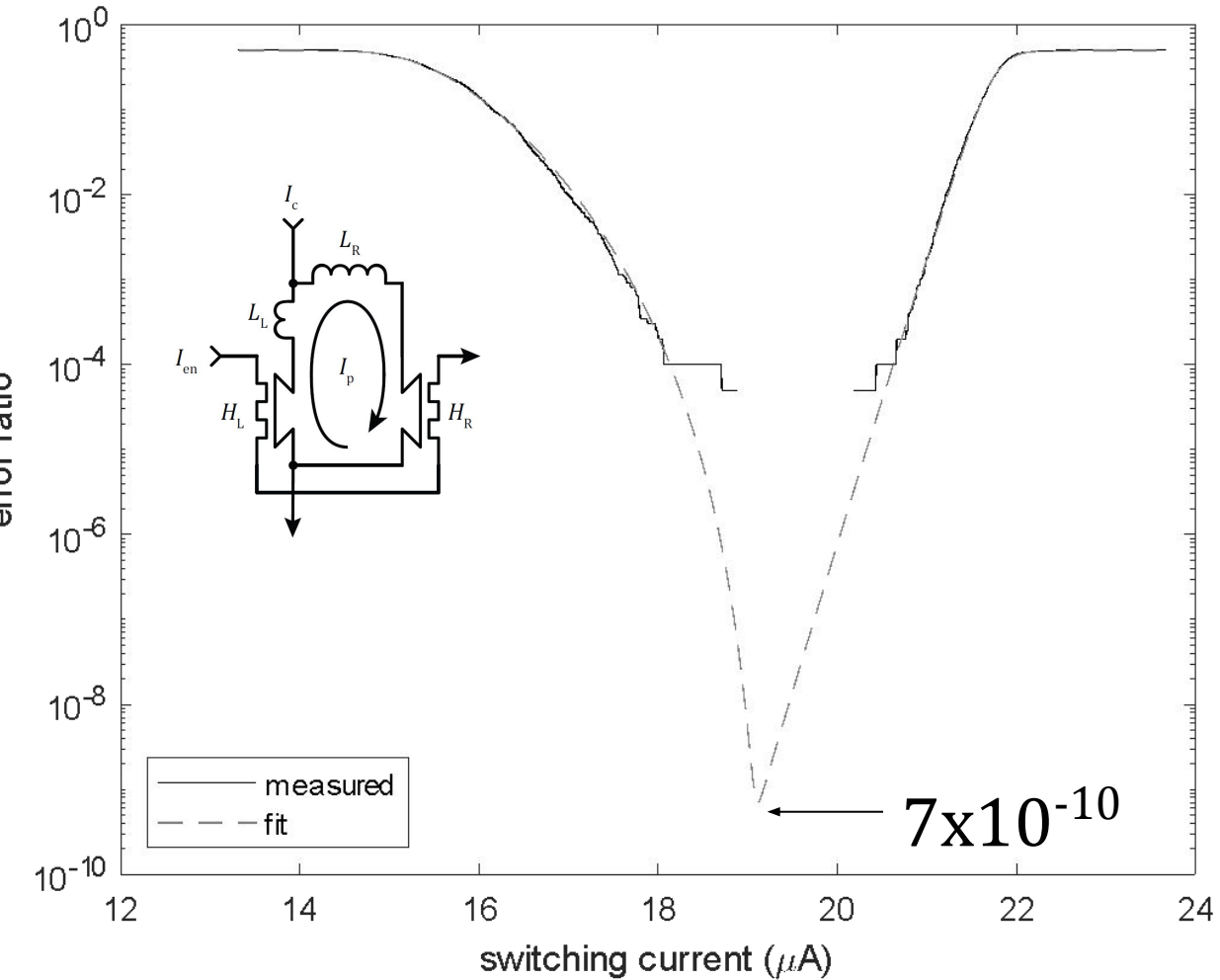
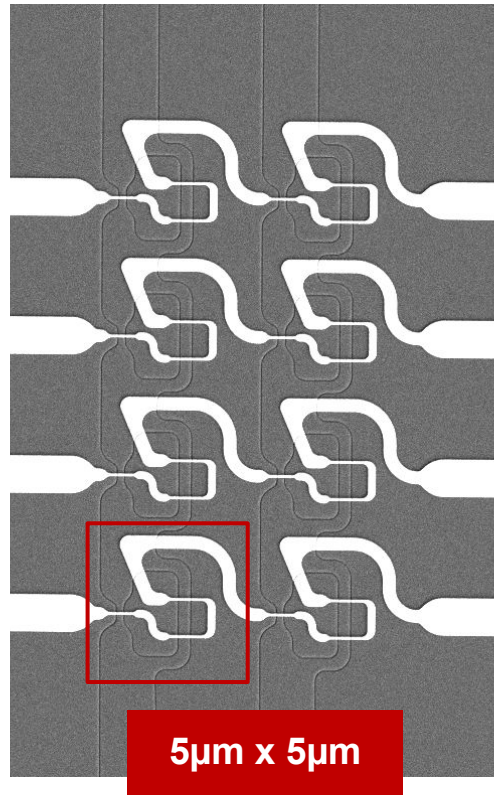
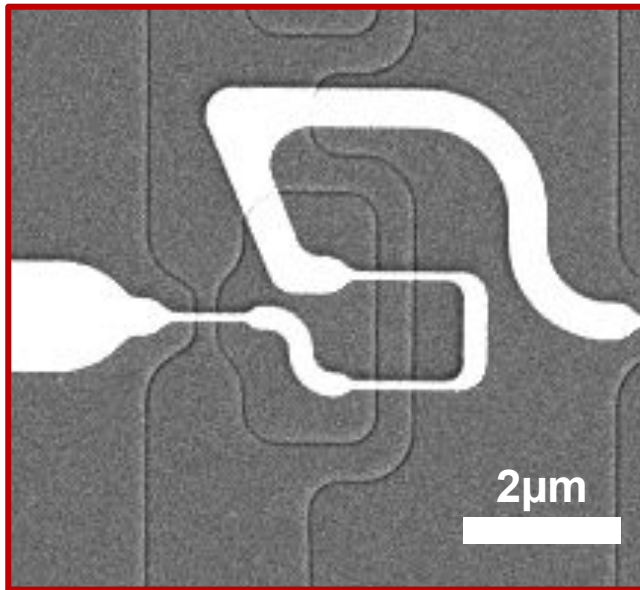
Writing



Reading



Switching Distributions

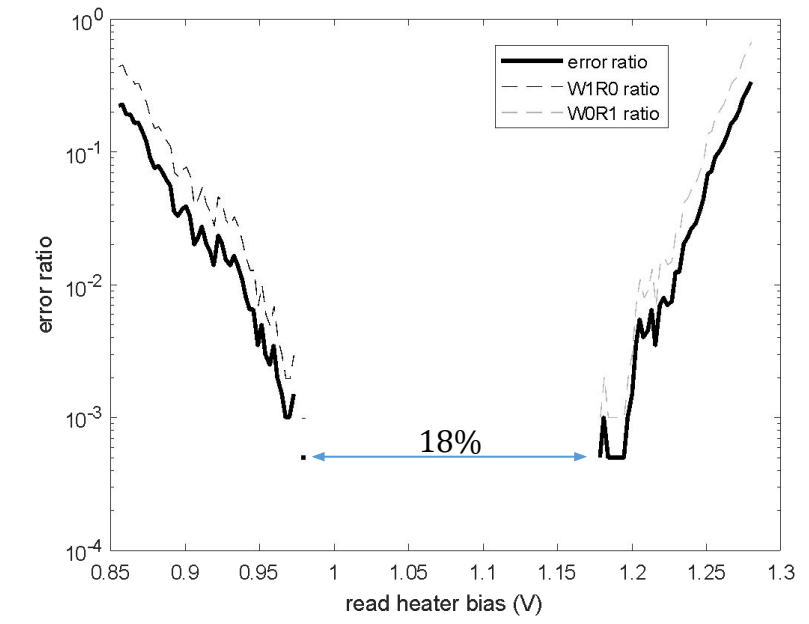
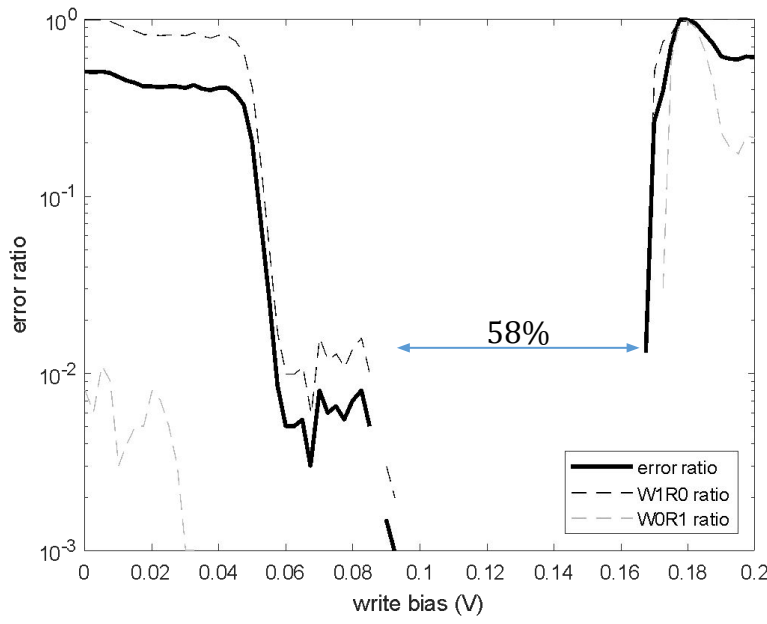
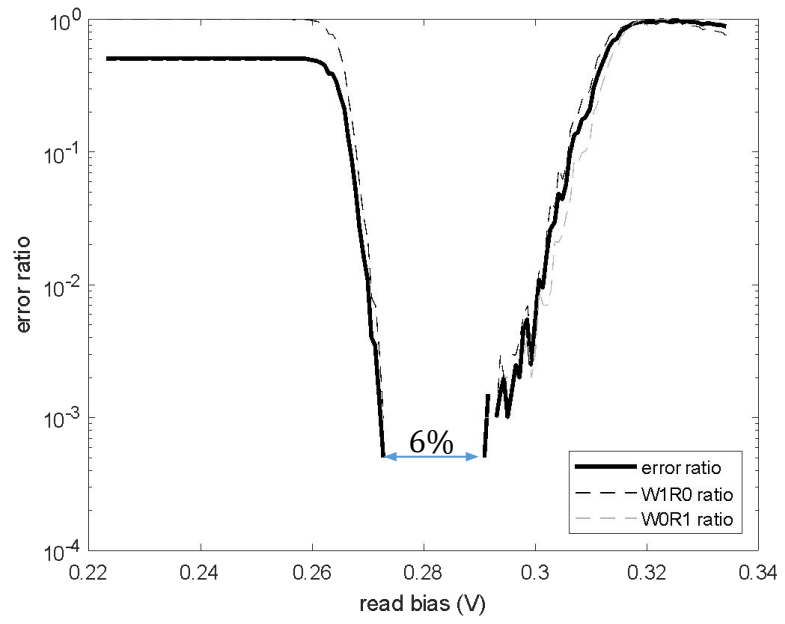


Comparison to existing superconducting memories

Table CEQIP-6 Superconductor Memory Status

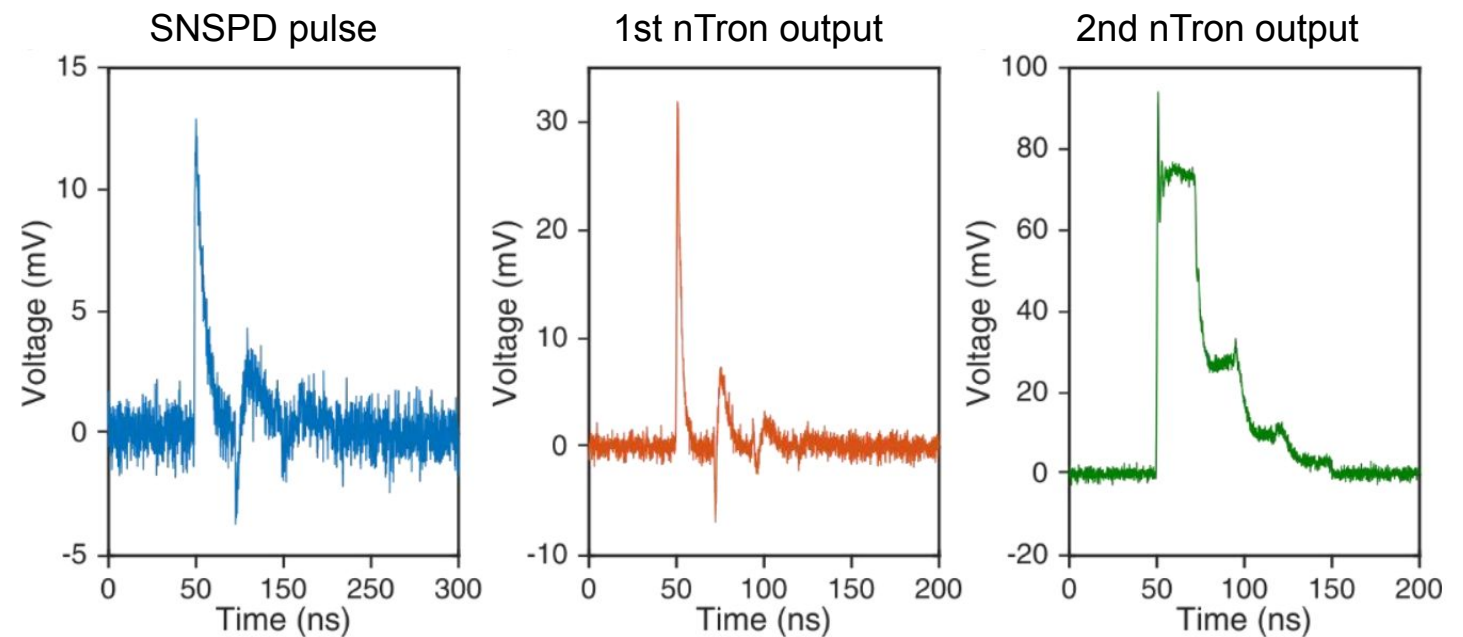
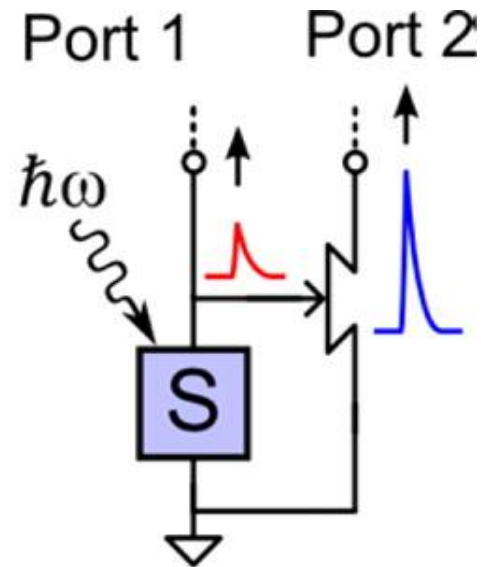
Name	References	RAM	Bit Cell Area [μm^2]	Latency [ns]		Energy [fJ]		Static Power	Bits
				Read	Write	Read	Write		
SR: shift register, ac-biased	[121]		300 (15×20)						202 280
SR: shift register	[339]			0.02	0.02	0.1	0.1	0.2 mW	64
VTM: vortex transition memory	[203 (VT2)]	✓	99 (9×11)	0.10	0.10	100	100		72
JJ-RAM: Josephson junction RAM	[199]	✓	484 (22×22)					4.5 mW	4096
RQL-RAM: reciprocal quantum logic	[200]	✓	1452 (33×44)						1024
PRAM: PTL-RAM	[201, 202]	✓	1452 (33×44)						512
SHE-MTJ: Spin Hall effect magnetic tunnel junction	[239]	✓	2470 (38×65)	0.10	2	1000	8000		16
SNM: superconducting nanowire memory	[107]	✓	26.5 (5×5.3)	0.10	3	10	10		8
Hybrid: JJ-CMOS	[659]	✓		2 ~ 4	2 ~ 4	100	100		65 536

Holmes, D. Scott. "Cryogenic Electronics And Quantum Information Processing." 2022
IEEE International Roadmap for Devices and Systems Outbriefs. IEEE, 2022.



Off-Chip Drivers

nTron Amplifier Example for SNSPDs

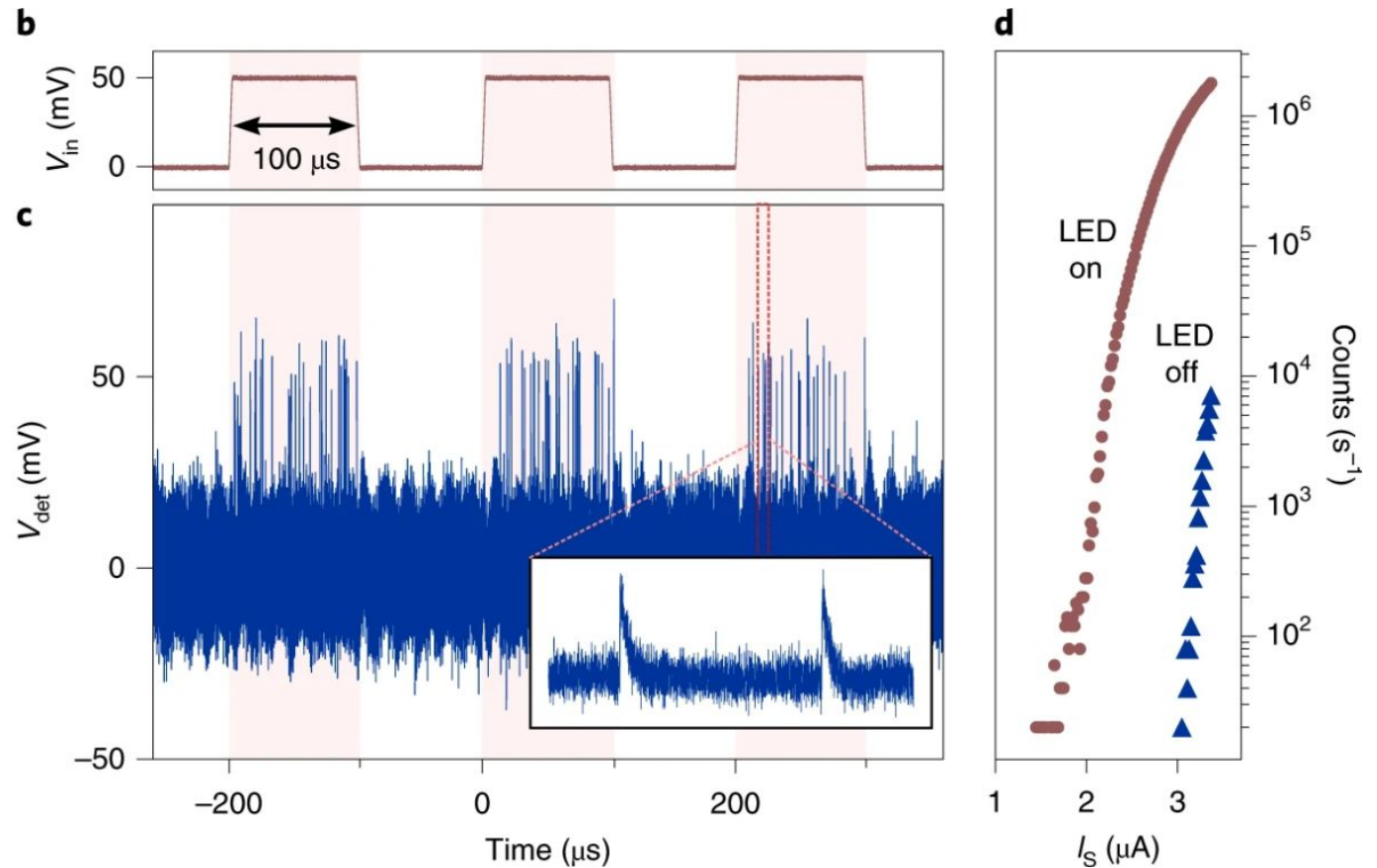
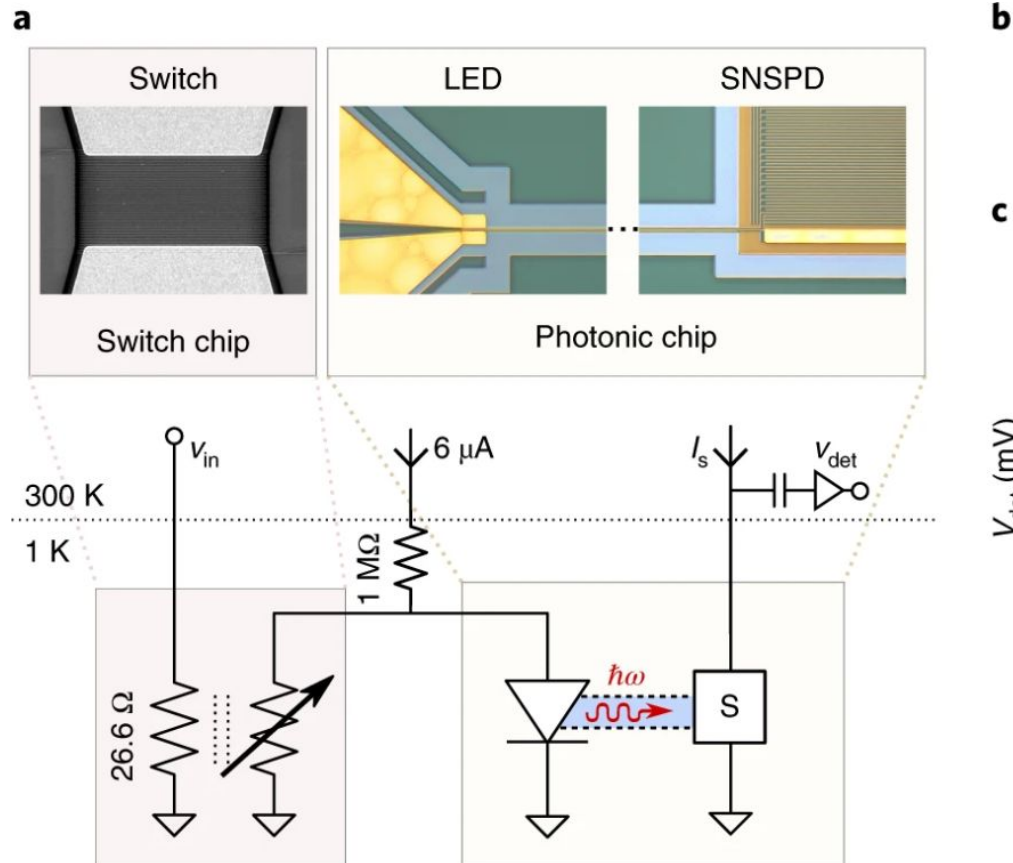


A. N. McCaughan and K. K. Berggren,
Nano Letters 14(10), 5748 (2014)

11/30/22 - Prof. K.K.Berggren

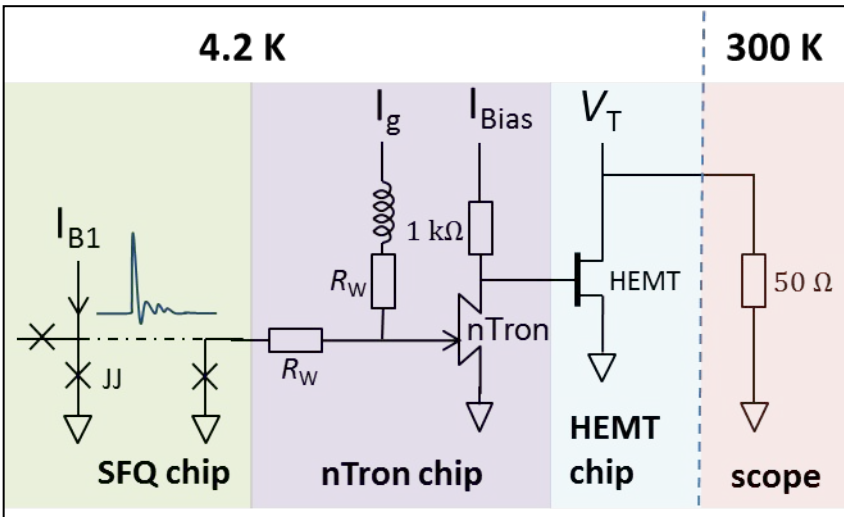
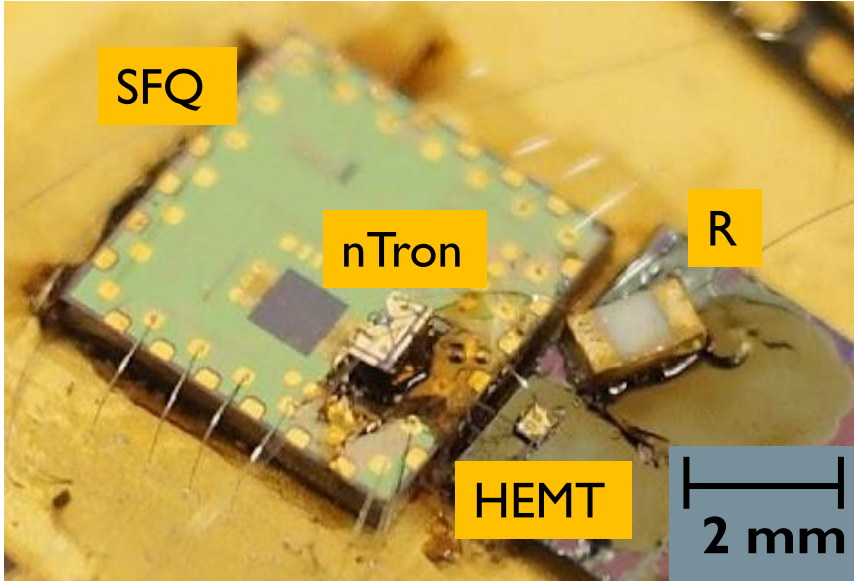
Zheng, K., Zhao, Q. Y., et al. "A Superconducting Binary Encoder with Multigate Nanowire Cryotrons." *Nano letters*, 20(5), (2020) 3553-3559. (Supporting Information)

The NIST Thermal Switch (hTron)



McCaughan, A.N., et al. "A superconducting thermal switch with ultrahigh impedance for interfacing superconductors to semiconductors." *Nat Electron* 2, 451–456 (2019). 68

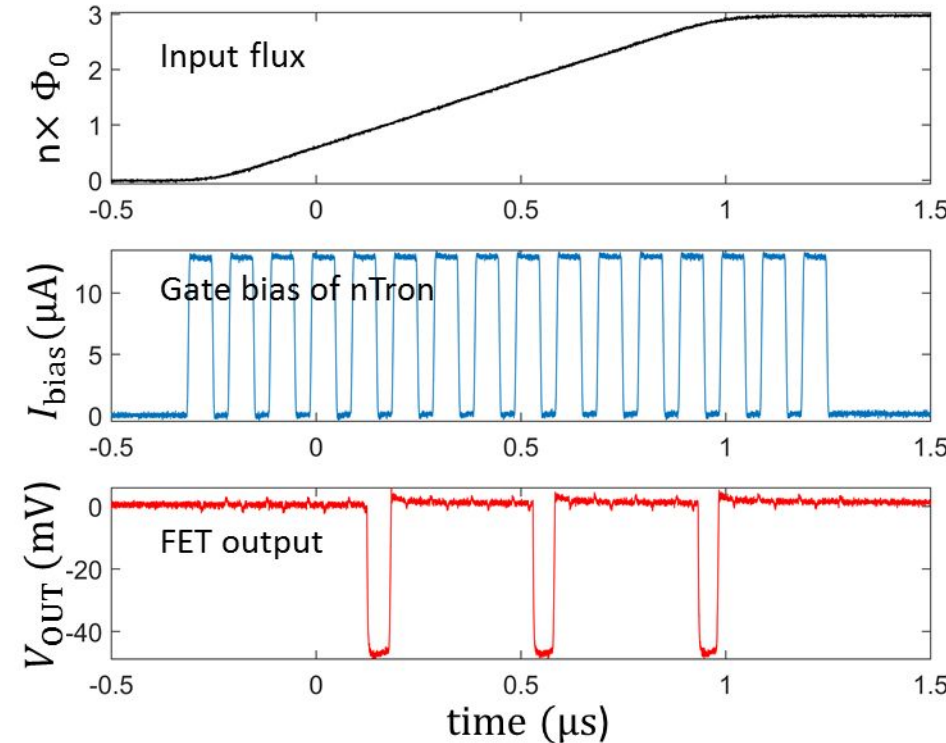
Interface between RSFQ & Semiconductors



Experimental demonstration

SFQ→nTron→HEMT

Josephson junction → nanowire → transistor



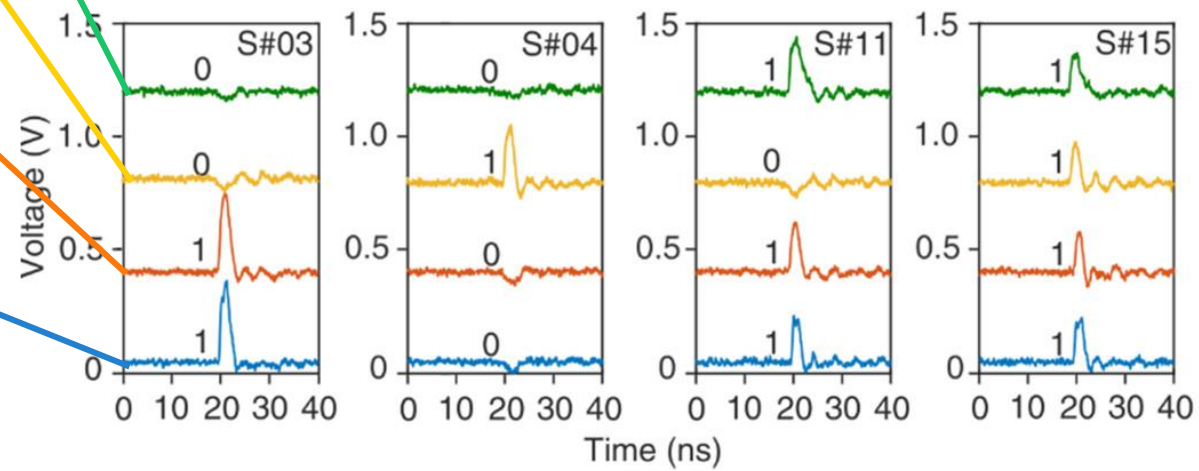
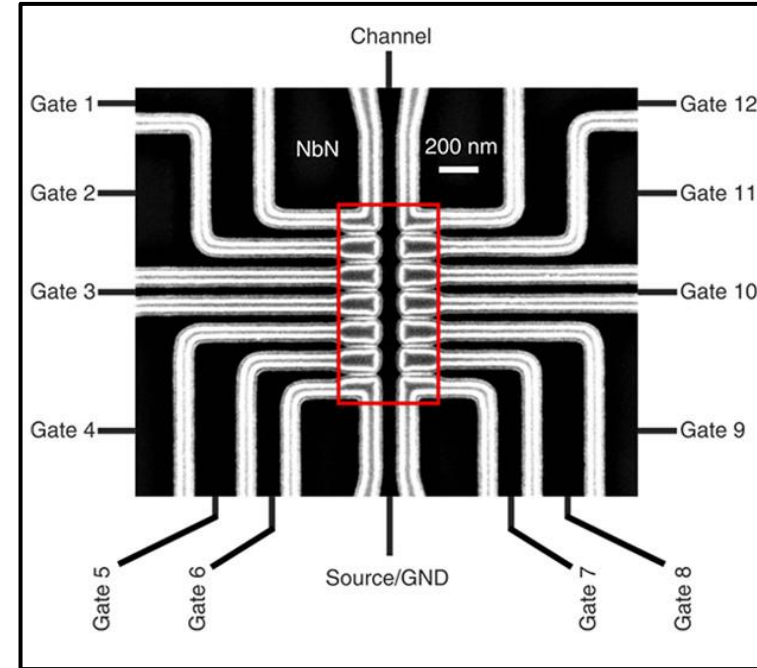
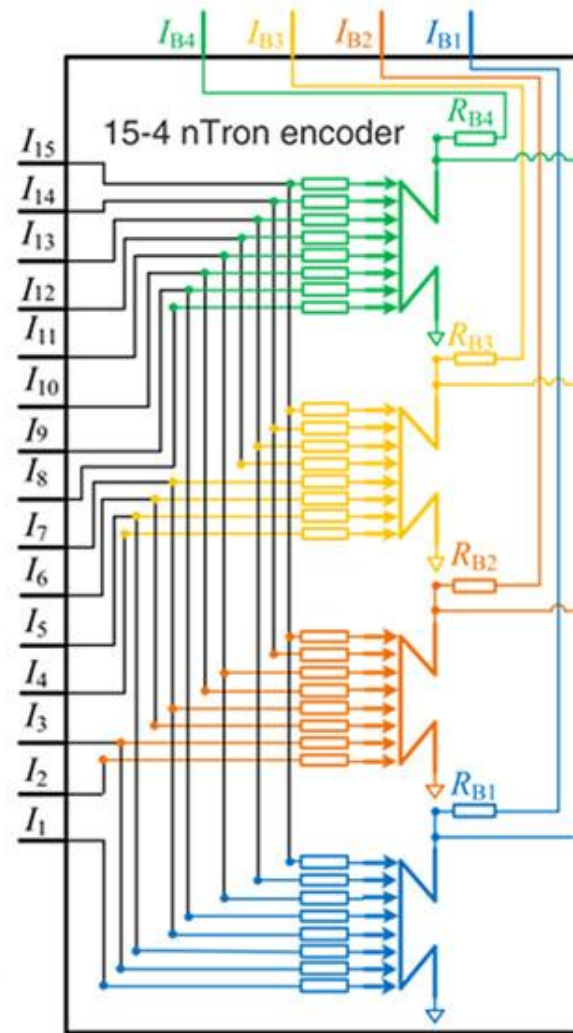
Encoders

A major need for superconducting electronics is the ability to do robust multiplexing onto and off chip.

The Nanjing Encoder



Qingyuan Zhao



Neuromorphic Circuits

Application to Neuromorphic Computing

- **Neuromorphic circuits are likely to require multiple modalities (e.g. flux, light, charge)**
- **Natural fit to spiking characteristic of physical neurons**



Emily Toomey
Grad student

In Collaboration With

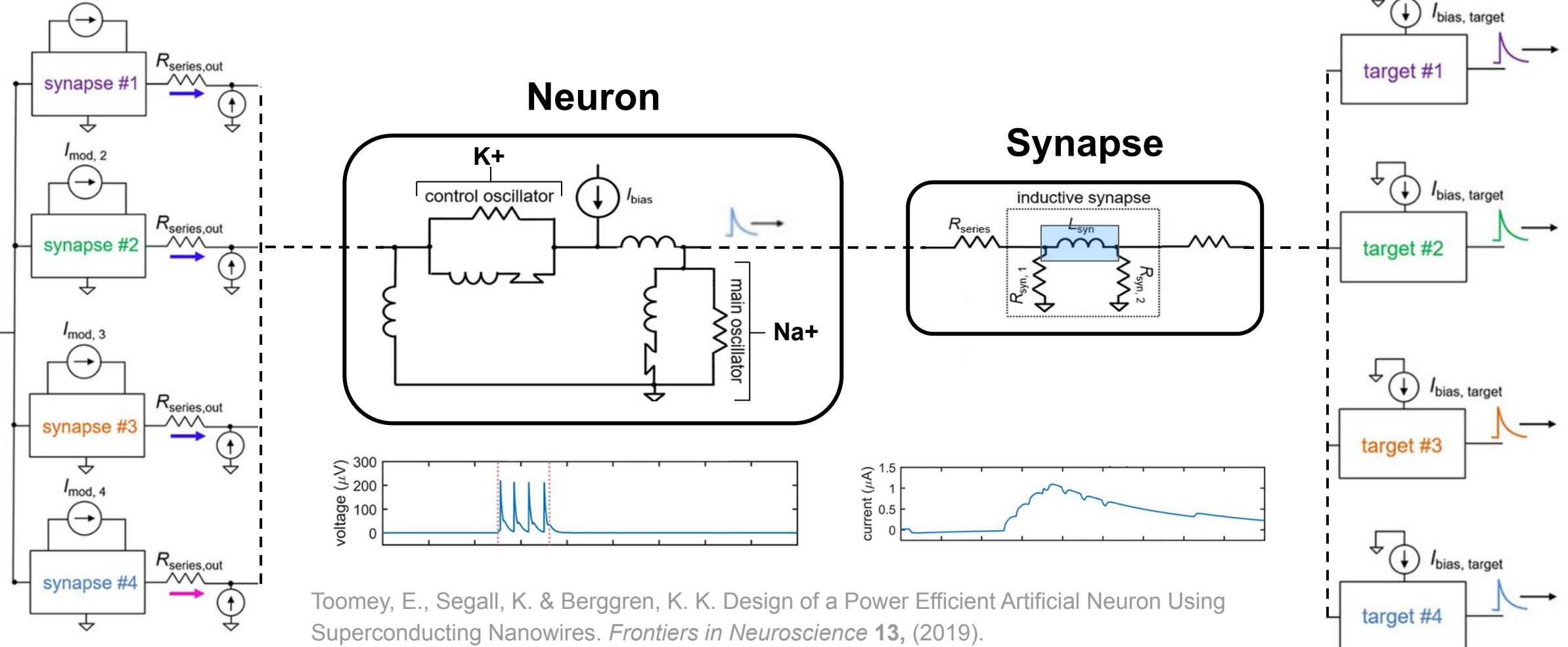


Ken Segall,
Colgate

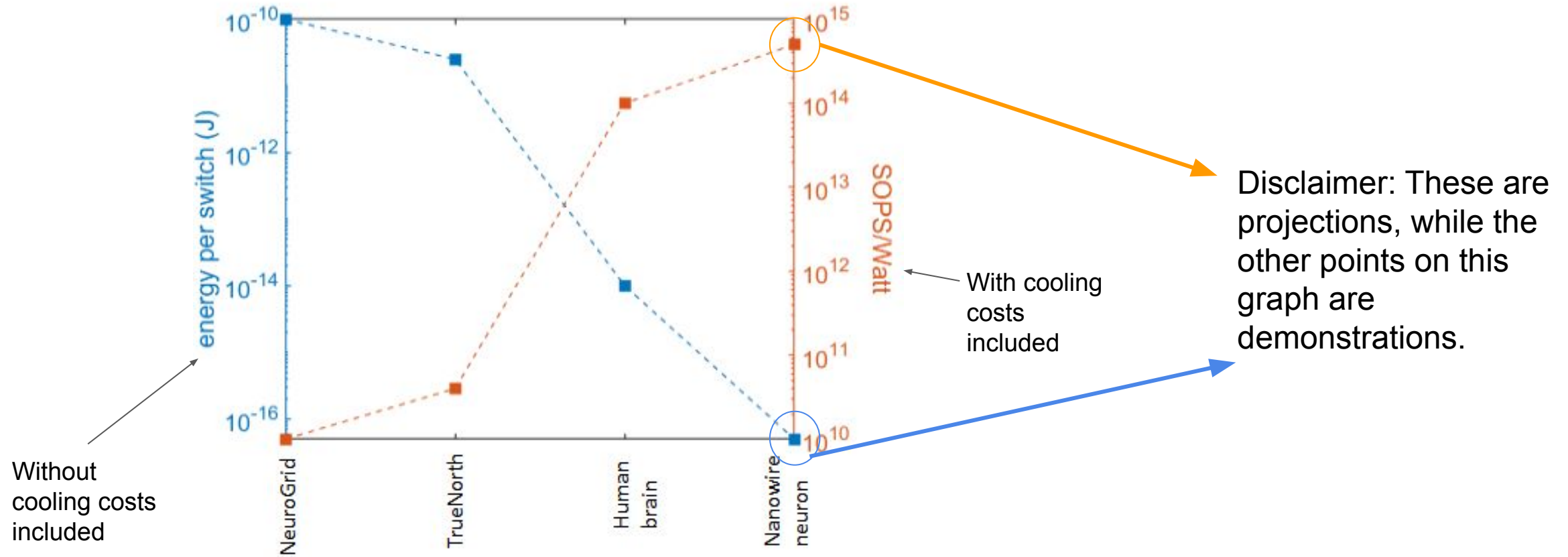


Nancy Lynch,
MIT

Applications to neuromorphic computing



Nanowire neuron: energy performance

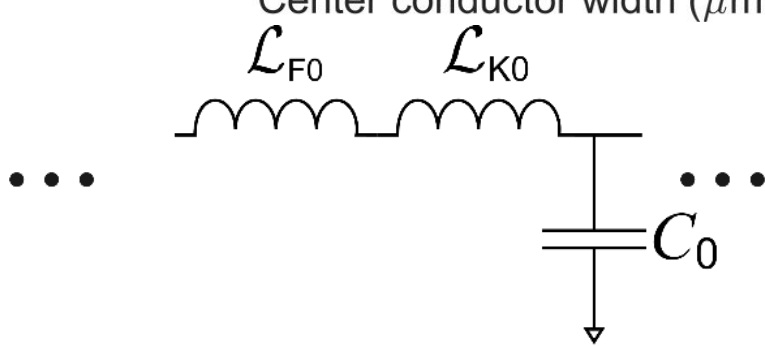
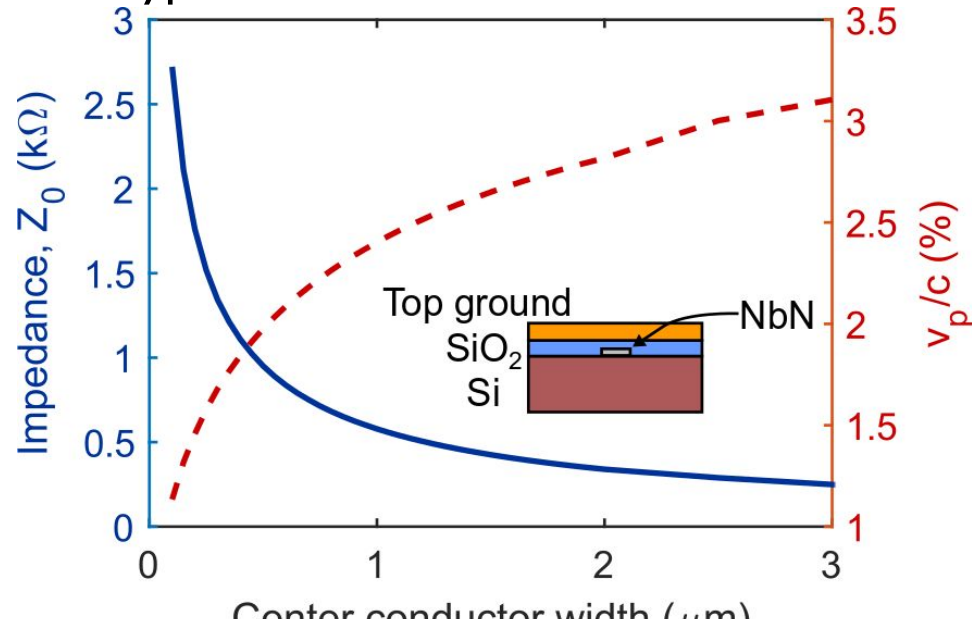


- Projected to have a figure of merit 4 orders of magnitude better than current CMOS architectures
- Additional advantage of no static power dissipation in the interconnects
- JJ neuron projected to have $\sim 10^{15}$ SOPS/Watt

Microwave Electronics

Slow-wave transmission line

A typical nanowire transmission line



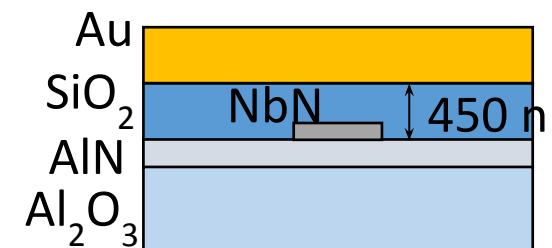
For a ~ 5 nm thick 300 nm wide NbN microstrip,

$$\mathcal{L}_{K0} \approx 212\mu_0 \quad \mathcal{L}_{F0} \approx 0.3\mu_0 \quad C_0 \approx 21\epsilon_0$$

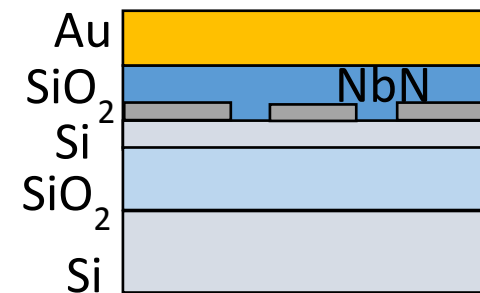
Measured group velocities to date



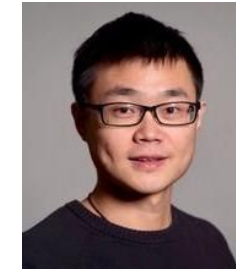
Signal speed $\sim 2\%c = 6 \mu\text{m} / \text{ps}$
Zhao et al. Nat. Photonics 11, 247 (2017)



Signal speed $1.6\%c = 4.8 \mu\text{m} / \text{ps}$
Zhu et al. Nat. Nanotech. 13, 596 (2018)



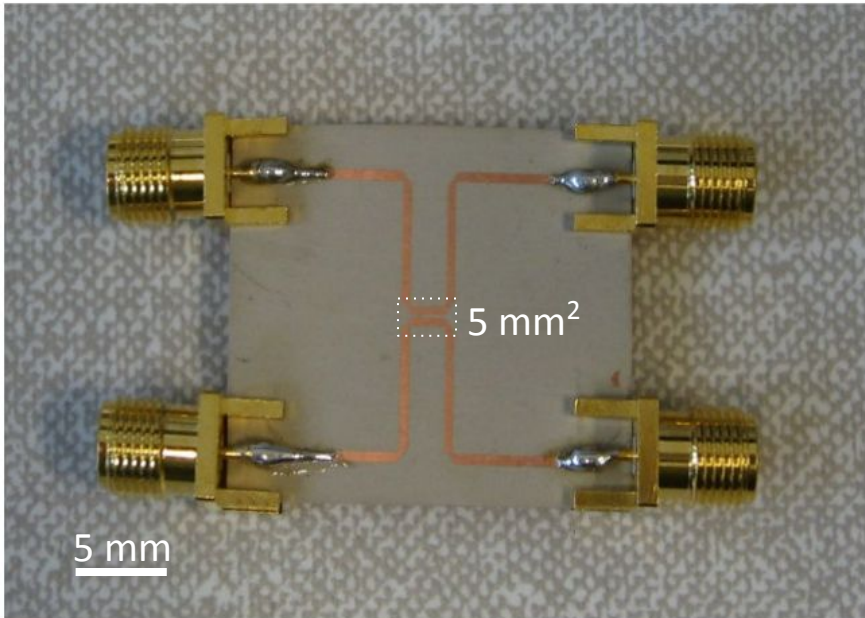
Signal speed = $2.7 \mu\text{m}/\text{ps}$
Zhu et al. (2018), unpublished



Di Zhu

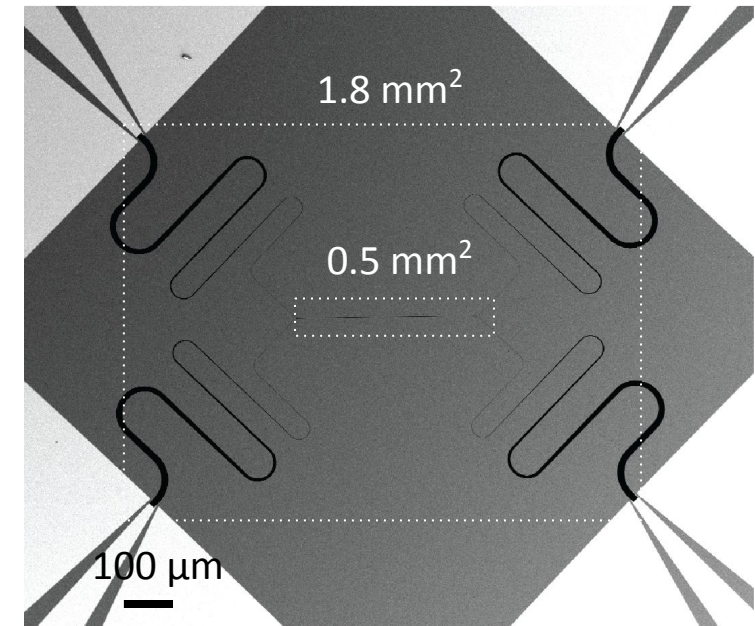
Extreme footprint reduction

@ 12 GHz - $\lambda = 1$ cm



Nanowire
Microstrip
Transmission Lines
 $\xrightarrow{10\times - 100\times}$
footprint reduction

@ 5 GHz - $\lambda = 1$ mm



Fauzi, Azahar, and Zairi Ismael Rizman. *Journal of Engineering Science and Technology* 11.3 (2016): 431-442.

12 GHz microstrip directional coupler (on RO6010)

- backward coupling
- $Z_0 = 50 \Omega$

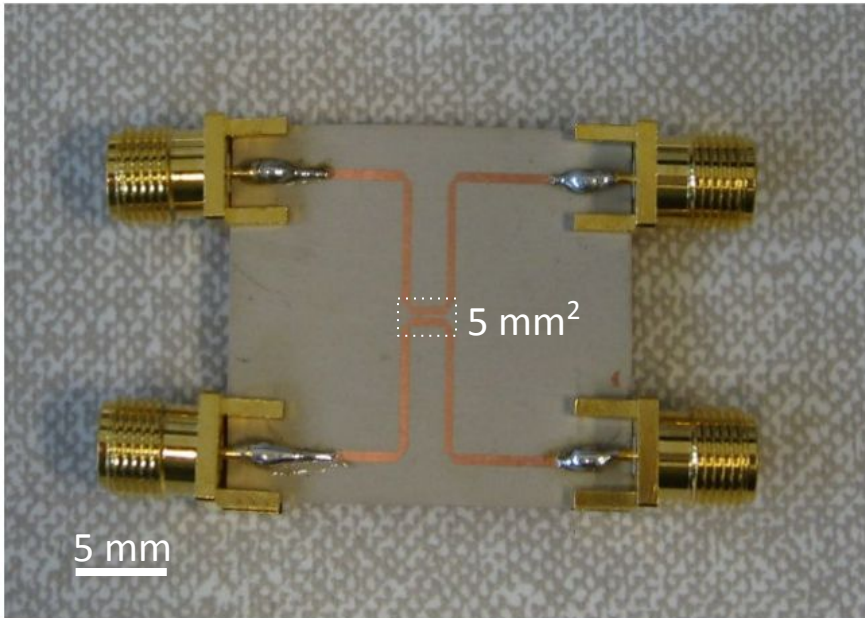
Colangelo, Marco, et al. "Compact and Tunable Forward Coupler Based on High-Impedance Superconducting Nanowires." *Physical Review Applied* 15.2 (2021): 024064.

5 GHz microstrip directional coupler

- forward coupling
- $Z_0 = 1446 \Omega$

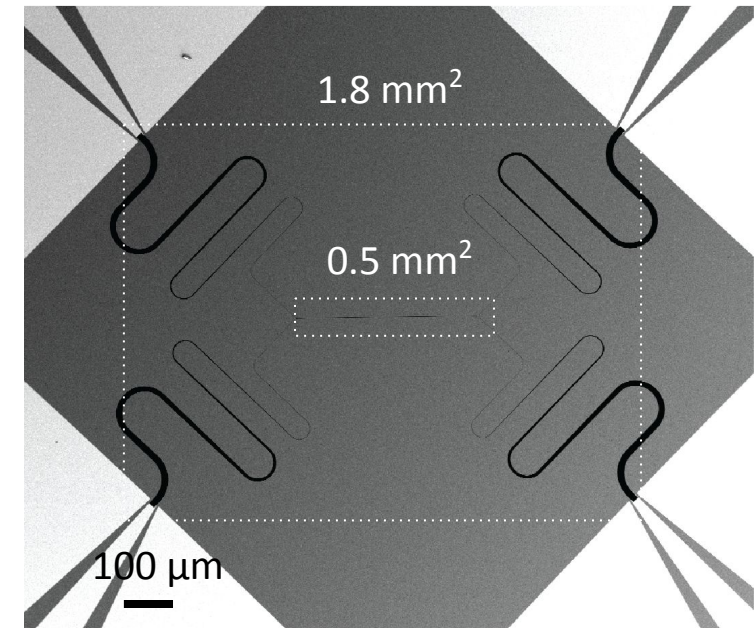
Extreme footprint reduction

@ 12 GHz - $\lambda = 1$ cm



Nanowire
Microstrip
Transmission Lines
 $\xrightarrow{10\times - 100\times}$
footprint reduction

@ 5 GHz - $\lambda = 1$ mm



Fauzi, Azahar, and Zairi Ismael Rizman. *Journal of Engineering Science and Technology* 11.3 (2016): 431-442.

12 GHz microstrip directional coupler (on RO6010)

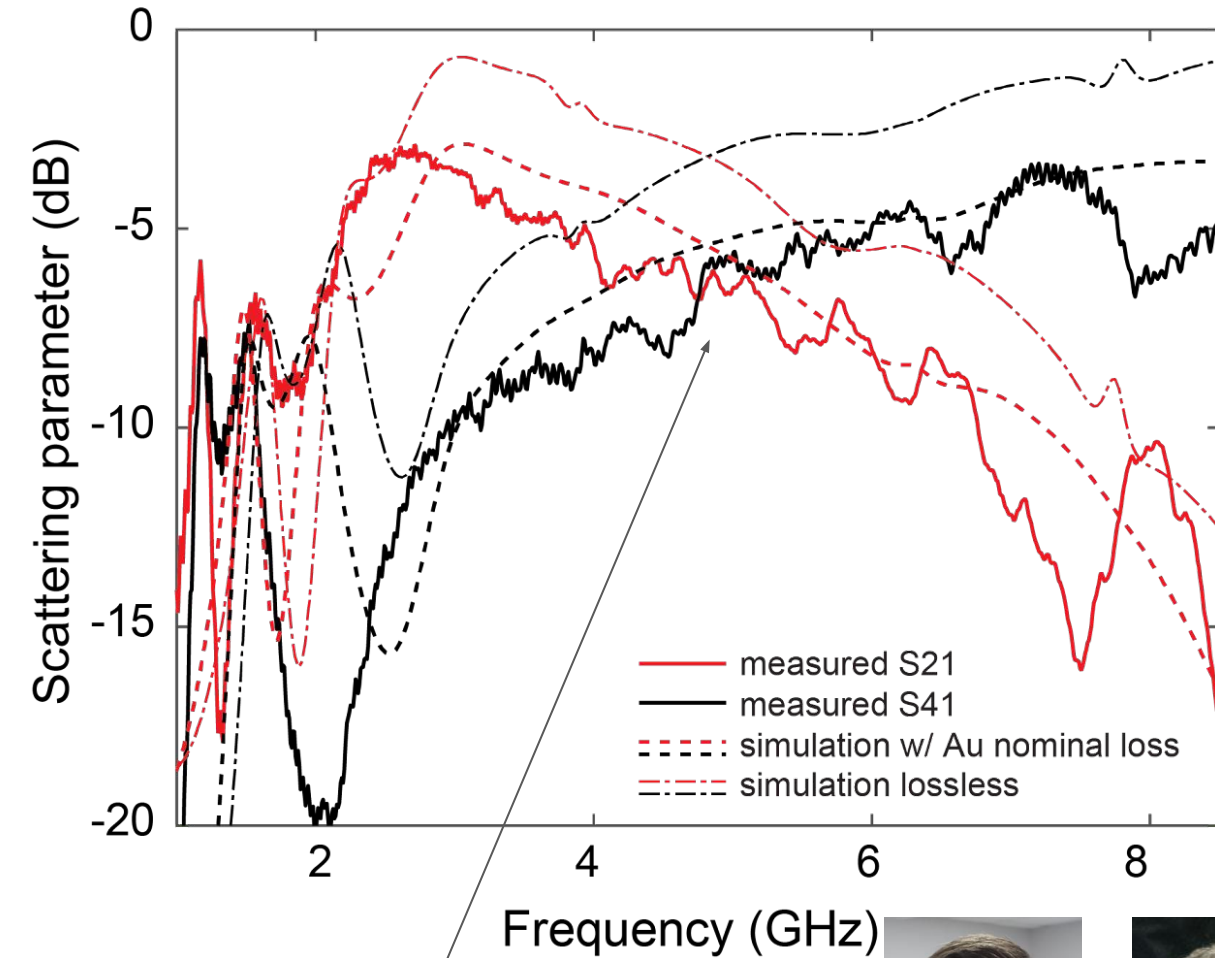
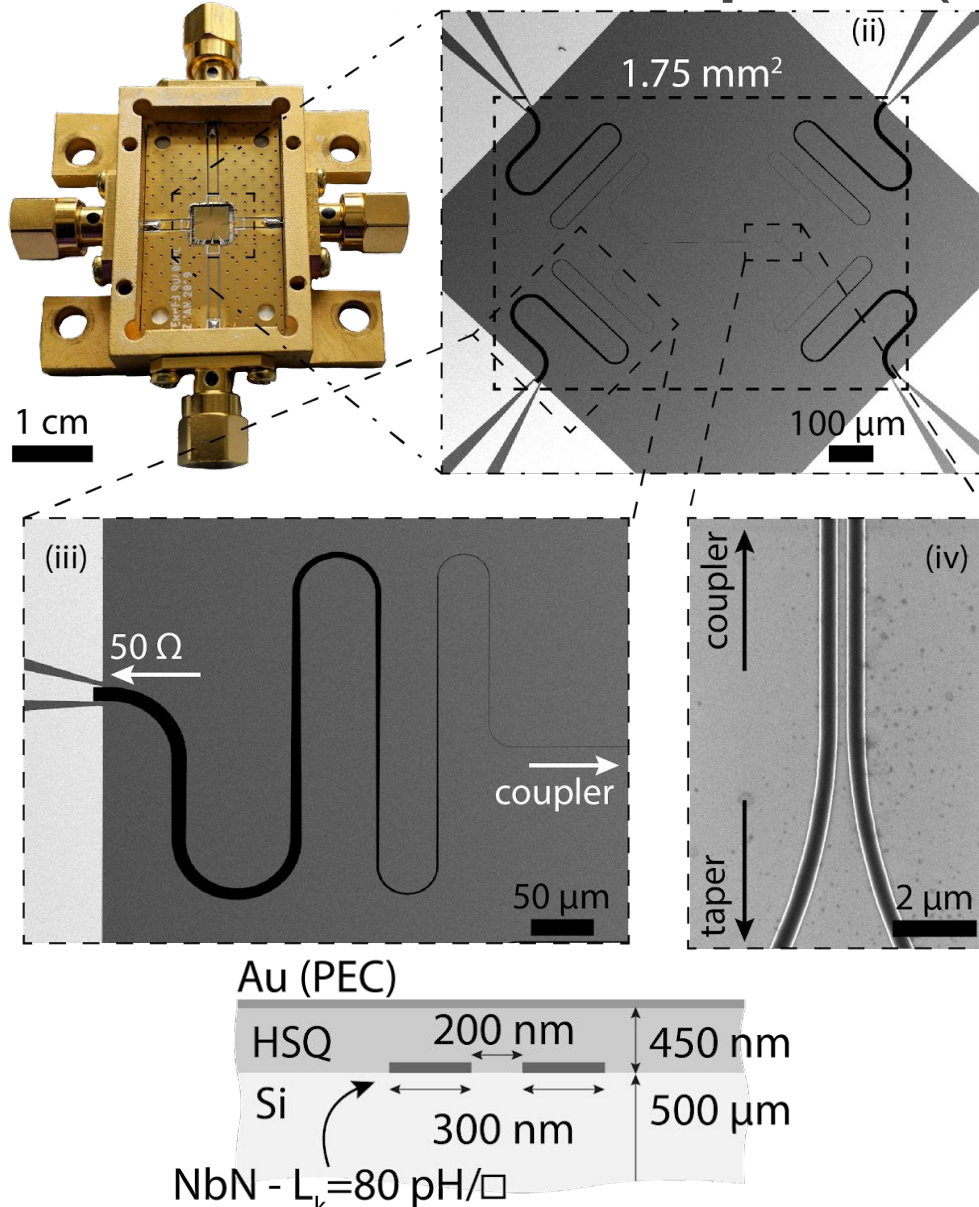
- backward coupling
- $Z_0 = 50 \Omega$

Colangelo, Marco, et al. "Compact and Tunable Forward Coupler Based on High-Impedance Superconducting Nanowires." *Physical Review Applied* 15.2 (2021): 024064.

5 GHz microstrip directional coupler

- forward coupling
- $Z_0 = 1446 \Omega$

Nanowire coupler (experiment)

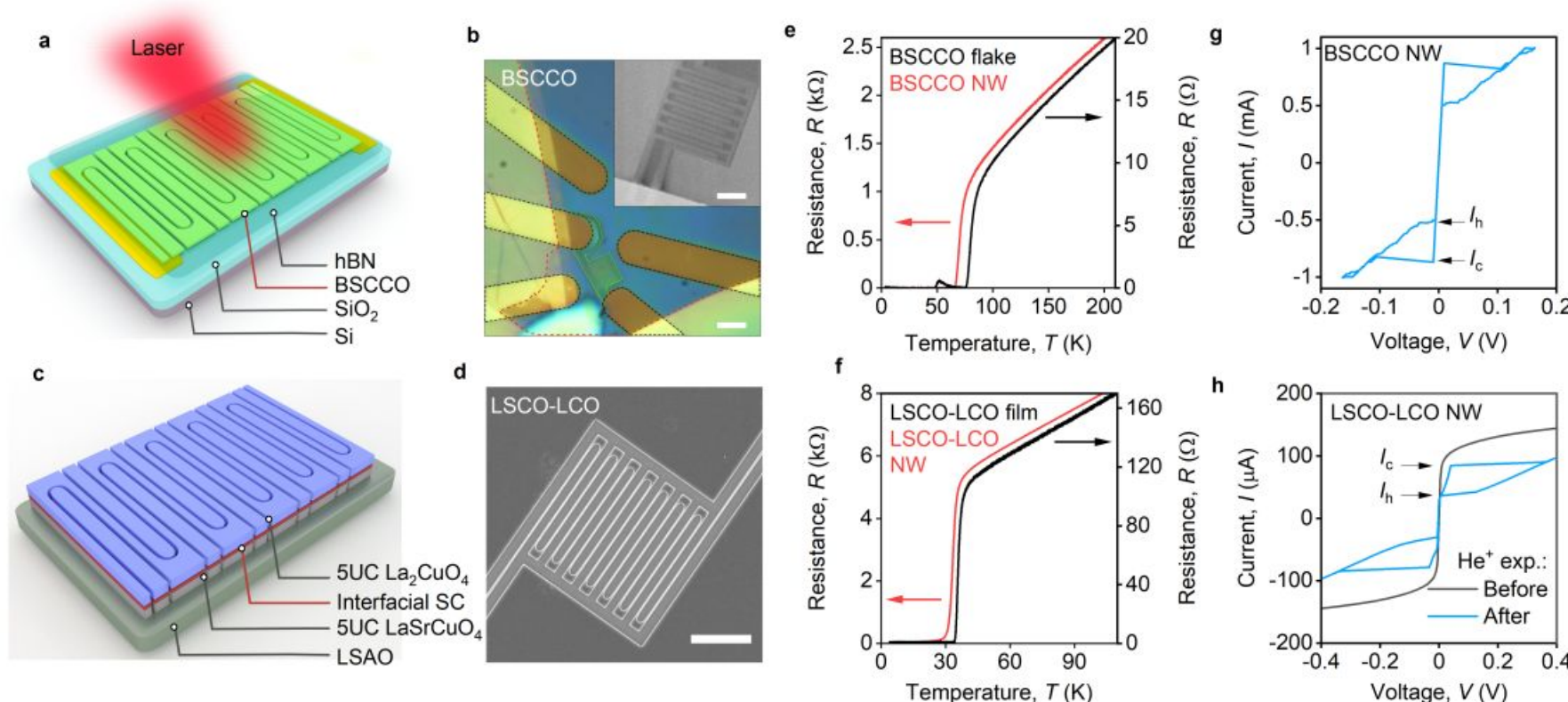


50:50 balanced coupling at 4.75 GHz



High-Temp Operation

Potential Future High-Temperature Operation



Charaev et al. 2022,
[arXiv:2208.05674](https://arxiv.org/abs/2208.05674)
[cond-mat.supr-con]

FIG. 1. **High- T_c superconducting nanowires.** **a**, Schematic of the BSCCO single-photon detector: A relatively thin flake of BSCCO is covered by a much thicker flake of hBN and transferred onto ultra-flat gold contacts. SNW region is defined by a helium beam exposure. **b**, Optical photograph of the BSCCO device. Scale bar is 3 μm. Inset: Example of the SEM image of the BSCCO SNW produced by the He⁺ beam exposure (similar but not identical to that from the photograph). The scale bar is 2 μm. **c**, Schematic of the LSCO-LCO single-photon detector: High- T_c two-dimensional superconductor is formed at the interface between the 5 UC of the LCO insulator and the 5 UC of the LSCO metal. 10 nm of chromium-gold was used for contact leads. **d**, An SEM image of a typical LSCO-LCO SNW device. The scale bar is 2 μm. **e-f**, Examples of the $R(T)$ dependencies for BSCCO (e) and LSCO-LCO (f) flake, film and SNWs. **g**, Typical I - V curve for the BSCCO SNWs measured at $T = 3.7$ K. **h**, Typical I - V curves of the LSCO-LCO SNWs measured at $T = 3.7$ K before and after He⁺ ion exposure.

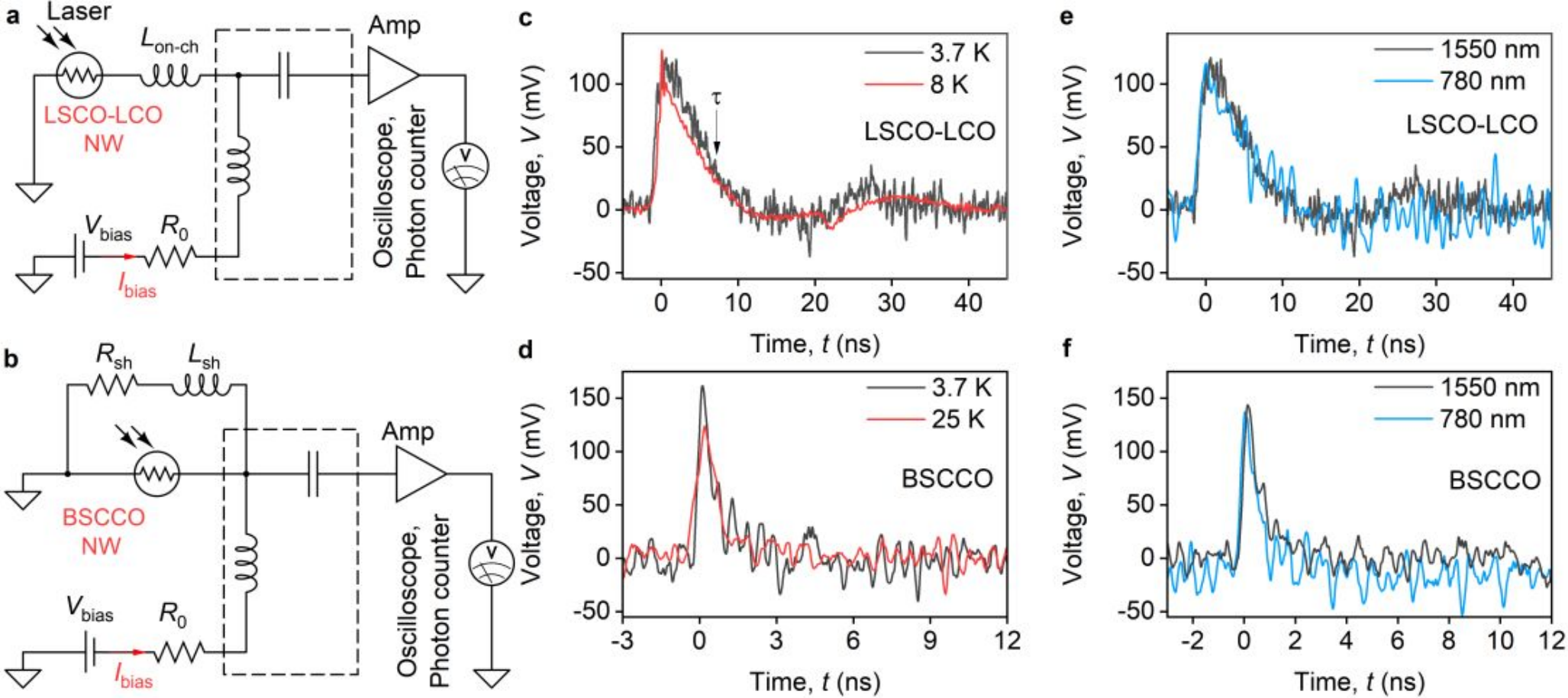


FIG. 2. Photovoltage generation in cuprate NW detectors. **a**, The simplified circuit diagram used to measure the photoresponse of the LSCO-LCO SNW detector. The SNW is current-biased by an isolated voltage source connected to the DC port of the bias tee (dashed rectangle) through a resistor, R_0 . Incident radiation triggers a voltage spike generating a short pulse that propagates through the AC port of the bias tee to the preamplifier and is read out using an oscilloscope or a photon counter. $L_{\text{on-ch}}$ is an on-chip kinetic inductor made out of the LSCO-LCO film. **b**, The simplified circuit diagram used to measure the photoresponse of the BSCCO SNW detector. R_{sh} and L_{sh} are the shunt resistor and the inductor connected in parallel with the BSCCO SNW to prevent it from latching. **c-d**, Photovoltage V_{ph} pulses measured in the LSCO-LCO (c) and BSCCO (d) photodetectors at given T and $\lambda = 1.5 \mu\text{m}$. The devices are biased to the 95% of their critical current for given T . **e-f**, The V_{ph} pulses measured at given λ for the LSCO-LCO (e) and BSCCO (f) devices at $T = 3.7 \text{ K}$ and $T = 16 \text{ K}$ respectively.

Vision & Conclusion

- **Nanowire-Based electronics**
 - Low power, high output impedance
 - Driving more conventional electronics
 - Simple manufacturing
- **Where is this going?**
 - High-temperature ($> 20K$) electronics for a range of applications (e.g. MgB_2)
 - Exploit microwave behaviors
 - Applications in neuromorphic, reversible, and other alternative computing paradigms
 - Scaling and shunting to speed up devices and lower power

Power Consumption: Rough Analysis

- **Switching energy, compare to Silicon**
 - $E \sim V^2$
 - $V \sim 100\times$ lower \rightarrow Energy $\sim 1e4$ lower
 - Cooling penalty $\sim 1e3$
 - ⇒ final advantage $\sim 10\times$
- **Switching energy, compare to RSFQ**
 - $E = \Phi^2 / 2 L$
 - $\Phi \sim 100 \times$ larger and $L \sim 100 \times$ larger
 - ⇒ final disadvantage $\sim 100\times$
- **V and Φ are scalable, potentially**

Remaining Concerns

- **Realistic models**
- **Reproducible fabrication processes**
 - Can critical current of a wire be controlled?
- **Scalable designs**

Likely Applications

- **Detector readout, where materials are already suitable for nanowire electronics**
- **Memories, where JJs struggle with footprint**
- **Off-chip drivers or memory-line drivers, where JJs struggle with high load impedances and bandwidth requirements are lower**
- **Radiation-sensitive applications (e.g. space, HEP) where dielectric barriers might degrade**

THANK YOU

- Current Funding
 - Dept. of Energy
 - DARPA
 - NSF
- Past Funding
 - U.S. Air force Office of Scientific Research
 - U.S. Office of Naval Research
 - IARPA, NASA, Skolkovo Inst. of Technology
- Many U.S. and international fellowships

Superconductivity Team in QNN Group



Emma Batson
(Grad Student)



Camron Blackburn
(Grad Student)



Matteo Castellani
(Grad Student)



Marco Colangelo
(Grad Student)



Torque Dandachi
(MEng Student)



Reed Foster
(MEng Student)



Stewart Koppell
(Post-Doc)



Owen Medeiros
(Grad Student)



Dip Joti Paul
(Grad Student)



Tony Zhao
(Post-Doc)

Graduated/Former

Nathan Abebe
Lucy Archer
Reza Baghdadi
Francesco Bellei
Brenden Butters
Alessandro Buzzi
Niccolo Calandri
Ilya Charaev
Ignacio Estay Forno
Andrew Dane
Yachin Ivry
Glenn Martinez
Adam McCaughan
Faraz Najafi
Murat Onen
Ashley Qu
Kristen Sunter
Emily Toomey
Hao-Zhu Wang
Qing-Yuan Zhao
Di Zhu

Thank you to Lara Ranieri and Rinske Wijtmans for assistance in preparing these slides for presentation

END OF PRESENTATION

berggren@mit.edu
[@karlberggren](https://twitter.com/karlberggren)